Western Graduate&PostdoctoralStudies

Electronic Thesis and Dissertation Repository

10-16-2014 12:00 AM

Seismicity Processes in the Charlevoix Seismic Zone, Eastern Canada

Azadeh Fereidoni, *The University of Western Ontario*

Supervisor: Dr. Gail Atkinson, *The University of Western Ontario*
A thesis submitted in partial fulfillment of the requirements for the Doctor of Philosophy degree in Geophysics
© Azadeh Fereidoni 2014

Follow this and additional works at: https://ir.lib.uwo.ca/etd

Part of the Geophysics and Seismology Commons

Recommended Citation

SEISMICITY PROCESSES IN THE CHARLEVOIX SEISMIC ZONE, EASTERN CANADA

(Thesis format: Integrated Article)

by

Azadeh <u>Fereidoni</u>

Graduate Program in Geophysics

A thesis submitted in partial fulfillment
of the requirements for the degree of
Doctor of Philosophy

The School of Graduate and Postdoctoral Studies
The University of Western Ontario
London, Ontario, Canada

Abstract

The Charlevoix Seismic Zone (CSZ) is the most seismically active region in eastern Canada, based on the historical and current rate of activity. Several papers contend that the current seismicity in the CSZ represents long-lived aftershock sequences of the 1663 M~7 earthquake, in which the aftershock activity has persisted for hundreds of years. The aim of this thesis is to explore the influence of the 1663 earthquake on the current seismicity in the CSZ. The first part of the thesis has focused on developing a comprehensive earthquake database required for analysis of seismicity. The second part of the thesis has been devoted to characterization of seismicity in the CSZ in both time and space, with the goal of developing greater insight into the nature of intraplate seismicity in this region. The evidence from statistical analysis suggests that the current seismicity in the CSZ is not predominantly composed of the aftershock activity of past large earthquakes; the ongoing seismicity is therefore expected to continue in the region, and the zone should be considered an ongoing source of seismic hazard. However, I emphasize that this does not eliminate the possibility that earthquake activity in Charlevoix is still influenced by the stress changes imparted by the 1663 earthquake in the surrounding crust. The Coulomb stress analysis used in the present thesis shows that the stress triggers and shadow cast by the 1663 earthquake still exert influence on earthquake occurrence in Charlevoix after centuries.

Keywords

Co-Authorship Statement

This thesis is prepared in integrated-article format and the following manuscripts were written by Azadeh Fereidoni and the co-authors. Azadeh is the lead author on studies of seismicity and related topics, and carried out the studies with some input and direction from the co-authors.

1) Fereidoni, A., Atkinson, G. M., Macias, M., & Goda, K. (2012). CCSC: A composite seismicity catalog for earthquake hazard assessment in major Canadian cities, *Seismological Research Letters*, **83**(1), 179-189.

2) Fereidoni, A., Atkinson, G. M. (2014). Aftershock statistics for earthquakes in the St. Lawrence Valley, *Seismological Research Letters*, **85**(5), 1125-1136.

3) Fereidoni, A., Atkinson, G. M. (2014). Correlation between coulomb stress changes imparted by historic earthquakes and current seismicity in Charlevoix Seismic Zone, eastern Canada (Accepted for publication in *Seismological Research Letters*)

Acknowledgments

The completion of this thesis was made possible by the help and cooperation of numerous people.

First and foremost, I would like to sincerely thank my supervisor Dr. Gail Atkinson for her guidance and encouragement throughout the course of my study program. I would like to thank her for providing me with the opportunity to study in the Geophysics program at Western, and to have this invaluable learning experience in her research group. Without her guidance and persistent help this dissertation would not have been possible. She will be an exemplary role model to me in my whole personal and career life.

My gratitude also extends to my advisory committee: Dr. Kristy Tiampo and Dr. Robert Shcherbakov for following up my progress during the annual meetings. My research benefitted from their technical advice and their helpful suggestions.

I would like to thank all the colleagues in the Engineering Seismology Research Group for their valuable friendship and suggestions during weekly group meetings. Special thank goes to Dr. Karen Assatourians for being a constant source of support despite his busy schedule. Invaluable discussions and cooperation with him made my research move forward.

Also I would like to thank the great administrative staff at the Department of Earth Sciences for spending their time on providing information to the graduate students. Special thanks to Marie Schell, for her constant love and help, and to John Brunet for a level of support which went beyond his responsibilities and was truly uncommon.

My parents and my lovely sisters definitely deserve special thanks for their ongoing support and their unconditional love.

Last, but not least, I thank my husband Afshin for his love, patience and encouragement throughout the course of this journey. He has always been my number one supporter during the long days of work. I can't put in the word how much I appreciate him.

Table of Contents

List of Tables

List of Figures

List of frequently-used symbols and acronyms

M	Earthquake magnitude
	Moment magnitude,
M	which is defined by the seismic moment of an earthquake
	(Kanamori and Hanks, 1979)
CSZ	Charlevoix Seismic Zone
ΔCFF	Change in Coulomb Failure Function
n	number of earthquakes
t	elapsed time from mainshoock
CCSC	Canadian Composite Seismicity Catalog
SHEEF	Seismic Hazard Earthquake Epicenter File
GSC	Geological Survey of Canada
ANSS	Advance National Seismic System
mb	Teleseismic body-wave magnitude
MN/mN	Nuttli magnitude
ML	Local magnitude
MS	Surface-wave magnitude
MC	coda magnitude
mD	Duration magnitude
SD	Standard Deviation
CI	95% Confidence Interval
MMI	Modified Mercalli Intensity
ENA	Eastern North America
WNA	Western North America
λ	Frequency of earthquake per unit time
MLE	Maximum Likelihood Estimation
M_e	Equivalent magnitude for stacked aftershock sequences
$\Delta\tau$	Shear stress change
$\Delta\sigma$	normal stress change
μ'	effective/apparent coefficient of friction

Chapter 1

1   Introduction

1.1   Motivation for this study

Although large earthquakes are rare in stable continental regions, they can present significant natural hazard to population and infrastructure centers as evidenced by the occurrence of disastrous intraplate earthquakes such as 2008 magnitude (M) 7.9 earthquake in Sichuan, China. Eastern Canada is no exception; large earthquakes in the past have proven to be damaging and deadly such as 1929 Grand Banks M7.2 earthquake which triggered a tsunami and killed 27 people (Lamontagne, 2008). The consequences of a significant earthquake near a major population centre in eastern Canada, such as Montreal, Ottawa, or Quebec City could be potentially disastrous today in terms of social and economic impact. An accurate and reliable assessment of seismic hazard is an essential prerequisite for effective mitigation measures in eastern Canada.

 In intraplate regions, characterization of seismicity plays a crucial role in evaluation of seismic hazard (Beauval et al, 2006; Atkinson and Goda, 2011). The intraplate seismicity in eastern Canada is concentrated in clusters of activity along the St. Lawrence and Ottawa valleys. In this study, I focus on the cluster of activity in the Charlevoix Seismic Zone (CSZ) of Quebec, which is seismically the most active region in eastern Canada. The zone experiences a continuing moderate-to-high level of seismic activity, including several historic damaging earthquakes in the magnitude 6 range (Adams and Basham, 1989). According to the National Seismic Hazard Map of Canada (Adams and Halchuk, 2003), as illustrated in Figure 1.1, the seismic hazard in the CSZ is as high as that in active plate-margin settings such as British Columbia. Based on historical accounts, Smith (1962) has identified the Charlevoix region as the focal area of the 1663 (M~7) earthquake. The 25 February 1663 earthquake, which is historically the largest earthquake to have occurred on land in eastern Canada, was felt as far as New England, and triggered major landslides along the St. Lawrence River (Ebel, 1996, Gouin, 2001). Like other intraplate earthquake zones, the causes of large earthquakes in the Charlevoix region are poorly understood.

A controversy over the nature of the seismic hazard at Charlevoix has developed during the

past three decades. Several papers contend that the current seismicity clusters along the St. Lawrence and Ottawa valleys represents long-lived aftershock sequences of previous large earthquakes occurring along Iapetan rift faults (e.g. Basham and Adams, 1983; Basham, 1989, Ebel et al, 2000; Ma and Eaton, 2007; Stein and Liu, 2009), where aftershock activity may persist for hundreds of years. The current high seismicity in the Charlevoix region might be of this type, with the 1663 M7 earthquake considered as a characteristic mainshock. This hypothesis might suggest that seismicity in Charlevoix is "near the end", so that the CSZ is no longer a source of significant hazard. Under this model, future large earthquakes would not necessarily be expected in currently-active zones, which would have important implications for hazard assessment.
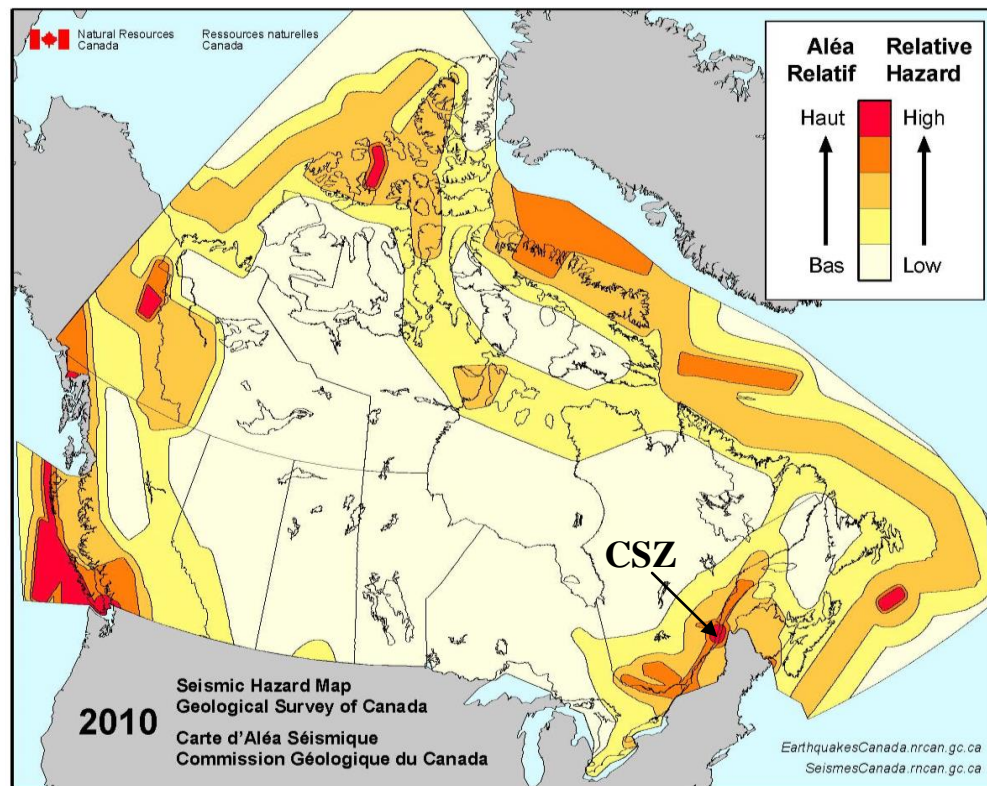
Figure 1-1 2010 Simplified Seismic Hazard Map of Canada (Source: http://www.earthquakescanada.nrcan.gc.ca/hazard-alea/simphaz-eng.php). CSZ denotes Charlevoix Seismic Zone.

In this work, I aim to shed light on whether the current seismicity is the CSZ is likely to be an aftershock sequence that is dying out with time. To do that I use well-known seismicity

clustering models to investigate the pattern of seismicity in both temporal and spatial domains. An accurate characterization of seismicity could yield better insight into the influence of large historical earthquakes on current seismicity in Charlevoix. Although this work examines the case of the CSZ, the results of our analysis could also improve our understanding of seismogenesis and seismic hazard in other intraplate earthquake zones.

1.2   Organization of work

The integrated research work presented in this thesis is organized in 5 chapters as follows. Chapter 1 describes the specific objectives of this work, and outlines the questions that have been addressed through the thesis. In this chapter, I also give a brief summary of seismicity models applied in succeeding chapters. In Chapter 2, I describe the development of a comprehensive, high-quality database of earthquake epicenters. The composite seismicity catalog provides a suitable baseline for my research work as well as other seismological studies in Canada. Chapter 3 provides an analysis of temporal behavior of seismicity in the St. Lawrence Valley, considering the aftershock activity of recent major earthquakes in the region. The findings of this statistical approach give useful insight into the length of aftershock activity in eastern Canada for both contemporary and historic mainshocks. In Chaptered 4, Coulomb stress theory is used to investigate the influence of past large earthquakes on the location of current seismicity in the CSZ. Chapter 5 provides concluding remarks, and discusses those aspects of the research work that warrant further investigation in future works.

1.3   Previous studies in the Charlevoix Seismic Zone

The Charlevoix Seismic Zone is located along the St. Lawrence River, 105 km NE of Quebec City. The active zone defines a 30 by 85 eclipse that covers an area of overlap between faults associated with Iapetan rifting in the Palezoic, and a Devonian-meteorite crater. The Charlevoix region lies in a complex geologic setting along the St. Lawrence rift fault. As pointed out in Lamontagne (1999), the main geological structures include features from several tectonic events: faulting during the 1100 Ma Grenvillian orogeny; rifting during the 700 Ma Iapetus Ocean opening; the 450 Ma Appalachian orogeny; and a large meteor impact at ~350 Ma (Rondot, 1979). Therefore, the CSZ fault zone occurs within a highly fractured volume, particularly within the impact structure. It is difficult to relate all of the seismicity to

the rifts fault, as similar structures elsewhere along the St. Lawrence River are not seismically active (Lamontagne et al, 2004).

Since the area has been settled in the 1600s, the CSZ has experienced 5 damaging events in the magnitude 6 range (Adams and Basham, 1989), including the 25 February 1663 earthquake. Recently, the magnitude of the 1663 earthquake was estimated to be possibly as large as **M**7.2-7.9 (Locat 2011; Ebel 2011). The complexity of CSZ seismicity might be modeled by a combination of factors. Based on the similarity between the spatial trend of seismicity at depth and orientation of rift faults, Anglin (1984) concluded that the earthquake activity in the Charlevoix is mostly related to the reactivation of the faults. However, most of the low-level background seismicity is located within the impact structure suggesting that this feature has significant influence on the concentration of seismicity in the region. Lamontagne (1987) proposed that the impact structure weakened the fault zone and created its own fractures. Adams and Basham (1989) discounted the link between these two structures, as the spatial extent of active zone goes beyond the crater boundaries. Moreover, other meteorite impacts in Canada are seismically inactive.

Hypocentral locations reveal that the seismicity is not uniformly distributed in the CSZ. The clustering of seismicity and variability in rupture plane orientations from microearthquake focal mechanisms imply that the fault zone in the CSZ occurs within a highly fractured volume, particularly within the impact structure (Lamontagne, 1999). Lamontagne et al (2004) suggested that these highly fractured areas respond to regional stresses; however, some smaller events are due to local changes in stress/strength.

The concentration of earthquakes in the CSZ while similar rift faults along the St. Lawrence River are not seismically active has puzzled researchers of seismicity in this region (Lamontagne et al, 2004). The hypothesis of the long-lived aftershock sequence in the Charlevoix region has been discussed since the 1980s (Basham and Adams, 1983; Basham, 1989). More recently, two studies (Ebel, 2000; Liu and Stein, 2009) suggested that the activity in Charlevoix is well characterized as a long aftershock sequence of the 1663 earthquake. These two studies, however, did not provide direct evidence whether the activity rate from 1663 to present could be reconciled by well-established aftershock decay models (e.g. Omori decay model). Such evidence exists for the 1891 Nobi (Japan) earthquake, where

the Omori decay model holds for more than a century after the mainshock (Utsu et al, 1995).

Previous studies of crustal deformation have shown detectable deformation in the Charlevoix Seismic Zone that is higher than the regional average across the St. Lawrence region. On the basis of earthquake statistics from the Canadian earthquake hazard model, Mazzotti and Adams (2005) estimated the seismic strain rate locally to be of the order of $3\text{-}23 \times 10^{-9}$ yr^{-1} in the CSZ which is higher than the typical strain rates of intraplate environments (10^{-13}–10^{-11} yr^{-1}). In another study, Mazzotti et al (2005) presented the Global Positioning System (GPS) measurements that constrain the average crustal strain rate in amplitude (1.7×10^{-9} yr^{-1}), style (mostly ESE-WNW shortening) , and origin (postglacial rebound) across the seismic zones of the lower St. Lawrence valley. For the case of CSZ, they estimated that the horizontal strain rate follows the regional pattern (shortening perpendicular to the St. Lawrence River) but its amplitude (3.7×10^{-9} yr^{-1}) is about twice the regional average. These geodetic measurements are in agreement with the deformation pattern indicated by the focal mechanism of large earthquakes. This amount of deformation from GPS data could account for very large earthquakes with recurrence periods of 400-1300 years which are not inconsistent with the seismic catalog statistics in Charlevoix.

1.4   February 5, 1663 Charlevoix earthquake

The earthquake at about 5:30 p.m. on February 5, 1663 (Local Time in Quebec) was one of the most important crises in eastern North America in historic time. The mainshock was of intensity > VIII between Gouffre River (47°26'N, 70°29'W) and La Malbaie (47°39'N, 70°09'W) and was reported felt over a large area, from Tadoussac to Montreal and to the south as far as Boston and New Amsterdam. At the time of the earthquake, the population of New-France was confined to the fortified posts of Quebec, Trios-Rivieries, and Montreal. A few missionaries and hunters were scattered throughout the territory. Much of the Jesuits Relations for the year 1663 is devoted to describing the profound effects of this earthquake, both on the land and on the people of New-France. The earthquake caused large landslides and sand volcanoes along the St. Lawrence River and its tributaries. It is believed that the sand volcanoes which occurred at the mouth of the Gouffre River indicate the epicentral region (Gouin, 2001). Smith (1962) has assigned the epicenter of the 1663 earthquake to the Charlevoix Seismic Zone where most of the epicenters of current seismicity are located.

However, the exact location remains doubtful due to the lack of definitive information. Based on the readings of the Relations and other historical accounts, the felt area of the 1663 earthquake is estimated to be in the range of $(3.5\text{-}4.0) \times 10^6$ km^2 (Gouin, 2001). The felt reports, which were of course written by non-professionals, are not sufficient in number and are not detailed enough to allow us to determine the exact intensities. Based on the widespread effects of this earthquake and its large felt area, Ebel (1996) assigned a magnitude of 7.0 ± 0.5 (mbLg scale) to the 1663 mainshock. Recently, its magnitude was estimated to be possibly as large as moment magnitude 7.2 to 7.9 (Locat, 2011; Ebel, 2011). Therefore, the magnitude of the 1663 earthquake still has an uncertainty of at least several tenths to one-half of a magnitude unit. As noted in Lamontagne et al (2004), a repeat earthquake of the 1663 M~ 7 earthquakes would result in serious damage to towns located in the epicentral zone on both shores of the St. Lawrence River. It would probably cause landslides and seriously damage to parts of Quebec City, where soft soils amplify ground motions.

1.5 Temporal clustering models

The lists of earthquakes that are regularly published by the international and national seismological agencies have shown that the seismicity is clustered on time scales. The terms of foreshocks, mainshocks, aftershocks, and earthquake swarms are related to the concept of the temporal clustering of the earthquakes. During the last century, several seismicity models have been developed to statistically investigate the various temporal features of seismic activity. These statistical models not only are remarkable tools for better understanding of seismicity patterns, but they also provide important frameworks for time-dependent seismic hazard assessment and forecasting the probabilities of earthquake occurrences. In this section, I emphasize the pioneering Omori formula, its modified forms and the point process models using these formulae (i.e. Epidemic-Type Aftershock Sequence), mainly from the statistical viewpoint. The physical explanations of these models and related observations are out of scope of this section. Extensive reviews of the development of the temporal seismicity models are given in Utsu et al (1995), Ogata (1999), Zhuang et al (2011, 2012).

Sequences of aftershocks commonly follow moderate-to-large earthquakes. It is widely

accepted that the aftershock activity dies off with time, after which the level of background or normal activity resumes in the focal area. Omori (1894 a,b) studied the aftershocks of the 1891Nobi earthquake and showed that the decrease of the frequency of aftershocks with time is well represented by

$$n(t) = \frac{1}{t} \tag{1.1},$$

where t is the time from the occurrence of the mainshock. The power law dependency of time separates the Omori formula from most decay laws in physics in which the dependency on time are described by an exponential function. The decay of aftershocks in the form of a power law implies its long-lived nature (Utsu et al, 1995).

When Utsu (1957) was studying the aftershocks of several earthquakes in Japan, he postulated that the decay of aftershock activity of several earthquakes varied from the original Omori formula, and developed a modified form of Equation (1.1) as follows:

$$n(t) = K(t)^{-p} \tag{1.2},$$

where K and p are constants to be determined. Since the function diverges at $t = 0$, he recommended the use of additional small positive constant c:

$$n(t) = K(t + c)^{-p} \tag{1.3}.$$

Equation (1.3) is now called the modified Omori formula or the Omori-Utsu formula. The modified form emphasizes that the decay of aftershock activity could be somewhat faster (i.e $p > 1$) or slower (i.e. $p < 1$) than that expected from the original Omori formula, since the slope of the curve of the cumulative number of aftershocks against $log\ t$ tends to change with time. In contrast, the original Omori formula predicts a constant slope for large t. Utsu (1995) reviewed the p values from more than 200 studies and reported that it ranges from 0.6 to 2.5 with a median of 1.1. A detailed discussion of the Omori parameters (K, c, p) is provided in next chapter.

It is preferable to assume that aftershock occurrence follow the non-stationary Poisson process and compute the Omori parameters using the maximum likelihood method, directly based on the occurrence times of individual shocks. With the use of numerical optimization

approaches, Ogata (1983) developed a procedure for obtaining the maximum likelihood estimates (MLE) of the Omori parameters by maximizing the logarithm of the likelihood function. For N aftershocks occurring at time t_i ($i = 1, 2, \ldots, N$) between T_s and T_e, likelihood function (L) is written as

$$L = \{\textstyle\prod_{i=1}^{N} \lambda(t_i)\} exp\left\{-\int_{T_s}^{T_e} \lambda(t) dt\right\} \qquad (1.4),$$

where intensity function (i.e $\lambda(t)$) is given by Equation (1.3). The Ogata's maximum likelihood procedure also has the advantage of providing the standard error of the MLE as a side product. Specifically, the inverse of the Fisher information matrix provides the variance-covariance matrix of the errors of the MLE.

The maximum likelihood estimation of the modified Omori formula provided a practical basis for developing a procedure for forecasting the probability of aftershock occurrence following a large mainshock. Reasenberg and Jones (1989) combined the modified Omori formula with the Gutenberg-Richter law of magnitude frequency and provided a routine procure for determination of probabilities, with the use of Bayesian aftershock statistics from a suite of California aftershock sequences.

It is often observed that the frequency of aftershocks in complex sequences does not follow the original or modified Omori formula. For example, it is not rare to observe that one or more large aftershocks in a sequence accompanied by many aftershocks of their own (secondary aftershocks). Such complex sequences cannot be modeled by a simple decay model expected by the modified Omori formula, but may be presented by superposition of primary and secondary aftershock sequences. The Epidemic-Type Aftershock Sequence model (ETAS) proposed by Ogata (1988) is the most popular of such models that covers the weak points of the Omori model.

The ETAS model generalizes the modified Omori formula by assuming that every earthquake triggers its own aftershock activity. The seismic activity of the region (i.e. $\lambda(t)$) includes the background activity with the occurrence rate of μ and the sum of the modified Omori functions of any shocks i with M_i magnitude which occurred at time t_i, as given by below equation:

$$\lambda(t) = \mu + \sum_{t_i < t} \frac{K_0 exp\{\alpha(M_i - M_z)\}}{(t - t_i + c)^{-p}} \qquad (1.5)$$

where M_z is the cut off magnitude of the dataset. The MLE of the five model parameters (μ, K_0, c, α, and p) can be obtained by maximizing the likelihood function L (Ogata et al, 1993) similar to the form given in Equation (1.4). In characterizing the seismicity of the region, α and p parameters are very important as p indicates the decay rate of aftershocks and α represents the magnitude dependency in generating the aftershocks in a broad sense.

There have been many applications of the ETAS model. The model fits well to various aftershock sequences including swarm type sequences; it is also extremely useful for the study of general seismicity where aftershocks accounts for a considerable part of the data set, such as the point process modeling of shallow seismicity. This advantage relies on the fact that the ETAS model does not require a distinction between triggering events (i.e mainshocks) and the other events. It is worthwhile to note that certain forms for extension of the ETAS to the spatial seismicity are proposed (e.g Ogata 1998). Here, I refer to Zhuang et al (2011) for further discussion. We focused in our study on the Omori formula to model the aftershock sequences, as there are insufficient catalog data in eastern Canada to effectively use the ETAS model.

1.6   Stress transfer models

Earthquake interaction is a fundamental feature of seismicity, leading to earthquake clustering. In the past two decades, numerous studies have focused on the role of stress changes in earthquake mechanics to understand earthquake interactions. Overall, the occurrence of a large earthquake produces a drop in the average stress in the source region. However, there is also a redistribution of the stress, which may cause local stress increases on the fault surface. The process by which a stress perturbation is communicated to the fault is usually referred to as "stress transfer". In this section, we discuss the role of elastic stress changes in earthquake interactions. However, stress can also transfer between faults through other mechanisms such as dynamic stresses and long-term viscoelastic effects. The review papers by Harris (1998), Stein (1999) and Steacy et al (2005) provide more complete discussion on stress transfer and earthquake triggering.

The relation between static stress changes and the location of subsequent earthquakes was

originally proposed in the pioneering work of Das and Scholz (1981). However, the study by Stein et al (1992), which explored the role of stress transfer in earthquake occurrence following the 1992 M7.3 Landers earthquake, brought the renewed attention of seismologists to this issue. Since then, the hypothesis of stress transfer has continued to gain credibility because of its ability to explain the location of aftershocks and other smaller events that follow a mainshock.

Coulomb stress transfer is one of the simple interaction mechanisms that provide a comprehensive description of the triggering mechanism. The Coulomb failure stress is calculated based on the idea (Jaeger and Cook, 1969) that displacement in the elastic upper crust due to the causative fault generates a tensoral stress change which will then be resolved on a target (receiver) fault into shear and normal stress components, as illustrated in Figure 1.2.
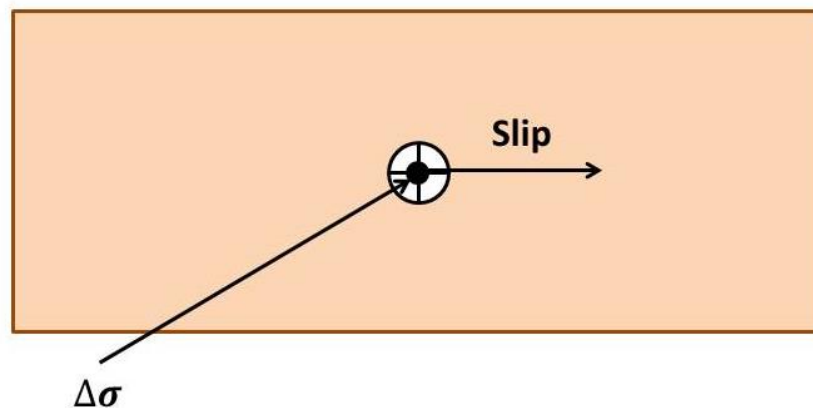
$$\Delta CFF = \Delta\tau + \mu(\Delta\sigma + \Delta p)$$
$$\approx \Delta\tau + \mu'\Delta\sigma$$

ΔCFF>0   fault plane loaded → Stress-triggering
ΔCFF<0   fault plane relaxed → Stress Shadow

Figure 1-2 ΔCFF, the change in Coulomb Failure Function, is calculated to evaluate if one event brought another event closer to, or further from failure. Δτ is the change in shear stress, and Δσ is the change in normal stress on the fault plane of second event (receiver fault). μ in the coefficient of friction and Δp is the change in pore pressure. It is common to simplify the equation by dropping the explicit calculation of pore pressure

and using apparent (effective) coefficient of friction, μ' (see Harris, 1998); schematic diagram produced after Harris (1998).

A large number of researchers have applied Coulomb stress calculations to the study of earthquake clustering. It is widely reported that the regions where stress increases (ΔCFF > 0, the stress triggering zone) match with areas where subsequent events cluster, whereas reduction in stress (ΔCFF < 0, the stress shadows) suppresses future tremors (Harris, 1998 and references therein). It appears that a small ΔCFF, as low as 0.01 MPa (0.1 bar), can influence the locations of subsequent events (e.g Reasenberg and Simpson, 1992; King et al, 1994), although this value is only a few percent of the total stress drop during the mainshock.

While the absolute value of stress is difficult to estimate, stress changes can be readily calculated for a given geometry of fault plane and slip direction. The uncertainty in the receiver fault orientation, slip distribution, and the input parameters for friction usually are sources of variability in the calculation of Coulomb stress changes. It is recommended to compare the stress changes map with the location of seismicity to test the quality and robustness of the calculation (Hainzl et al, 2010).

The Coulomb stress analysis could generally define the location of future earthquakes but not their timing. By using the long-term stressing rate through Dietrich (1994)'s rate-and-state relation, one could potentially obtain a prediction about the timing of stress-triggered events. By incorporating the concept of rate/state friction into Coulomb stress analysis, several researchers (see Stein 1999 and reference therein) have converted their static stress changes model into time-dependent seismic hazard assessments.

Although the Coulomb stress model has gained widespread use in explaining triggered seismicity over the past decades, the results from several studies suggest that its applicability varies between different sequences. As an example, a comprehensive statistical test by Hardebeck et al (1998), considering the **M**6.7 1994 Northridge, California earthquake, showed that the static stress change model cannot explain the first month of the Northridge aftershock sequence. The lack of consistency in the performance of the static stress change triggering model in explaining different sequences may be due in part to the limitations of the modelling. Simplicity of the assumed slip model, approximating the Earth as a homogeneous elastic half-space, and fixed receiver fault mechanism affect the computed values of the

ΔCFF for the subsequent events. The variability of the results for different sequences may also imply that there are other triggering mechanisms involved, such as dynamic strain [e.g., Anderson et al., 1994; Hill et al., 1993], transient changes in pore pressure due to dynamic strain [e.g., Hill et al., 1993], long-term changes in pore pressure due to pore-fluid movements [e.g., Hill et al., 1993], and increase in pore pressure by dynamic strain via rectified diffusion [Sturtevant et al., 1996]. Thus although the static stress change triggering model can be useful in explaining aftershock triggering, it is not consistently applicable for all events, or even consistently-applicable within an event sequence. Consequently, Coulomb stress modeling may not be generally applicable to seismic hazard assessment applications, at least not until additional factors such as tectonic regime, regional stress levels, and fault strength can be adequately incorporated into the model.

1.7 References

Adams, J., and S. Halchuk (2003). Fourth generation seismic hazard maps of Canada; values for over 650 Canadian localities intended for the 2005 National Building Code of Canada, *Open-File Report - Geological Survey of Canada*.

Adams, J., P. W. Basham, and S. Gregersen (1989). Seismicity and seismotectonics of Canada's eastern margin and craton, *NATO Advanced Study Institutes Series.Series C: Mathematical and Physical Sciences* **266,** 355-370.

Anderson, J. G., J. N. Brune, J. N. Louie, Y. Zeng, M. Savage, G. Yu, and Q. Chen (1994). Seismicity in the western Great Basin apparently triggered by the Landers, California, earthquake, 28 June 1992, *Bulletin of the Seismological Society of America* **84,** 863-891.

Anglin, F. M. (1984). Seismicity and faulting in the Charlevoix Zone of the St. Lawrence Valley, *Bulletin of the Seismological Society of America* **74,** 595-603.

Atkinson, G. M., and K. Goda (2011). Effects of seismicity models and new ground-motion prediction equations on seismic hazard assessment for four Canadian cities, *Bulletin of the Seismological Society of America* **101,** 176-189.

Basham, P. W. (1989). Problems with seismic hazard assessment on the eastern Canadian continental margin, *NATO Advanced Study Institutes Series.Series C: Mathematical and Physical Sciences* **266,** 679-686.

Basham, P. W. (1989). Problems with seismic hazard assessment on the eastern Canadian

continental margin, *NATO Advanced Study Institutes Series.Series C: Mathematical and Physical Sciences* **266,** 679-686.

Basham, P. W., J. Adams, and C. Kitzmiller (1983). Earthquakes on the continental margin of Eastern Canada; need future large events be confined to the locations of large historical events? *Open-File Report - U.S.Geological Survey* 456-467.

Beauval, C., S. Hainzl, and F. Scherbaum (2006). Probabilistic seismic hazard estimation in low-seismicity regions considering non-Poissonian seismic occurrence, *Geophysical Journal International* **164,** 543-550.

Das, S., and C. H. Scholz (1981). Off-fault aftershock clusters caused by shear stress increase? *Bulletin of the Seismological Society of America* **71,** 1669-1675.

Dieterich, J. (1994). A constitutive law for rate of earthquake production and its application to earthquake clustering, *Journal of Geophysical Research* **99,** 2601-2618.

Ebel, J. E. (2011). A new analysis of the magnitude of the February 1663 earthquake at Charlevoix, Quebec, *Bulletin of the Seismological Society of America* **101,** 1024-1038.

Ebel, J. E. (1996). The seventeeth century seismicity of northeastern North America, *Seismol.Res.Lett.* **67,** 51-68.

Ebel, J. E., K. Bonjer, and M. C. Oncescu (2000). Paleoseismicity; seismicity evidence for past large earthquakes, *Seismol.Res.Lett.* **71,** 283-294.

Gouin, P. (2001). Historical earthquakes felt in Quebec (from 1534 to March 1925), *Guérin, Montréal*.

Hainzl, S., S. Steacy, and D. and Marsan (2010). Seismicity models based on Coulomb stress calculations, *Community Online Resource for Statistical Seismicity Analysis*.

Harris, R. A. (1998). Introduction to special section; stress triggers, stress shadows, and implications for seismic hazard, *Journal of Geophysical Research* **103,** 24-24,358.

Hardebeck, J. L., J. J. Nazareth, and E. Hauksson (1998). The static stress change triggering model: Constraints from two southern California aftershock sequences, *Journal of Geophysical Research: Solid Earth (1978–2012)* **103,** 24427-24437.

Hill, D., P. Reasenberg, A. Michael, W. Arabaz, G. Beroza, D. Brumbaugh, J. Brune, R. Castro, S. Davis, and W. Ellsworth (1993). Seismicity remotely triggered by the magnitude 7.3 Landers, California, earthquake, *Science* **260,** 1617-1623.

Jaeger, J. C., and N. G. W. Cook (1969). Fundamentals of rock mechanics, Canada (CAN).

King, G. C. P., R. S. Stein, and J. Lin (1994). Static stress changes and the triggering of earthquakes, *Bulletin of the Seismological Society of America* **84,** 935-953.

Lamontagne, M., M. Beauchemin, and T. and Toutin (2004). Earthquakes of the Charlevoix seismic zone, Quebec, *CSEG RECORDS* **October,** 41-44.

Lamontagne, M. (2008). Casualties directly caused by an earthquake in Canada; first contemporaneous written accounts from the M 6.5 Charlevoix, Quebec, earthquake of 20 October 1870, *Bulletin of the Seismological Society of America* **98,** 1602-1606.

Lamontagne, M. (1987). Seismic activity and structural features in the Charlevoix region, Quebec, *Canadian Journal of Earth Sciences = Revue Canadienne des Sciences de la Terre* **24,** 2118-2129.

Lamontagne, M. Rheological and geological constraints on the earthquake distribution in the Charlevoix seismic zone, Quebec, Canada, Ph.D. Theses, .

Locat, J. (2011). La localisation et la magnitude du seisme du 5 fevrier 1663 (Charlevoix) revues a l'aide des mouvements de terrain, *Canadian Geotechnical Journal = Revue Canadienne de Geotechnique* **48,** 1266-1286.

Mazzotti, S., and J. Adams (2005). Rates and uncertainties on seismic moment and deformation in eastern Canada, *Journal of Geophysical Research: Solid Earth (1978–2012)* **110,** .

Mazzotti, S., T. S. James, J. Henton, and J. Adams (2005). GPS crustal strain, postglacial rebound, and seismic hazard in eastern North America: The Saint Lawrence valley example, *Journal of Geophysical Research: Solid Earth (1978–2012)* **110,** .

Ma, S., and D. W. Eaton (2007). Western Quebec seismic zone (Canada); clustered midcrustal seismicity along a Mesozoic hot spot track, *Journal of Geophysical Research* **112,** B06305.

Ogata, Y. (1999). Seismicity analysis through point-process modeling: A review, *Pure Appl.Geophys.* **155,** 471-507.

Ogata, Y. (1998). Space-time point-process models for earthquake occurrences, *Annals of the Institute of Statistical Mathematics* **50,** 379-402.

Ogata, Y. (1988). Statistical models for earthquake occurrences and residual analysis for point processes, *Journal of the American Statistical Association* **83,** 9-27.

Ogata, Y. (1988). Statistical models for earthquake occurrences and residual analysis for point processes, *Journal of the American Statistical Association* **83,** 9-27.

Ogata, Y. (1983). Estimation of the parameters in the modified Omori formula for aftershock frequencies by the maximum likelihood procedure, *Journal of Physics of the Earth* **31,** 115-124.

Omori, F. (1894b). On after-shocks of earthquakes, *J. Coll. Sci. Imp. Univ. Tokyo* **7,** 111-200.

Omori, F. (1894a). On after-shocks, *Rep. Imp. Earthq. Inv. Corn.* **2,** 103-138.

Reasenberg, P. A., and L. M. Jones (1989). Earthquake hazard after a mainshock in California, *Science* **243,** 1173-1176.

Rice, J. R. (1992). Fault stress states, pore pressure distributions, and the weakness of the San Andreas Fault, Acad. Press, San Diego, CA, San Diego, CA, United States (USA).

Rice, J. R., and M. P. Cleary (1976). Some basic stress diffusion solutions for fluid‐saturated elastic porous media with compressible constituents, *Rev.Geophys.* **14,** 227-241.

Simpson, R. W., and P. A. Reasenberg (1994). Earthquake-induced static-stress changes on Central California faults, *U.S.Geological Survey Professional Paper* F55-F89.

Smith, W. E. T. (1962). Earthquakes of eastern Canada and adjacent areas 1534-1927, *Publications of the Dominion Observatory, Ottawa* **26,** 271-301.

Steacy, S., J. Gomberg, and M. Cocco (2005). Stress transfer, earthquake triggering, and time-dependent seismic hazard, *Journal of Geophysical Research* **110,** variously paginated.

Stein, R. S. (1999). The role of stress transfer in earthquake occurrence, *Nature (London)* **402,** 605-609.

Stein, R. S., G. C. King, and J. Lin (1992). Change in failure stress on the southern San Andreas fault system caused by the 1992 magnitude = 7.4 Landers earthquake, *Science* **258,** 1328-1332.

Stein, S., and M. Liu (2009). Long aftershock sequences within continents and implications for earthquake hazard assessment, *Nature (London)* **462,** 87-89.

Utsu, T. (1957). Magnitudes of earthquakes and occurrence of their aftershocks , *Zisin, Ser. 2* **10,** 35-45.

Utsu, T., Y. Ogata, and R. S. Matsu'ura (1995). The centenary of the Omori Formula for a decay law of aftershock activity, *Journal of Physics of the Earth* **43,** 1-33.

Zhuang, J., D. Harte, M. J. Werner, S. Hainzl, and S. Zhou (2012). Basic models of

seismicity: Temporal models, *Community Online Resource for Statistical Seismicity Analysis*.

Zhuang, J., M. J. Werner, S. Hainzl, D. Harte, and S. Zhou (2011). Basic models of seismicity: spatiotemporal models, *Community Online Resource for Statistical Seismicity Analysis.*

Chapter 2

2　CCSC: A composite seismicity catalog for earthquake hazard assessment in major Canadian cities[1]

We have developed a composite Canadian seismicity catalog (CCSC) containing seismicity data to 2009. The primary source of information for the CCSC is the seismicity catalog from the Geological Survey of Canada. Location, magnitude, and focal depth parameters are then supplemented by the addition of available complementary data from other sources. For each event, the set of all available magnitude types is compiled, and a preferred conversion to moment magnitude is provided. The CCSC provides a valuable database for earthquake hazard analysis of major Canadian cities.

2.1　Introduction

The development of a comprehensive, high-quality catalog of earthquake events is the most fundamental step in seismic hazard analyses and related studies (Woessner and Wiemer 2005). The current national seismic hazard maps of Canada (as used in the 2010 National Building Code of Canada) adopt the information in the Seismic Hazard Earthquake Epicenter File (SHEEF) catalog provided by the Geological Survey of Canada (GSC), covering the earthquake activity through 1991 (Adams and Halchuk 2003). Since that time, a significant amount of data has been added to the Canadian earthquake catalog, and significant improvements in unifying magnitude scales have been made. To integrate the improved knowledge on seismicity parameters during the past two decades, we have developed the 2009 Composite Canadian Seismicity Catalog (CCSC), suitable as a baseline database for seismic hazard analyses in major Canadian cities. The intent is to update the catalog each year by adding new events.

The primary source for the CCSC is the most updated version of the SHEEF catalog

---

[1] A version of this chapter has been published. Fereidoni, A., Atkinson, G. M., Macias, M., & Goda, K. (2012). CCSC: A composite seismicity catalog for earthquake hazard assessment in major Canadian cities. *Seismological Research Letters*, **83**(1), 179-189.

(Halchuk 2009); it is enhanced using other local and global databases. The fundamental idea is to preserve the information of the primary dataset and to modify and extend the catalog by addition of available complementary data from other sources. For each event, we compiled the set of all available magnitude types and assigned a preferred magnitude depending on availability and quality of data. All magnitude measures are retained in the CCSC to provide the most complete event characterization. This is an important distinction between the SHEEF and the CCSC; the SHEEF provides a single preferred magnitude measure while the CCSC tabulates all magnitude measures.

We have unified the composite catalog with respect to moment magnitude (**M**). In western Canada, the moment magnitude conversions are mostly based on empirical conversion equations derived in the present study. However, we considered pre-existing models from the literature (e.g., Dewberry and Crosson 1995) when the data were insufficient to derive a reliable empirical conversion model. In eastern Canada, due to the paucity of moment magnitude measurements, the conversions are based on available models from the literature (e.g., Johnston 1996; Kim 1998; Sonley and Atkinson 2005). In all cases, moment magnitudes obtained by detailed studies in previous publications have been adopted in the composite catalog in preference to values converted by empirical relationships.

The catalog provides the output information in 24 fields, as listed in Table 2.1, and currently includes earthquake events through December 2008. The output files for eastern and western Canada (where the dividing line is 110°W), ccsc09east.txt and ccsc09west.txt, are available online for download, along with comprehensive documentation, at http://www.seismoto-olbox.ca/Catalogs.html. Updated files will be provided on the Web site on an annual basis[2].

---

[2] We have since updated the catalog.

Table 2-1 List of fields in output catalog files

Field No.	Data	Comments
1-5	Origin time: year, month, day, hour, minute	As integers
6-7	Location: latitude and longitude	In decimal degree, with 3 decimal places
8-16	Reported magnitudes: mb, MN, ML, MS, mD, **M**, MM, MZ	The last two variables are generated and used for unknown magnitude type
17-18	Preferred magnitude value and type	Selected from all the reported magnitudes based on the quality of data using the logic described in our online documentation
19	Depth value	In km, with 2 decimal places
20	Depth designation	Indicating how the depth value is determined or assigned in the source catalog (See the corresponding catalog documentation for detailed information on coding). In cases where the depth designation is left blank, the code Z is used
21	Source catalog flag	Points to the catalog from which earthquake event is adopted: 0-SHEEF08, 1-MASE, 2-PETW, 3-PETE, 4-ANSS, 5-PGCW, and 6-RIST
22	Seismic source zone flag	Refers to the associated source zone
23	Conversion Factor	With 2 decimal places, used for **M** calculation from the preferred catalog magnitude
24	Assigned moment magnitude	Our best estimate of **M**

2.2 Contributing earthquake catalogs

The CCSC incorporates information from eight local and international earthquake catalogs: the GSC's SHEEF (Adams and Halchuk 2003; Halchuk 2009), the Ma and Atkinson (2006) catalog (MASE), the Canadian Pacific Geosciences Centre's (PGC) Canadian Earthquake Epicenter File (PGCW, G. Rogers, personal communication, 2008), the GSC's Canadian Earthquake Epicenter File (GSCE, S. Halchuk, personal communication 2008), the U.S. Geological Survey's (USGS) catalogs for the United States (PETE, PETW, Petersen et al. 2008), the Advanced National Seismic System's (ANSS) catalog (http://earthquakes.usgs.gov/research/monitoring/anss), and the Ristau (2004) moment tensor solution catalog (RIST).

Table 2.2 gives a summary of the catalog properties. We have provided a more thorough review of the catalogs and other supplementary reports used to compose and enhance the

CCSC in the online documentation. Hereafter the catalogs are referenced using the nicknames assigned in Table 2.2.

2.3   Removing duplicates from SHEEF catalog

The primary data for the development of CCSC is the updated version of the SHEEF catalog used by Adams and Halchuk (2003) as the basis for the fourth-generation seismic hazard maps of Canada (Note: the fourth-generation maps used data to 1991, but the GSC has since updated the catalog). The SHEEF catalog covers all of the Canadian territory, including earthquakes at a minimum distance of 200 km from the south- western and northwestern boundaries and 300 km from the southeastern boundary.

Table 2-2 List of input catalogs

Catalog	Nickname	Time Period	Minimum Magnitude	Comment
SHEEF	SHEEF08	1600-2008	2.5	The original version (through 1991), later updated through 2008 by the GSC
GSC's CEEF	GSCE	1550-1991	-	Remarkable source of information on reported magnitudes in Eastern Canada
PGC's CEEF	PGCW	1550-1991	-	Primary source of information on reported magnitudes in Western Canada
Ma and Atkinson	MASE	1980-2006	-	High-quality estimates of hypocentral location in eastern North America
Catalog for the Central and Eastern North America	PETE	1700-2006	3.0	The basis for the 2008 update of the U.S. national seismic hazard maps (Central and Eastern US)
Catalog for the Western North America	PETW	1850-2006	4.0	The basis for the 2008 update of the U.S. national seismic hazard maps (Western US)
ANSS	ANSS	2007-2008	2.5	Extension of US database through 2008
Ristau	RIST	1976-2004	3.4	High-quality moment magnitudes for Western Canadian earthquakes

The SHEEF catalog is based on the earthquake epicenter and magnitude information in

GSC's Canadian Earthquake Epicenter File (CEEF), which has been maintained and augmented for about a century (Halchuk 2009). Through the development of the SHEEF catalog, the primary source has been augmented and extended by inclusion of events from various earthquake databases. The procedure of updating and integration of the solutions has resulted in multiple solutions for a single event (S. Halchuk, personal communication 2010).

The updated version of the SHEEF catalog is available online through the GSC's Open File Report 6208 (Halchuk 2009). The report is accompanied by the full solution lines of the database and lists of aftershocks removed from the main database for hazard calculation purposes. It also includes the list of events identified as duplicates by the GSC in late 2009. Our initial investigation uncovered some duplicates still in the full solutions, and we needed to conduct a comprehensive investigation to clean the SHEEF data of replicated information.

We applied a semi-automatic procedure to identify duplicate events in the SHEEF. A set of possible candidate pairs (potential duplicates) was extracted based on the occurrence of the events within the same one-minute time window. Each pair was examined individually; a coincident pair in time is identified as duplicate unless there is a legitimate reason to consider it as two separate events, such as the distance between events or their occurrence within an aftershock sequence. Since the accuracy of earthquake location varies significantly over time and space in the SHEEF data (Halchuk 2009), it was impossible to set automatic criteria for determining the reasonable distance between two separate earthquakes, so we decided subjectively for each pair.

2.4   Composing the earthquake parameters in CCSC

The fundamental idea in the development of the CCSC is to preserve the primary dataset and to enhance and extend it through the inclusion of data from secondary sources. The procedure applied to integrate the information is thoroughly described in the online documentation. In summary, for events common to more than one catalog, we added additional magnitude values to the primary solution based on the availability and quality of data, and for non-common events we added all the information. In some cases (described below), values from a "preferred" secondary source are used to replace those from the primary source. Figure 2.1 shows a general representation of the development procedure and gives the order in which information is processed.

Once we cleaned the SHEEF of duplicate information, we merged the SHEEF and MASE datasets. The MASE catalog focuses on northern Ontario and western Quebec, and provides high-quality hypocenter locations. Therefore, the MASE catalog is preferred for the epicentral location and the depth of eastern events. The GSCE and PGCW provide a rich source of information on additional magnitude estimates (on several different magnitude scales) and we subsequently used them to enhance the completeness of reported magnitude values for eastern and western events, respectively.

As the earthquakes beyond the country's boundaries have the potential to cause damage within Canada (Halchuk 2009), we extended the CCSC using American sources. We used the PETE and PETW as the source of information in the United States; these catalogs were developed for the 2008 update of the U.S. national seismic hazard maps and cover seismicity to the end of 2006. We then supplemented the U.S. database using the ANSS catalog for the period of 2007–2008 inclusive. Next we used the RIST catalog, which provides high-quality moment magnitude values for a suite of western earthquakes, to add in moment magnitude information where available. Each one of the events in the final ensemble is referred to its original database by using the source catalog flags.

Since the seismotectonic setting may have bearing on the moment magnitude conversions (described below), we classified all events according to seismic source zonation. The source zone classification in this study is mainly based on the R model of seismicity published by Adams and Halchuk (2003). We provide a numerical flag in the composite catalog that indicates the assigned seismic source zone. The relation between the numeric flags used in the CCSC and the abbreviation code given by Adams and Halchuk (2003), along with the spatial distribution of each seismic zone, are explained in our online documentation.

Finally, the output database is filtered in space ($-110° \leq$ longitude $\leq -45°$, $35° \leq$ latitude $\leq 80°$) for the eastern region and ($-160° \leq$ longitude $< -110°$, $43.5° \leq$ latitude $\leq 75°$) for the western region, to provide convenient spatial coverage of the composite catalog for further analyses.
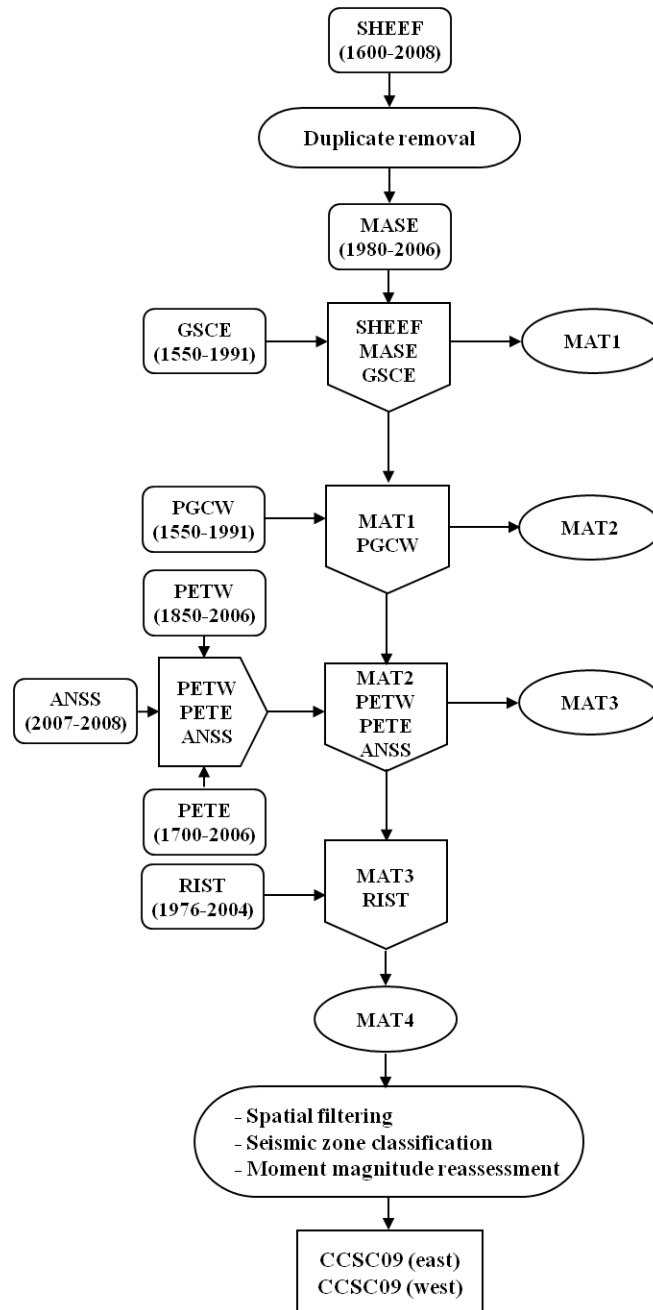
Figure 2-1 Schematic representation of the process used to develop the Canadian Composite Seismicity Catalog (CCSC). MAT1, MAT2, MAT3, and MAT4 are internal ensembles that contain the output from each section of the process.

2.5 Moment magnitude assignment in the CCSC

Current approaches in seismic hazard assessment require the input catalog of seismicity to be unified and homogenized in terms of magnitude, with moment magnitude (**M**) being the

preferred magnitude scale (Johnston 1996; Atkinson and McCartney 2005; Bent 2009; Yadav et al. 2009). For many events, we adopt **M** values from previous special studies, including modeling studies from the literature and moment values from the RIST catalog. For the remaining events, we apply empirical relationships either derived in this study or presented in the literature, between moment magnitude and instrumental magnitude scales (e.g. teleseismic body-wave magnitude *mb*, Nuttli magnitude *MN*, local magnitude *ML*, surface-wave magnitude *MS*, coda magnitude *MC*, and duration magnitude *mD*). We describe these conversions in the following sections.

2.5.1   Moment magnitude for western Canada

The complex seismotectonic setting of western Canada may considerably influence the regional moment magnitude conversions. We divide western Canada into seven subregions for these investigations as given in Table 2.3 and Figure 2.2. The spatial coordinates and details of the subregions are provided in the online documentation.

To derive the conversion relationships, we assumed that the gradient between **M** and any of the other magnitude types is equal to 1.0. Under this assumption, the moment magnitude values are obtained by simply adding a conversion factor to the corresponding reported magnitude:

$$\mathbf{M} = M + \text{Conversion Factor}, \qquad (2.1)$$

where *M* is any instrumental magnitude scale. To test this, we plot the reported **M** values against the different types of magnitude scales, as shown on Figures 2.3 to 2.7. The assumption of slope = 1.0 is supported for *mb*, *MN*, and *ML*, for which the number of **M**-*M* pairs allows the delineation of trends. For these cases, the conversion factors are calculated as the mean value of the residuals (moment magnitude minus instrumental magnitude) for each subregion. It should be noted that the validity of some of the **M**-ML pairs at small magnitudes are questionable based on the linear pattern of data points in the subregions 1, 2, and 3 (Figure 2.5), which arises from questionable information in the source catalogs. For consistency, these values are retained in the composite catalog, but we note that the actual moment magnitudes of these smaller events require further investigation.

As the number of *mb* values is small, we combined the **M**-*mb* data pairs in subregions 2 and 3; both these subregions cover offshore events, and thus the merging of these subregions is reasonable. We also combined the data pairs in subregions 1, 4, 5, 6, and 7 together to increase the amount of data used in conversion factor estimation. For *MN*, the data in all western subregions are combined to derive the **M**-*MN* conversion factor. The *MN* magnitude scale is reported only for the crustal events, so the offshore subregions do not contribute to the estimations in this case. Table 2.4 gives the mean conversion factors, along with their standard deviations, and the number of **M**-*M* data pairs in each subregion for the *mb*, *MN*, and *ML* scales.

There are more than 90 western earthquakes with both **M** and *MC* values reported. However, the validity of some *MC* values in this dataset is questionable (based on the strange pattern of data points in Figure 2.6). For consistency, these values are retained in the composite catalog, but we refrained from deriving an **M**-*MC* conversion relationship. Instead, the regional model proposed by Dewberry and Crosson (1995) is applied for estimating **M** from *MC*:

$$\mathbf{M} = 0.96MC + 0.19 \qquad\qquad (2.2)$$

Equation 2.2 was also used for converting 18 values of *mD* in the western dataset to **M**; these are events from the USGS database (Petersen et al. 2008) that have no reported **M** values. Finally, because the **M**-*MS* data pairs do not follow the model with slope of 1.0 (Figure 2.7), we applied a standard linear regression to derive a relationship between the **M** and *MS* magnitude scales:

$$\mathbf{M} = 0.81MS + 1.3 \qquad\qquad (2.3)$$

The estimated **M** values and the corresponding conversion factors are listed in the CCSC. When a specific conversion model is applied (*MS*, *MC*, and *mD*), the conversion factor listed is the difference between the **M** estimate and the corresponding instrumental magnitude. For *mb*, *MN*, and *ML*, the conversion factors in Table 2.4 are simply added to the instrumental magnitudes.

Table 2-3 Defined subregions of western Canada

Subregion	Expected Event Type [*]	Code for Seismic Source Zones [**]
1	Transition, Shallow	BRO, HECR
2	Offshore, Interface, Transition	EXP, NOFR, OFS, WS2
3	Offshore, Transition	GOA, QCFR, WW
4	Shallow crustal, Interface, Continental	CASR, CST, FHL, ROC, SBC, WSE
5	Continental	DENR, MMB, NBC, RMN, RMS, SOY, WE
6	Interface, Inslab, Continental	ALC, ALI, BFT, NYK, YAK, WNE, WNW
7	Interface, Inslab, Transition	GSP, JDFF, JDFN, WS1

[*] The event type column is just given as a reference and is not used for M assignment in the CCSC (See Atkinson (2005) for more detailed description on the event types in the region).
[**] See the online documentation for more detailed descriptions.

Table 2-4 Western Canada moment magnitude conversion factors (mean ± one standard deviation) for mb, MN, and ML magnitude types and for seismic source subregions as defined in Table 2-3

Subregion	*mb*		*MN*		*ML*	
	Factor ± SD	# Pairs	Factor ± SD	# Pairs	Factor ± SD	# Pairs
1	-0.06 ± 0.31	3	0.05 ± 0.29	0	0.57 ± 0.15	74
2	0.37 ± 0.32	47	0.05 ± 0.29	0	0.63 ± 0.15	1268
3	0.37 ± 0.32	12	0.05 ± 0.29	0	0.55 ± 0.21	251
4	-0.06 ± 0.31	6	0.05 ± 0.29	3	0.12 ± 0.37	36
5	-0.06 ± 0.31	3	0.05 ± 0.29	6	-0.18 ± 0.30	80
6	-0.06 ± 0.31	2	0.05 ± 0.29	1	0.03 ± 0.35	33
7	-0.06 ± 0.31	4	0.05 ± 0.29	0	0.60 ± 0.48	16

SD – Standard deviation
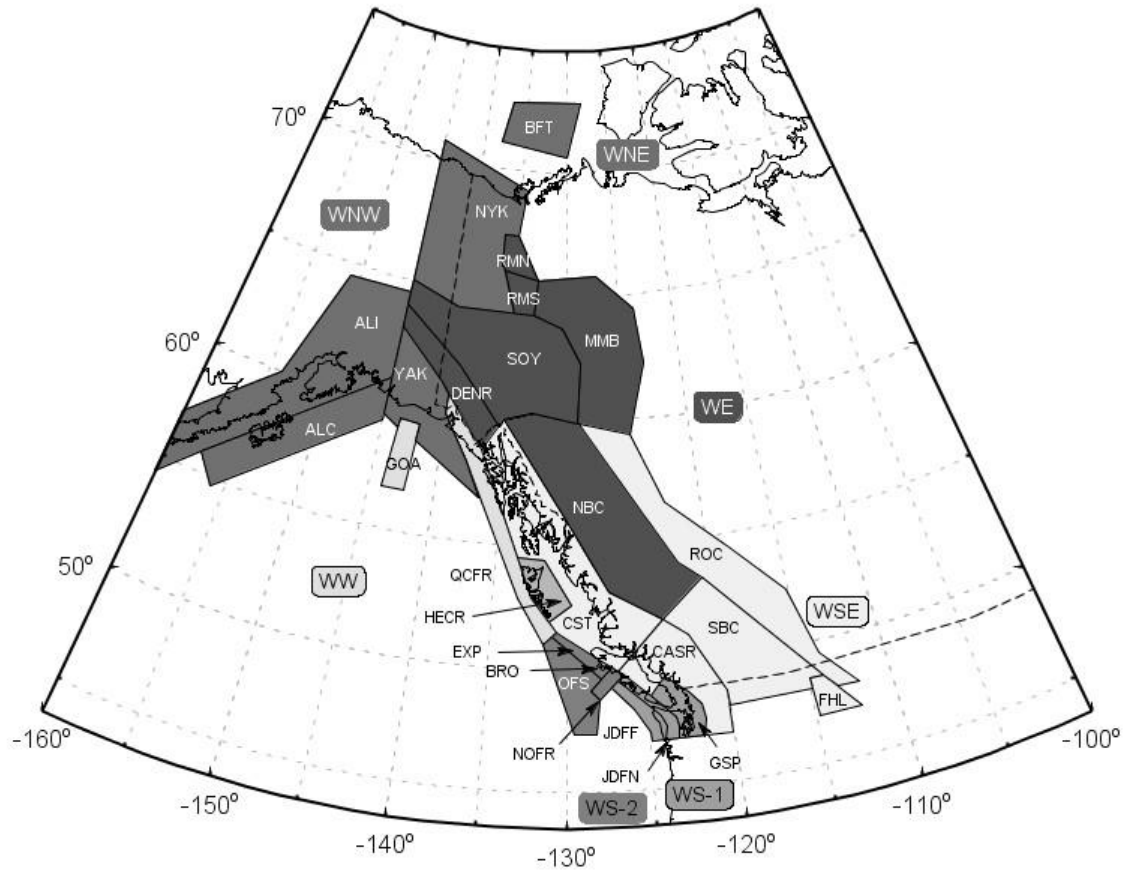
Figure 2-2 Western Canada seismic source zones (Adams and Halchuk 2003) used to classify events included in the CCSC catalog. Shadings identify subregions (used to assign moment magnitude in the catalog) that are described in Table 1-3. Source zones WNE, WE, WSE, WS-1, WS-2, WW, and WNW are extra zones not defined in Adams and Halchuk (2003) that are used to cover the whole region.
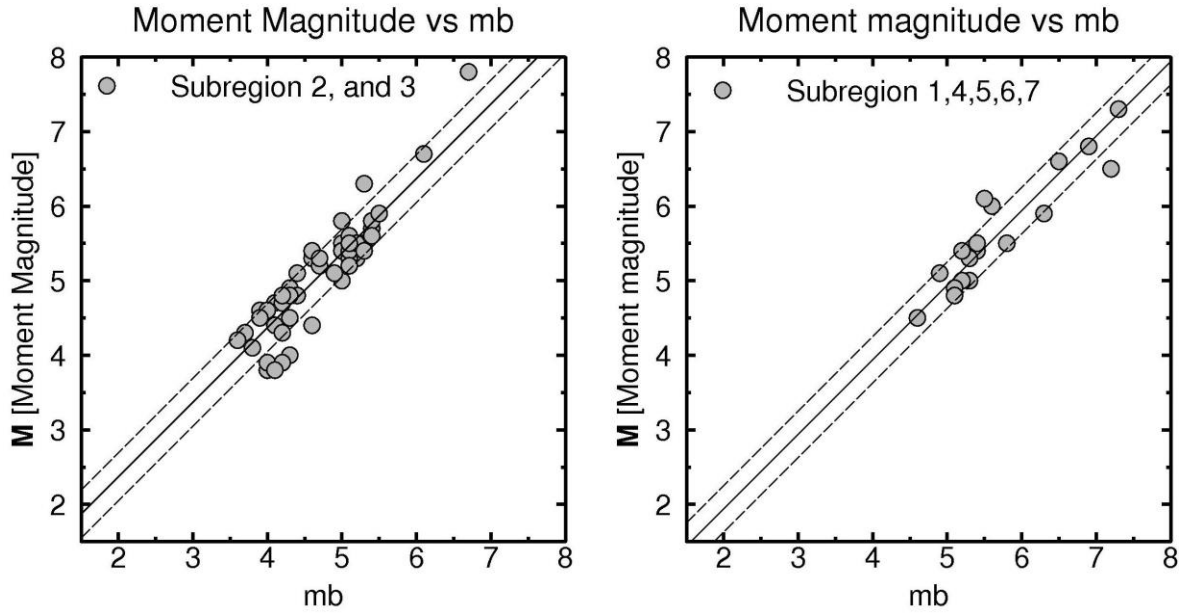
Figure 2-3 Moment magnitude-*mb* data pairs in western Canada. The solid lines are the moment magnitude calibration models derived in this study and dashed lines indicate the 68 percent confidence (±one standard deviation) limits on the models.
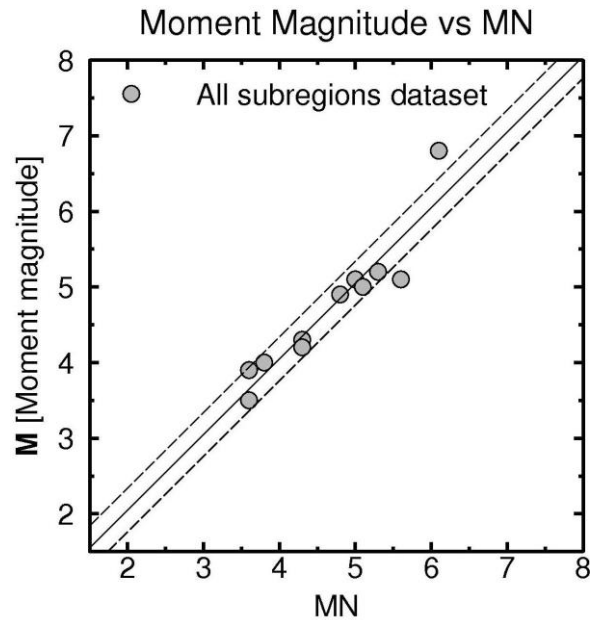
Figure 2-4 Moment magnitude-*MN* data pairs in western Canada. The solid line is the moment magnitude calibration model derived in this study and dashed lines indicate the 68 percent confidence (±one standard deviation) limits on the models.
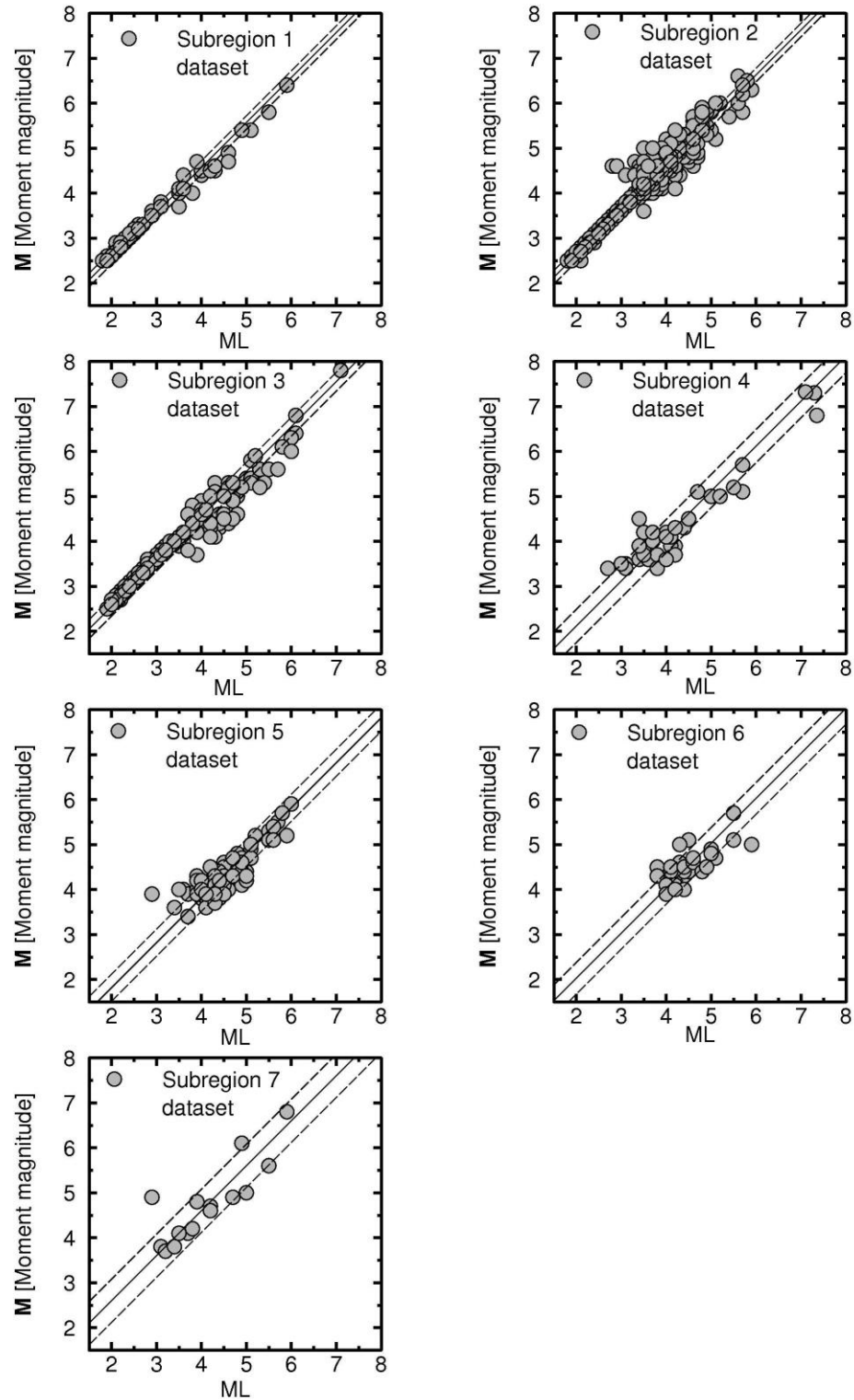
Figure 2-5 Moment magnitude-*ML* data pairs in western Canada. The solid lines are the moment magnitude calibration models derived in this study and dashed lines indicate the 68 percent confidence (±one standard deviation) limits on the models.
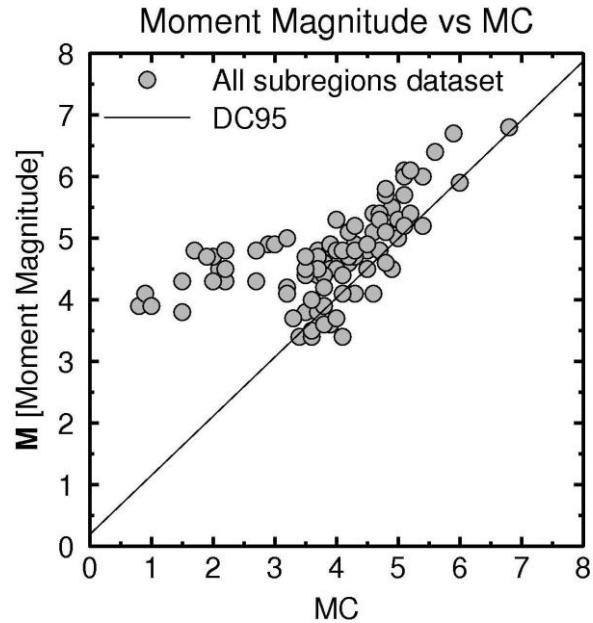
Figure 2-6 Moment magnitude-*MC* data pairs in western Canada; the solid line indicates Dewberry and Crosson (1995) model (DC95).
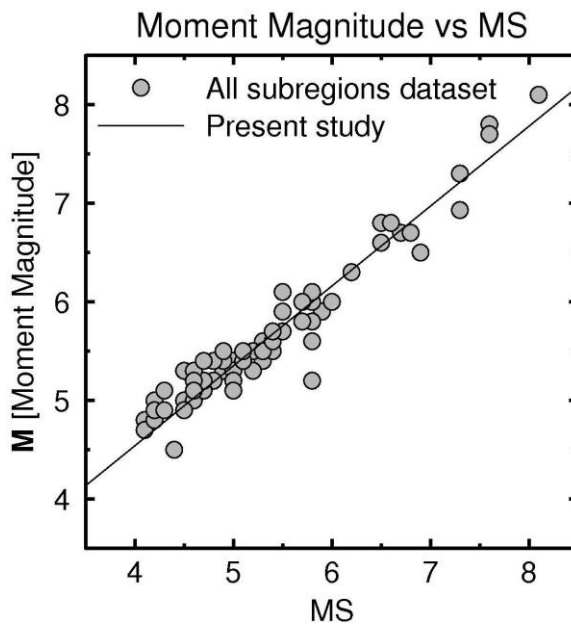
Figure 2-7 Moment magnitude-*MS* data pairs in western Canada; the solid line shows the empirical model derived in the present study.

2.5.2   Moment magnitude for eastern Canada

The number of earthquake events with a reported value of moment magnitude in eastern

Canada is very limited. Therefore, we use published relationships for magnitude conversions. Four different relationships between **M** and different *M* types are applied. Figure 2.8 shows how the applied relationships compare to available data.
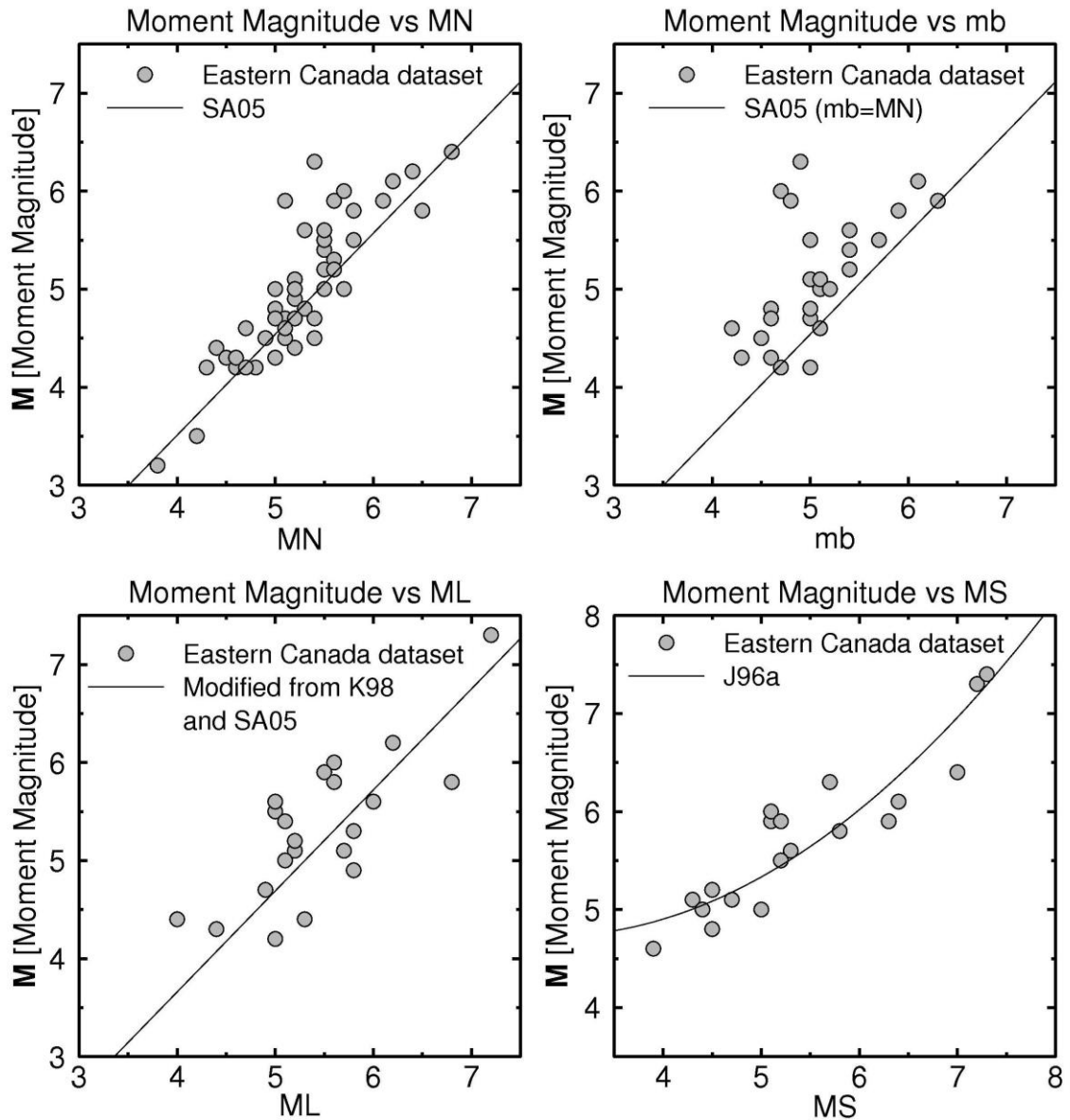
Figure 2-8 Moment magnitude-*M* (different instrumental magnitude types) data pairs in eastern Canada. The solid lines are the adopted moment magnitude conversion models (J96a— Johnston 1996; K98 —Kim 1998; SA05 —Sonley and Atkinson 2005).

For *MN*, we adopted the Sonley and Atkinson (2005) model (Equation 2.4) as the most completely documented equation over all magnitude ranges from 2 to 7:

$$\mathbf{M} = 1.03MN - 0.61 \qquad\qquad (2.4)$$

Because the slope is near unity, the conversion factor from *MN* to **M** is approximately -0.50 units for the *MN* 3 to 5 range over which this equation is commonly applied. The Sonley and Atkinson (2005) model is also assumed to apply for converting *mb* to **M**, under the assumption that *mb = MN*; however, we infer from Figure 2.8 an offset of about 0.2 units between *mb* and **MN** (in terms of its relationship with **M**). Thus one could argue that 0.2 units should be added to any **M** values estimated from mb in eastern Canada; this was not applied in the CCSC09 catalog but may be considered for future revisions.

Kim (1998) developed an *ML* scale for eastern North America (ENA) and explored the differences between *ML* and *MN*. Using the Kim (1998) empirical relationship between *ML-MN*, as well as Equation 2.4, we derived a model for estimating moment magnitude from *ML* values:

$$\mathbf{M} = 1.03ML - 0.46 \qquad\qquad (2.5)$$

This provides a conversion factor of approximately -0.35 units for events in the range of *ML* 3 to 5. For *MC* and *mD*, due to the limited data, we assume *MC = mD = ML*. For *MS*, we applied the regression relation of Johnston (1996) for stable continental regions for estimating **M**. The Johnston (1996) relation can be written as:

$$\mathbf{M} = 5.742 - 0.722MS + 0.128MS^2 \qquad\qquad (2.6)$$

2.6   Adoption of actual moment magnitude values

When **M** is converted from other instrumental magnitudes, the associated uncertainty is generally high. Thus moment magnitudes obtained by other means in previous studies have been adopted in the composite catalog where available. Preference has been given to the values determined by detailed earthquake source studies and moment tensor solutions. The use of Modified Mercalli Intensity (MMI) data in special studies was the second choice; felt data provide a good indication of the overall event size and are likely superior to instrumentally converted values for historical events for which the station coverage was poor and the magnitude determination methods were poorly documented. Two recent sources of moment magnitude values are consulted: Atkinson and Boore (2006) [AB06]

and Bent (2009) [B09]. We adopt the **M** values reported in AB06 except in cases where the B09 study provides new or additional information. The **M** values from these studies have been added to the catalog in the "Mw" column of the file and have been used directly as the assigned **M** value (last column of the catalog). For these events, the conversion factors are simply zeroes. For events from the B09 catalog for which we adopted Bent's moment magnitude estimate based on intensity (rather than a direct estimate of moment), we have changed the preferred magnitude type to be denoted as "*MI*" and used Bent's estimated moment magnitude as the assigned **M** value (last column of the catalog); however, these converted estimates of **M** do not appear in the "Mw" column in the catalog because they are not true values of moment magnitude. The process described above ends with the **M** assignment for each event and the generation and recovery of the two output files, ccsc09west.txt and ccsc09east.txt.

2.7 Overview of CCSC output files

The compiled information in the CCSC is contained in two separate catalogs. The spatial coverage of the catalogs is as follows:

CCSCwest: [−160° ≤ longitude < −110°] and [43.5° ≤ latitude ≤ 75°]

CCSCeast: [−110° ≤ longitude ≤ −45°] and [35° ≤ latitude ≤ 80°]

The CCSC09west and CCSC09east include more than 26,700 and 9,200 earthquakes from the period of 1700 and 1550 through December 2008, respectively. The catalog files contain 24 fields.

The CCSC catalog is available for download at http://www.seismotoolbox.ca/Catalogs.html as two space-delimited ascii files (ccsc09west.txt and ccsc09east.txt). It is also accompanied by comprehensive documentation (CCSC09.doc), which describes the compilation process of the CCSC in more detail. We plan to update the composite catalog periodically and post the updated versions online (CCSC10, etc.). Figures 2.9 and 2.10 show the earthquakes in the CCSC09 with moment magnitude of 2.5 or greater in the vicinity of major cities in western and eastern Canada, respectively.

It should be noted that we have included the data in the CCSC as provided in the source catalogs, with no set magnitude range in event selection. Consequently, it is recommended that the user should apply a magnitude completeness analysis to determine the threshold magnitude in the catalog over time and space, as required for the user's purposes.

Figure 2.11 uses the CCSC to show the frequency magnitude distribution of seismicity at different time periods in the Charlevoix Seismic Zone of Quebec, which is the area of interest in this thesis. The change in catalog completeness over time is apparent in the plot, and discussed in more detail in the next chapter.

Additionally, we acknowledge that the process of integrating information from several sources has probably resulted in the inclusion of some ghost events in the composite catalogs. The term "ghost" refer to an earthquake that is reported in the seismic catalogs, but is not really an earthquake, just an erroneous interpretation of some report. An example in eastern Canada is the earthquake of 1534 which is currently listed in the composite catalog as an entry. Gouin (1994) showed that this event was entirely fictitious and, consequently, should be removed from earthquake catalogs.
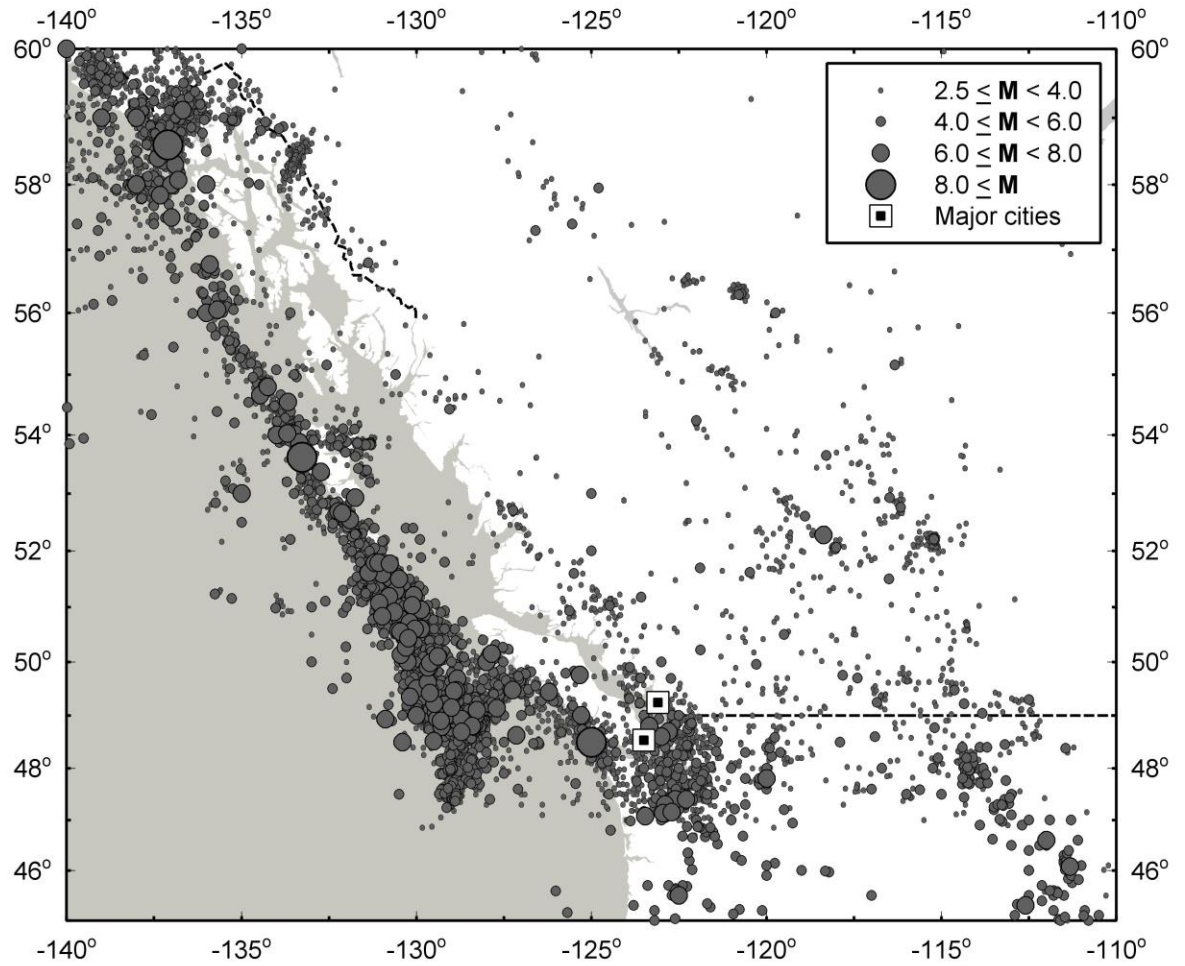
Figure 2-9 Earthquakes in the CCSC09 west catalog. All earthquakes with moment magnitude of 2.5 and greater are included in the western coastal region. Victoria (left) and Vancouver (right) are also marked on the map.
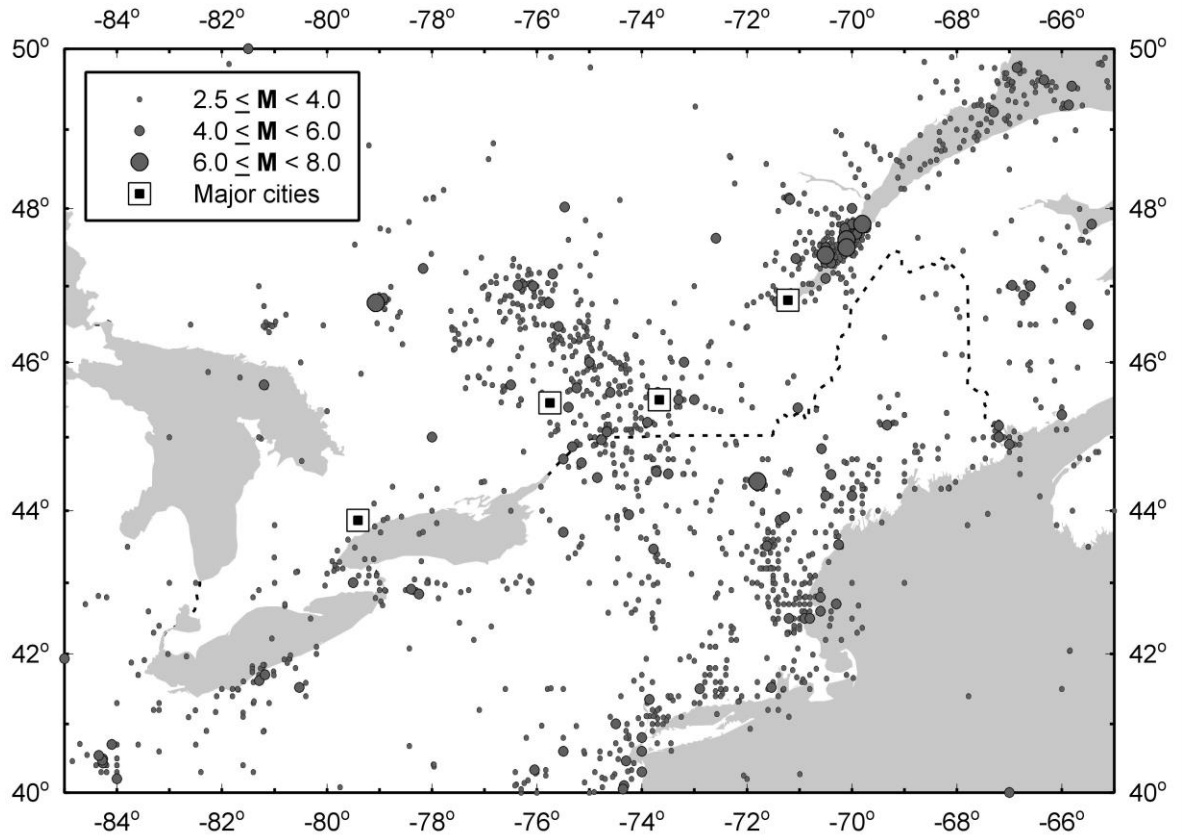
Figure 2-10 Earthquakes in the CCSC09 east catalog. All the earthquakes with moment magnitude of 2.5 or greater in the vicinity of four major cities in eastern Canada are included (from left to right: Toronto, Ottawa, Montreal, and Quebec City).
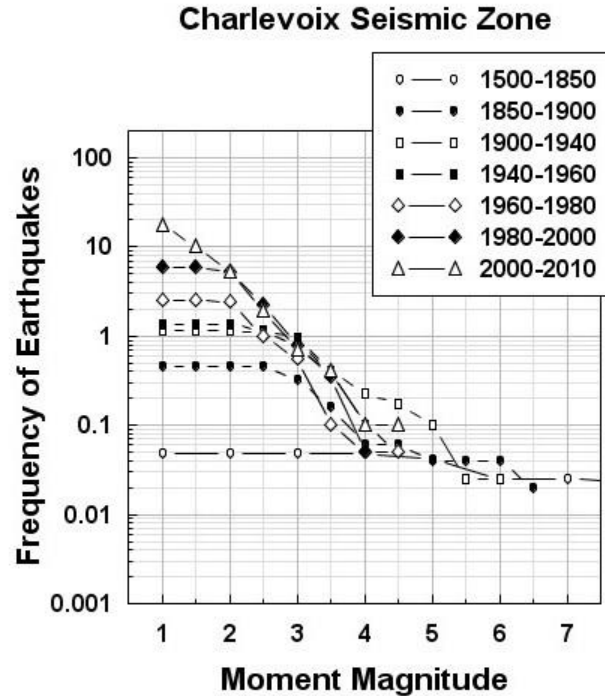
2-11 Observed cumulative annual frequency of earthquake occurrence for the events in Charlevoix seismic zone in various time intervals.

2.8 Summary

We have developed the Canadian Composite Seismicity Catalog (CCSC) for use in hazard studies in Canada. For each event, all available magnitude types, including *mb*, *MN*, *ML*, *MS*, *MC*, *mD*, and **M** are compiled, and a preferred estimate of moment magnitude is assigned depending on the availability and the quality of data.

The CCSC was largely compiled through an automatic procedure, but required manual judgment in selection of the preferred earthquake characterizations. We have applied our best efforts to associate the most complete and reliable information in the composite catalog. However, we acknowledge that the CCSC contains incomplete and uncertain information; this is unavoidable in the creation of a composite catalog.

2.9 References

Adams, J., & Halchuk, S. (2003). Fourth generation seismic hazard maps of Canada: Values for over 650 Canadian localities intended for the 2005 National Building Code of

Canada. *Geological Survey of Canada, Open File 4459* , 155 p.

Atkinson, G. M. (2005). Ground motions for earthquakes in South-western British Columbia and North-western Washington: crustal, in-slab, and offshore events. *Bulletin of the Seismological Society of America* **95**, 1027-1044.

Atkinson, G. M., & Boore, D. M. (2006). Earthquake ground motion prediction equations for eastern North America. *Bulletin of the Seismological Society of America* **96**, 2181-2205.

Atkinson, G. M., & McCartney, S. (2005). A revised magnitude-recurrence relation for shallow crustal earthquakes in southwestern British Colombia, considering the relationship between moment magnitude and regional magnitude scales. *Bulletin of the Seismological Society of America 95, 334-340.*

Bent, A. L. (2009). A moment magnitude catalog for the 150 largest eastern Canadian earthquakes. *Geological Survey of Canada, Open File 6080* , 23p.

Dewberry, S., & Crosson, R. (1995). Source scaling and moment estimation for the Pacific Northwest seismograph network using S-Coda amplitudes. *Bulletin of the Seismological Society of America* **85** , 1309-1326.

Halchuk, S. (2009). Seismic Hazard Earthquake Epicenter File (SHEEF) used in the fourth generation seismic hazard maps of Canada. *Geological Survey of Canada, Open File 6208* , 15p.

Johnston, A. C. (1996). Seismic moment assessment of earthquakes in stable continental-I. Instrumental seismicity. *Geophysical Journal International* **124** , 381-414.

Kim, W. Y. (1998). The ML scale in eastern North America. *Bulletin of the Seismological Society of America* **88** , 935-951.

Ma, S., & Atkinson, G. M. (2006). Focal depths for small to moderate earthquakes (MN $\geq$ 2.8) in western Quebec, southern Ontario, and northern New York. *Bulletin of the Seismological Society of America* **96** , 609-623.

Petersen, M., Frankel, A., Harmsen, S., Mueller, C., Haller, K., Wheeler, R., Wesson R., Zeng Y., Boyd O., Perkins D., Luco N., Field E., Wills C., and Rukstales K. (2008). Documentation for the 2008 Update of the United States National Seismic Hazard Maps. *U.S. Geological Survey, Open-File Report 2008-1128*, 61p.

Ristau, J. (2004). Seismotectonics of western Canada from regional moment tensor analysis, Ph.D. dissertation. School of Earth and Ocean Sciences, University of Victoria,

Biritish Columbia.

Sonley, E., & Atkinson, G. M. (2005). Empirical relationship between moment magnitude and Nuttli magnitude for small-magnitude earthquakes in South-eastern Canada. *Seismological Research Letters* **76**, 752-755.

Woessner, J., & Weimer, S. (2005). Assessing the quality of earthqauke catalogs: Estimating the magnitude of completeness and its uncertanity. *Bulletin of the Seismological Society of America* **95** , 684-698.

Yadav, R. B.S., Bormann, P., Rastogi, B. K., Das, M. C., and Chopra S (2009). A homogenous and complete earthquake catalog for northeast India and the adjoining region. *Seismological Research Letters* **80(4),** 609-627.

Chapter 3

3   Aftershock statistics for earthquakes in the St. Lawrence Valley[3]

Understanding the behavior of aftershock sequences is important to obtain a reliable evaluation of seismic hazard. It has been hypothesized that in continental intraplate regions, such as eastern Canada, aftershock sequences may persist for hundreds of years following a strong mainshock. In this study, we statistically characterize the behavior of aftershocks in the St. Lawrence Valley, the most seismically active region in eastern Canada. The observed aftershocks of moderate recent earthquakes in the region are used to calibrate the parameters of the Reasenberg and Jones aftershock decay model. The average values found for the region fall in the range of the corresponding values of the parameters for earthquakes in California; however, the aftershock sequences in eastern Canada are less energetic on average, and one event (the 1982 Miramichi earthquake) had a longer-than-average aftershock sequence. We use aftershock models for the region, considering the range of parameters obtained from the moderate events, as well as the corresponding parameters for a generic California model, to compute the expected activity rates in the area of the 1663 Charlevoix earthquake, in order to gain insight into how much of the contemporary activity might be considered part of a prolonged aftershock sequence. We conclude it is very unlikely that contemporary seismicity in Charlevoix represents aftershocks from the 1663 earthquake.

3.1   Introduction

Sequences of aftershocks commonly follow moderate-to-large earthquakes. It is widely accepted that the aftershock activity dies off with time, after which the level of background or normal activity resumes in the focal area. At plate boundaries, the transition from decaying aftershock to normal activity generally occurs within tens of years after the mainshock. However, in slowly deforming continental regions such as eastern North America, it has been

---

[3] A version of this chapter has been published for publication in *Seismological Research Letters*. Fereidoni, A., Atkinson, G. M., Aftershock statistics for earthquakes in the St. Lawrence Valley. *Seismological Research Letters*, September/October 2014, v. 85, p. 1125-1136, doi:10.1785/0220140042

suggested that the aftershock sequences may be hundreds to thousands of years in duration (Basham and Adams, 1983; Basham, 1989; Ebel et al, 2000; Ma and Eaton, 2007; Stein and Liu, 2009).
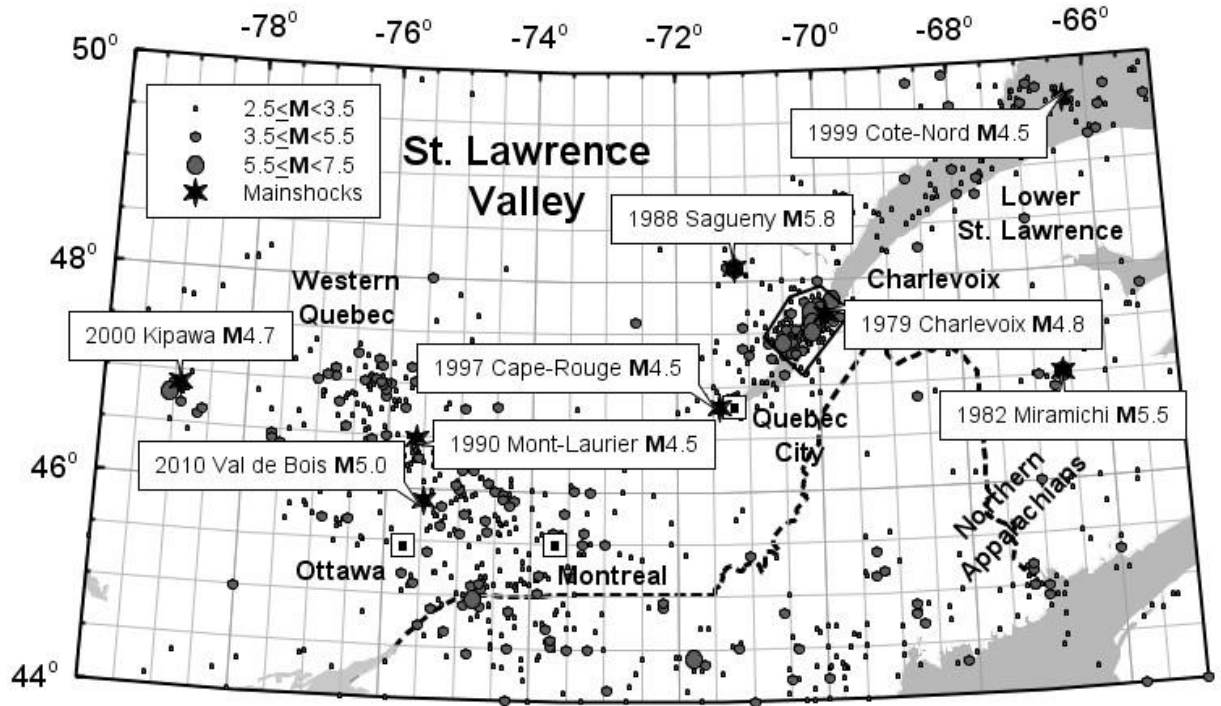
Figure 3-1 Earthquakes of the St. Lawrence region, from the CCSC catalog. The major clusters of the seismicity in southeastern Canada according to Basham and Adams (1989) are marked along with the epicenter of the earthquakes in Table 3-1.

In this study, we focus on aftershock activity in the St. Lawrence Valley, the most seismically active region in eastern Canada, as illustrated in Figure 3.1. Currently, hundreds of earthquakes are recorded there every year, though most of them are too small to be felt. Historically, the zone has experienced several damaging earthquakes in the magnitude (M) 6 to 7 range. There is a widely-discussed hypothesis that contemporary clusters of seismicity in the St. Lawrence region represent the long aftershock sequences of previous large earthquakes. Recognizing such long aftershock sequences is crucial for seismic hazard evaluations, in order to avoid potential overestimation of hazard in contemporary seismicity clusters and underestimation elsewhere (Stein and Liu, 2009). Although the long-lived aftershock hypothesis for eastern North America has been discussed since the 1980's, it is only recently that rigorous statistical studies have been undertaken. Fereidoni and Atkinson

(2012) and Page and Hough (2014) statistically studied the seismicity in the Charlevoix seismic zone and the New Madrid seismic zone, respectively, to investigate whether the current seismicity in the focal regions of past large earthquakes follow the well-known aftershock decaying models.

There have been a few studies of the temporal decay rate of aftershocks in continental intraplate regions. For example, Ebel et al (2000) and Ebel (2009) investigated the statistics of intraplate aftershock sequences around the world by uniformly processing the observed aftershock activities on a global basis. In this study, we focus specifically on the temporal behavior of aftershocks in the St. Lawrence Valley. We aim to achieve a better understanding of the contemporary seismicity in the region by statistically analyzing the aftershock sequences in this active intraplate region.

Significant historic earthquakes in the St. Lawrence region include the following events (where **M** is moment magnitude and mN is Nuttli magnitude): 1663 **M**7 Charlevoix, 1732 mN5.8 near Montreal, 1791 **M**5.5 Charlevoix, 1860 **M**6.1 Charlevoix, 1870 **M**6.6 Charlevoix, and 1925 **M**6.4 Charlevoix (Basham et al, 1982; Fereidoni et al, 2012). Quantifying the aftershock behavior of these sequences is important to the interpretation of seismicity in the region. However, the task is subject to considerable uncertainty, because the available catalogues of aftershocks following the larger historic events (e.g. Smith, 1962; Ebel, 1996; Gouin, 2001) are not complete at small magnitudes.

In this study we seek to improve our understanding of aftershock decay patterns in the region by first analyzing aftershock sequences of recent significant earthquakes for which reliable catalogs are available. We can then use the representative aftershock parameters for the region to compute the expected number of major aftershocks following the 1663 earthquake. The comparison of the predicted rate with the observed activity can shed new light on the duration of the aftershock sequence of this significant event. The process of aftershock generation is thought to be governed by regional geology and physical conditions of the fault zone. Therefore, the uniform and consistent analysis of recent aftershock activities can provide useful insights into the temporal features of sequences expected for the region as a whole (e. g. Utsu et al, 1995; Kisslinger, 1996; Ogata, 1999).

The results of our analysis have important implications for seismic hazard in the region. For

example, in conventional probabilistic seismic hazard assessment, the assumption of a Poissonian distribution of earthquakes necessitates the removal of aftershocks clusters (dependent events) from seismicity catalogs, requiring identification of such events. Moreover, the knowledge of average behavior of aftershocks in the region can be used to assess the probability of seismic activity following a large mainshock. Therefore knowledge of regional aftershock decay parameters provides useful information for long-term and short-term hazard assessment.

3.2 Method of analysis

There are several empirical relations that characterize the distribution of aftershocks in time, space, and magnitude. The temporal decay of aftershock activity is commonly modeled by the modified Omori relation (Utsu 1961). The Gutenberg-Richter relation can be used to characterize the magnitude distribution of aftershocks in a sequence (Gutenberg and Richter, 1954). These empirical relations have been used widely to study the behavior of aftershocks worldwide (e.g. Reasenberg and Jones, 1989; Felzer et al, 2004; Ebel, 2009; Shcherbakov et al, 2013). Reasenberg and Jones (1989) unified these relations to obtain a more complete characterization of aftershock decay rate as a function of time and magnitude. The resulting relationship provides a consistent framework for forecasting occurrence rate of aftershocks following a mainshock with a given magnitude. In our study, we aim to calibrate the aftershock parameters included in the Reasenberg and Jones (1989) model for the St. Lawrence Valley by analyzing the aftershock sequences of recent significant earthquakes in the region.

We begin our analysis by considering the temporal decay of aftershock activity after a large earthquake, which may be modeled by the modified Omori relation (Utsu, 1961):

$$N(t) = K(t + c)^{-p} \qquad\qquad (3.1)$$

where, $N(t)$, the rate function, is the frequency of aftershock per unit time (1 day, 1 months, etc) at time t after the mainshock, and K, c, p are constant parameters to be determined. The parameter p controls the decay of aftershock activity with time, and is thought to reflect the physical conditions of the fault zone (Kisslinger, 1996; Ogata, 1999). The constant c eliminates the uniqueness of occurrence rate at time zero, and is introduced in the formula to

compensate for the fact that the early part of an aftershock sequence often is not well modeled by a regular decay rate (Kisslinger, 1996). The productivity constant, K, is a normalizing parameter that depends on the total number of aftershocks.

In terms of magnitude distribution, an aftershock sequence can be modeled following the Gutenberg-Richter relation (Gutenberg and Richter, 1954), $N(M) = A10^{-bM}$, where $N(M)$ is the cumulative number of events with magnitude M or larger. A more complete description of aftershock decay rate can be presented by combining the modified Omori relation with Gutenberg-Richter relation, in which the aftershock productivity constant can be written as a function of the mainshock magnitude, M_m, and the aftershock magnitude, M:

$$K = 10^{a+b(M_m-M)} \tag{3.2}$$

Reasenberg and Jones (1989) proposed the following form of aftershock rate function:

$$\lambda(t, M) = 10^{a+b(M_m-M)}(t + c)^{-p} \tag{3.3}$$

where λ is the rate of aftershocks with magnitude equal to or greater than M at time t after the mainshock of magnitude M_m, p is the decay constant from modified Omori relation, b is the b-value from Gutenberg-Richter relation, and a is a constant that controls the productivity of the sequence. They used this form of Omori's relation to parameterize the aftershock sequences in California. By averaging parameter values over the events in their dataset, they obtain values of $a = 1.67$, $b = 0.91$, and $c = 0.05$ for generic aftershock sequences in California.

We carry out two separate steps to estimate the aftershock parameters in the Reasenberg and Jones formulation for each aftershock sequence in the St. Lawrence Valley. In the first step, we use the Ogata (1983) method to compute the maximum likelihood estimation (MLE) of the K, and p parameters in the modified Omori relation, with the c parameter held fixed. We choose to constrain the c parameter, using the generic value of 0.05 reported by Reasenberg and Jones (1989), because the numbers of aftershocks in the early hours of each sequence are insufficient to robustly determine this parameter. Using the Ogata (1983) method, it is possible to simultaneously obtain the standard error of the maximum likelihood estimates of the aftershock parameters. The standard error of the MLE parameters is obtained by taking

the square root of the corresponding diagonal elements of the inverse Fisher information matrix (Ogata, 1983).

The *b*-value in the Gutenberg-Richter relation can be estimated using the maximum likelihood method, or simply by visual inspection of the frequency-magnitude distribution of aftershock sequences, provided there are sufficient numbers of events. In our case, most of the observed sequences in the St. Lawrence Valley have relatively small numbers of aftershocks, which necessarily translates into uncertainty in the estimation of *b* for these sequences. We therefore choose to constrain the *b*-value in Equations 3.2 and 3.3 using typical published values for the region. For this purpose, we compile a list of published *b*-values for sequences in the region, as well as for other available aftershock parameters from previous studies. Once *b* and *K* are known, one can compute the *a*-value using Equation 3.3.

3.3 Database for analysis

We use the Canadian Composite Seismicity Catalog (CCSC, Fereidoni *et al.*, 2012) as the primary source of information in our analysis. The composite catalog provides an up-to-date and complete earthquake data in the study area, and has the advantage of being homogenized in terms of moment magnitude (**M**). Although all the currently used magnitude scales (e.g. local magnitudes ML, body wave magnitude mb, Nuttli magnitude mN, surface-wave magnitude MS, moment magnitude **M**) were intended to yield consistent results, the difference in magnitude value between different scales could be about $\pm$ 0.5 units or greater (for example see Fereidoni *et al*, 2012). In particular, mN is typically about 0.5 units higher than **M** for small-to-moderate events. It is therefore useful to unify all magnitudes with respect to one scale, with moment magnitude being the preferred scale in most modern earthquake catalogs (*e.g*. US Geological Survey catalogs).

We extend the time period of the catalog to 2011 by adding data from the Geological Survey of Canada's (GSC) National Earthquake Database. The CCSC was developed primarily for earthquake hazard assessment purposes; therefore, in this catalog aftershock data at smaller magnitudes are generally insufficient for robust estimation of aftershock parameters of the modified Omori relation. We further enhance the aftershock records in our dataset by including the data from a number of published studies containing information on specific

aftershock sequences. To maintain consistency in the dataset, all magnitudes from additional data sources are converted to moment magnitude, if applicable, using the same conversion applied in Fereidoni *et al*. (2012).

To obtain the rate of aftershock activity in the St. Lawrence Valley we develop a list of recent mainshock-aftershock sequences in the region by searching for eligible mainshocks in the Canadian composite catalog. We limit our selection to those mainshocks for which aftershock activity has been well-monitored by a permanent or portable seismic network. This criterion ensures that for each sequence we have a relatively complete list of aftershocks down to small magnitudes. Table 3.1 provides an initial list of 8 eligible events in the study area; the magnitude of the mainshocks ranges from **M**4.5-**M**5.8. The geographical distribution of these events is shown in Figure 3.1.

Table 3-1 List of recent significant mainshocks in the St. Lawrence valley from CCSC

Event	Date	Latitude	Longitude	Time (UT)	Depth (km)	M	Comment
Val des Bois	2010/06/23	45.88	-75.48	17:41:41	22	5.0	
Kipawa	2000/01/01	46.88	-78.92	11:22:57	12	4.7	Low aftershock activity [1]
Cote-Nord	1999/03/16	49.61	-66.32	12:50:48	20	4.5	
Cape-Rouge	1997/11/06	46.80	-71.41	2:34:33	22	4.5	Low aftershock activity [2]
Mont-Laurier	1990/10/19	46.47	-75.59	7:01:57	11	4.5	
Saguenay	1988/11/25	48.12	-71.18	23:46:04	29	5.8	Low aftershock activity [3]
Miramichi	1982/01/09	47.00	-66.60	12:53:00	7	5.5	
Charlevoix	1979/08/19	47.67	-69.90	22:49:31	10	4.8	Low aftershock activity [4]

[1] Bent et al (2002)
[2] Nadeau et al (1998)
[3] Du Beger et al (1991)
[4] Hasegawa and Wetmilller (1980)

In the next stage, a more detailed event selection is carried out to eliminate sequences with low aftershock activity for which parameters cannot be reliably determined. Four of the mainshocks (2010 Val des Bois, 1999 Cote-Nord, 1990 Mont-Laurier, and 1982 Miramichi)

had active aftershock sequences, while the other four (2000 Kipawa, 1997 Cape-Rouge, 1988 Saguenay, and 1979 Charlevoix) did not. The small number of events in the latter four sequences would necessarily translate into large uncertainty in the estimation of their aftershock parameters. We therefore focus our analysis on the four events with the most productive aftershock sequences. However, we consider later in the manuscript the effect that inclusion of the other less-productive events might have on our overall conclusions regarding typical aftershock parameters.

3.4 Aftershock parameters in the St. Lawrence Valley

The temporal decay rate of aftershocks in the St. Lawrence region is analyzed by determining the parameters in the Reasenberg and Jones (1989) model for the aftershock sequences of the 2010 Val des Bois **M**5.0, 1999 Cote-Nord **M**4.5, 1990 Mont-Laurier **M**4.5, and 1982 Miramichi **M**5.5 events. We use the maximum likelihood method of Ogata (1983) to determine the parameters of the Omori relation for each sequence (parameters K and p with parameter c fixed at 0.05) and their 95% confidence intervals. After obtaining the parameter K, we select appropriate b-values from published studies for each sequence, and then compute the parameter a in Equation 3.3. The results of the analysis are presented in this section separately for each sequence. Later, we discuss the variation of the parameters, and compare them to the statistics for these parameters computed by Reasenberg and Jones (1989) for California sequences.

The aftershock sequence of the 2010 Val des Bois earthquake- has the most recent and complete data among the events studied here. The sequence occurred inside the Western Quebec (WQU) seismic zone (Adams and Basham, 1989), which encloses the Ottawa Valley from Montreal to Timiskaming; the region is monitored by a network of local stations from the Canadian National Seismic Network (CNSN). With the current permanent network, all earthquakes larger than about Nuttli magnitude (mN) 1.7 (corresponding to moment magnitude **M**~1.2; see Fereidoni *et al*., 2012) would be detected by the network and located by the analysis of the Geological Survey of Canada (Lamontagne, 2013; personal communication). In the hours following the mainshock, a portable seismographic network was installed by the GSC to record aftershocks, further lowering the magnitude of completeness. More than 200 aftershocks were located during the three months following the

event. We analyze the aftershock sequence of the Val des Bois earthquake using the data from GSC's National Earthquake Database, which includes the aftershock records from the temporary network. Figure 3.2(a) provides a log-log plot of the number of events per day against time. The curve fitted to the data points is drawn using the maximum likelihood estimate (MLE) of the parameters: $K = 7.44 \pm 2.27$, $p = 1.41 \pm 0.17$ with c constrained at 0.05 as noted previously. Visual inspection suggests that the aftershock decay sequence for the Val des Bois is well-represented by the derived Omori model. Moreover, the Omori parameters are consistent with those obtained for the same sequence by Ma and Motazedian (2012).
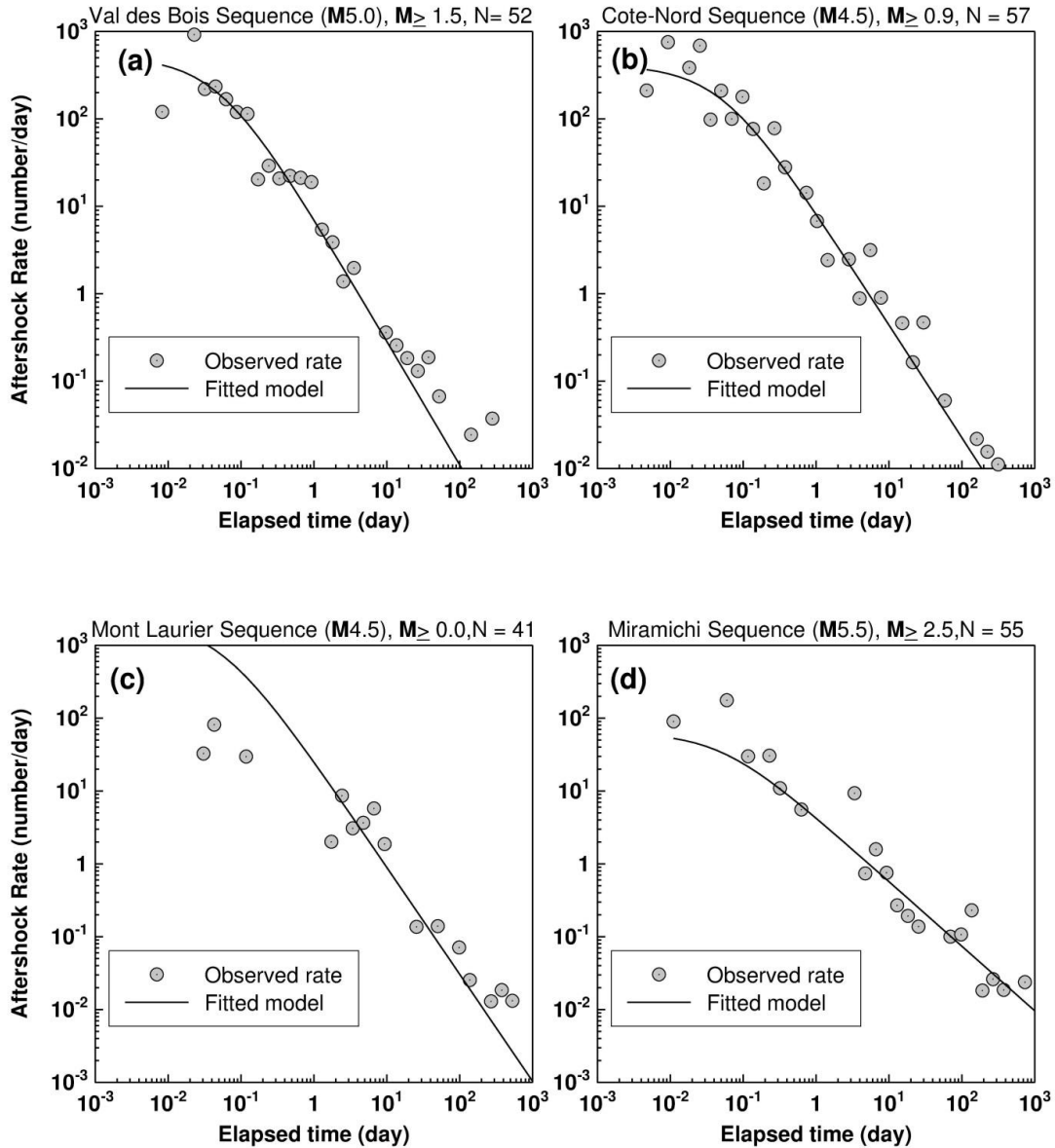
Figure 3-2 log-log plot of the number of events per day against time for aftershock sequences in Table 3-2. The curve fitted to the data points is drawn using the maximum likelihood estimate of the *K* and *p* parameters, with *c* constrained.

The aftershock sequence of the 1999 Cote-Nord earthquake-is one the most active sequences ever recorded in eastern Canada, considering its moderate magnitude (**M**4.5). Its focal region lies within the Lower St. Lawrence seismic zone (LSZ), which was defined based on a clustering of earthquakes under the estuary of the St. Lawrence River. Since 1991 the Geological Survey of Canada has monitored the seismicity of the LSZ with a good regional

seismic network. Considering the distribution of the seismic stations, every earthquake with mN ≥ 2.0 would be located by the network (Lamontagne et al, 2004). However, following the 1999 Cote-Nord earthquake, an analyst from GSC carefully scanned the continuous recordings of the closest station in the focal area to ensure all aftershocks equal to or greater than mN1.5 (~**M**0.9) were detected (Lamontagne et al, 2004). Using the list of aftershocks reported in Lamontagne *et al* (2004), we compute the values of $K = 8.61 \pm 2.45$, $p = 1.29 \pm 0.16$, while the c parameter is held fixed at 0.05. The distribution of the aftershocks in time is shown in Figure 3.2(b). Our estimation of the temporal aftershock parameters is consistent with characterization of the sequence in the work of Lamontagne *et al* (2004) with $K = 7.83$, $p = 1.34$, $c = 0.03$, and $b = 0.97 \pm 0.17$.

The 1990 Mont-Laurier Earthquake- occurred inside the Western Quebec seismic zone. Its aftershock sequence was recorded by the GSC, with the permanent network being enhanced by a portable seismic network deployed in the epicentral area following the mainshock. Proximity of the event to the closest station of GSC's permanent network ensures the detection of earthquakes with magnitude larger than ML0.0 (or **M**~-0.61) (Lamontagne *et al* 1994). Using the aftershock data from GSC's catalog, we obtain $K = 26.75 \pm 15.61$, $p = 1.47 \pm 0.22$, while c is constrained at 0.05. The frequency of aftershocks and the fitted Omori model are shown in Figure 3.2(c). One might argue that fixing the c-value at 0.05 might not be an appropriate approach for the Mont-Laurier sequence, as the observed data apparently show a c-value that is significantly higher than that assumed in this study. As very careful observation of aftershock activity did not started immediately after the mainshock, it is difficult to estimate the true c-value for this sequence. The apparent high c-value in the Mont-Laurier sequence may partially reflect the effect of incomplete detection of aftershocks shortly after the mainshock. There is an alternative interpretation in Shcherbakov et al (2004) and Shcherbakov and Turcotte (2006) which proposes that the c-value in the modified Omori formula is not constant and scales with the magnitude cutoff t of the data set, this could be the case for the Mont-Laurier sequence for which we considered $M_c = 0$. However, Enescu et al (2009) argue that the physical scaling proposed in these papers is the effect of the incomplete aftershock data (see also Kagan, 2004).For this reason, we disregard the early stage of the aftershock sequence and calculate the aftershock parameters based on the most complete part of the data (after 1.375 days). We have also tested our parameters by not

considering the *c*-value as a fixed parameter. Although there is difference in the *c*-values between suchcases, the decay rate (*p*-value) which is of particular importance in our study shows no significant difference. We use the results of the fixed *c*-value as the obtained parameters have smaller uncertainty and are more consistent with parameters from other sequences.

The aftershock sequence of the 1982 Miramichi earthquake- represents a notable earthquake sequence, both in regards to the duration of the aftershock activity and the significant size of the events (Burke *et al*, 1989). The epicentral region is situated in the Northern Appalachian seismic zone, which includes most of New Brunswick and extends into New England. For years following the mainshock, the GSC monitored the continuing aftershock activity of the sequence by a permanent seismograph station in close proximity, and by other stations of the regional network. In addition to the monitoring of activity by the permanent network, GSC conducted aftershock studies using portable seismic stations over several time periods (Wetmiller *et al*, 1984; Burke *et al*, 1989). Using data from the temporary field network, Wetmiller *et al* (1984) reported that the Miramichi sequence had a frequency magnitude distribution (*b*=0.7) similar to the regional distribution. They computed the value of $p = 0.8$ for the aftershock decay parameter, and concluded that the aftershock activity of the Miramichi sequence decayed slower than typical aftershock sequences (which have *p*-values larger than 1). Another study of the Miramichi aftershock sequence by Ebel *et al* (2000) gives the value of 1.01 for the *p* parameter. In our analysis, we use the GSC's catalog and compute the characteristic aftershock parameters for the Miramichi sequence: $K = 4.42 \pm 1.69$, $p = 0.89 \pm 0.10$. Our estimation of the *p* parameter is comparable to the value determined by Wetmiller *et al* (1984), and is slightly smaller than that determined by Ebel *et al* (2000).

We next use Equation 3.2 and the published *b*-values for each sequence to compute the *a* parameter in the Reasenberg and Jones (1989) formulation. Table 3.2 lists the *a*, *b*, and *p* parameters as well as the threshold magnitude considered for each sequence in our analysis. While one might argue that there are too few samples to compute reliable average regional parameters for the St. Lawrence Valley, the parameters from Table 3.2 can at least be

compared with statistics for these parameters in California. Figure 3.3 presents this comparison.

All of the aftershock parameters found for the four St. Lawrence aftershock sequences in this study fall within the range of values reported by Reasenberg and Jones (1989) for the sequences from California. The *p*-values in the St. Lawrence are between 0.89 and 1.47 (mean value = 1.27 ± 0.26, median = 1.35). The *b*-value varies from 0.76 to 1.23 (mean value = 0.94 ± 0.21, median = 0.89). The *a*-value ranges from -1.75 to -3.43 (mean value = -2.44 ± 0.75, median = -2.29). An interesting observation is that, while the parameters fall within the range of California observations, even discounting less-active sequences, the *a* values for the sequences in the St. Lawrence region tend to be lower than the average value for California, sometimes significantly so, while the *p* values tend to be higher than average values for California. This suggests that sequences in the St. Lawrence region may be less energetic and productive than those in California, on average, and die out more quickly with time. An exception is the Miramichi sequence, as discussed further below. The low productivity of aftershock sequences in the St. Lawrence may have important implications for assessing the aftershock hazard following a major event in the region.

Table 3-2 Aftershock parameters

Sequence	Mainshock Mag.	Seismic Zone	p-values from Previous Studies	Minimum Mag.	Elapsed Time from Mainshock (in days)*	b	p ± CI	c	a
Val des Bois	5.0	Western Quebec	1.5 [1]	≥1.5 [1]	0.1-100	1.23(mN≥2.0) [2]	1.41 ± 0.17	0.05	-3.43
Cote-Nord	4.5	Lower St. Lawrence	1.34 [2]	≥0.9 [3]	0-40	0.98 [3]	1.29 ± 0.16	0.05	-2.60
Mont Laurier	4.5	Western Quebec		≥0.0 [4]	1.375-405	0.76[5]	1.47 ± 0.22	0.05	-1.99
Miramichi	5.5	Northern Appalachians	0.8 [6]	≥2.5	0.01-1000	0.8 [6]	0.89 ± 0.10	0.05	-1.75

Magnitudes are in moment magnitude scale.
* Duration used for calculation of aftershock parameters.
c parameter is constrained.
CI : 95% Confidence Interval
[1] ; Lamontagne (2013, personal communication); [2] Ma and Motazedian, 2012; [3] Lamontagne et al, 2004;

Although the number of aftershocks in a sequence generally correlates with the magnitude of the mainshock, regional variations in the aftershock productivity rate have been observed in several studies (e. g. Sing and Suarez, 1988; Yamanaka and Shimazaki, 1990; McGuire *et al*, 2005). For example, Arabasz and Hill (1994) found that the aftershock sequences in Utah are less productive than suggested by the generic California model (Reasenberg and Jones, 1989), by approximately a factor of two. Regional differences in the aftershock productivity may be attributable to differences in source and crustal characteristics.

Overall, the occurrence of a mainshock produces a drop in the average stress in the source region. However, there is also a redistribution of the stress, which may cause local stress increases that are then released as aftershocks. We might therefore expect that the occurrence of aftershocks would be related to the stress and the strength heterogeneity of the fault zone, as discussed by Utsu (1971). Numerical modeling by Mikumo and Miyatake (1979) shows that homogenous faults should produce few aftershocks, because the whole fault surface fails in the initial rupture. We therefore speculate that the low aftershock productivity in the St. Lawrence region may be related to the relatively homogenous crust and systematic high stress drop of mainshocks in eastern North America in comparison to those in the west (e.g. Kanamori and Anderson, 1975; Atkinson, 1984; Boore and Atkinson, 1987).
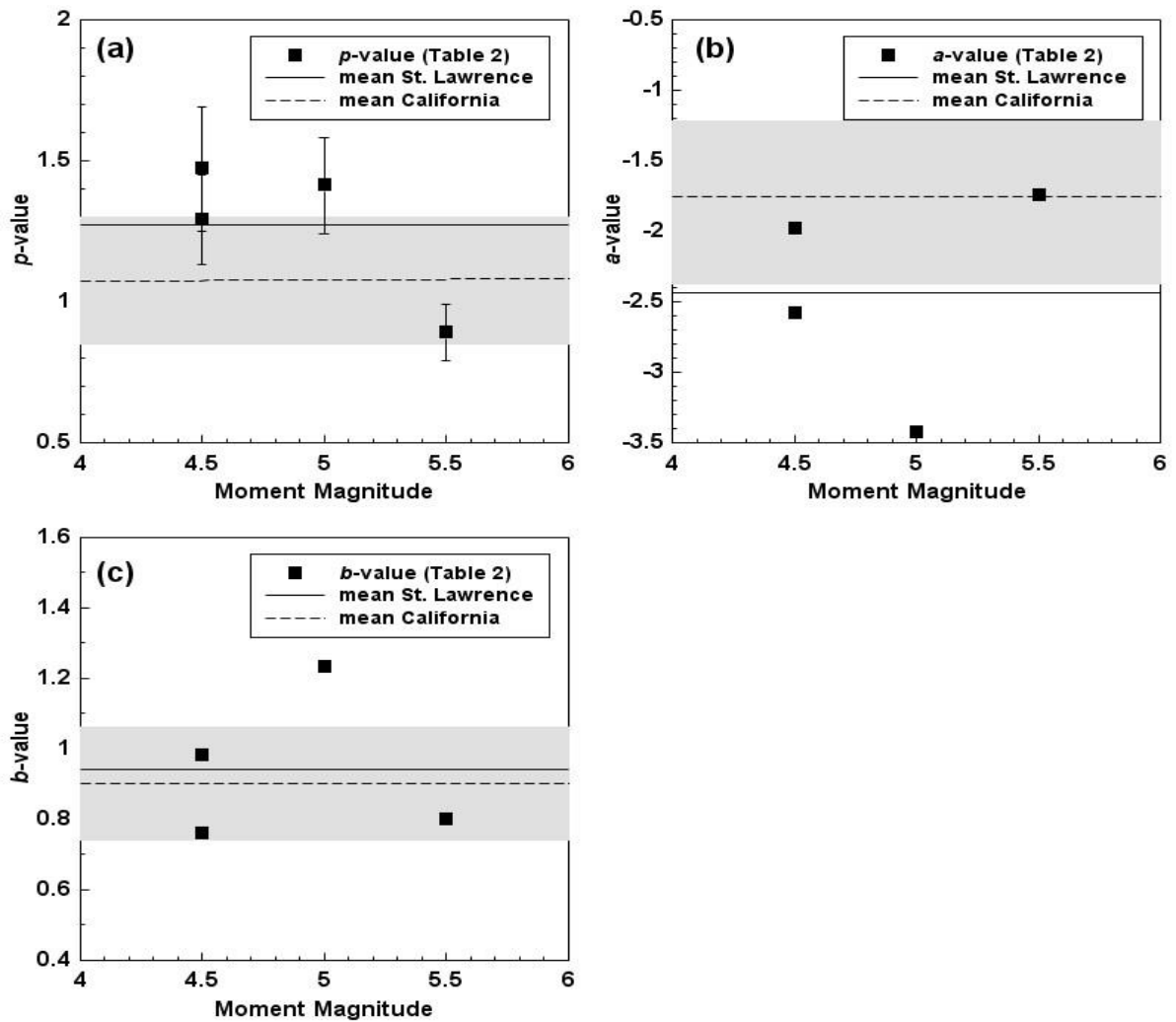
Figure 3-3 (a) *p* values (b) *a* values and (c) *b* values for 4 aftershock sequences in Table 3-2. The solid line and dashed lines show the average in the St. Lawrence and California, respectively. The gray area shows standard deviation of the California values.

It is also interesting and important that the aftershock sequences throughout the St. Lawrence region have similar values of the aftershock decay parameter (*p*-value); this may be representative of the seismicity regime in the region. An apparent exception is the *p* parameter for the Miramichi sequence, which has a value below 1. Visual inspection of Figure 3.2(d) reveals that for a long period of time after the Miramichi mainshock, the rate of activity in the epicentral region followed the modified Omori relation. The Miramichi earthquake and its significant aftershock activity are due to shallow (<10 km) thrust faulting

within the Northern Appalachians rocks, which have been thrust over the older Grenville bedrock. By contrast, the other three earthquakes studied here are deeper thrust events, which occurred within the Grenville cratonic bedrock, along reactivated faults of the ancient Iapetan rift system along the St. Lawrence and Ottawa valleys (Adams and Basham, 1989). We hypothesize that the slower Miramichi decay sequence may be related to the different seismogenic processes in the Appalachian region, in comparison to the processes within the rifted Grenville formations.

3.5   Aftershock rate from the 1663 Charlevoix earthquake

The 1663 Charlevoix earthquake, with an estimated moment magnitude of 7.0 (Ebel, 1996), is the largest known felt event in the St. Lawrence Valley, and so is of particular importance in the interpretation of seismicity in the study area. By scrutinizing firsthand historical accounts, Smith (1962) located the epicenter of the event in the Charlevoix region. The Charlevoix seismic zone is the most active region along the St. Lawrence Valley, and experiences a continuing moderate-to-high level of seismic activity, including several historic earthquakes in the magnitude 6 range, and several pre-historic large earthquakes (Tuttle and Atkinson, 2010). The boundary of the zone is shown in Figure 3.1.

In this section we explore the implications of the idea that the current cluster of seismicity in the Charlevoix Seismic Zone could be continuing aftershocks of the 1663 event. For this purpose, we again use the Reasenberg and Jones (1989) relationship (Eq. 3.3), and calculate the expected decay rate of activity following the 1663 **M**7.0 earthquake. The approach is to compare the expected rate with the observed seismicity, up to the present time. For this exercise, we use the Canadian Composite Seismicity Catalog (Fereidoni et al, 2012), which was primarily developed based on the GSC's Seismic Hazard Earthquake Epicentre File

(Adams and Halchuk, 2003). We supplement the historical seismicity catalog, particularly for the years following the 1663 earthquake, by scrutinizing the catalogs compiled by Smith (1962), Ebel (1996) and Gouin (2001) and adding events from those sources that were missing from the historical catalog. In comparing the observed and expected activity rates, the magnitude of completeness of the catalog is an important issue. The magnitude of completeness is usually defined as the minimum magnitude above which it is thought that all

earthquakes are reliably reported (Woessner and Wiemer, 2005). GSC's national earthquake hazard report provides an estimate of completeness magnitudes for the Charlevoix seismic zone in different time windows (Adams and Halchuck, 2003), as shown in Figure 3.4. Moreover, we will consider how different potential judgments regarding the magnitude of completeness could affect the conclusion reached.
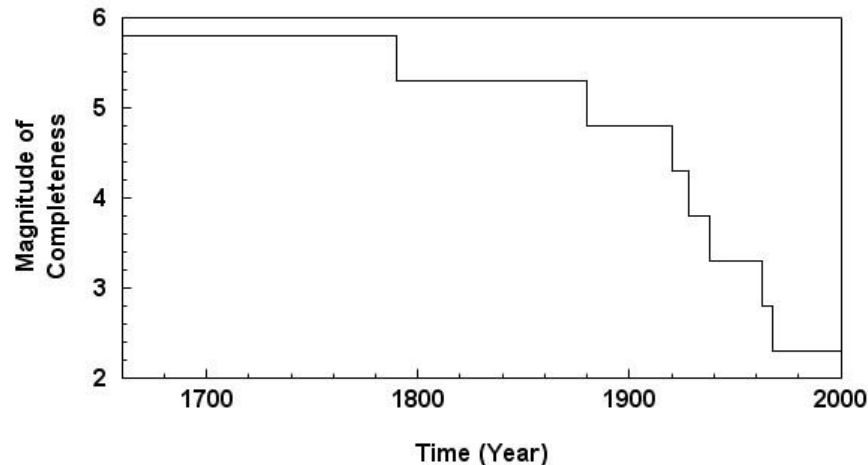
Figure 3-4 Magnitude completeness (in moment magnitude) of earthquake reporting in the Charlevoix Seismic Zone according to GSC's National Earthquake Hazard Report (Adams and Halchuk, 2003). Note that the catalog magnitudes are converted to moment magnitude for this illustration.

Figure 3.5 shows the rate of activity observed after the 1663 event up to the present time, along with the expected rate for the aftershock sequence of a **M**7.0 earthquake in the St. Lawrence region. To account for uncertainty in the aftershock parameters, the expected rates are calculated using three plausible sets of model parameters: 1) The St. Lawrence model (mean parameters determined from the four St. Lawrence aftershock sequences in this study); 2) a "generic California" aftershock model, using parameters from Reasenberg and Jones (1989); and 3) the Miramichi model (the aftershock parameters estimated here for the Miramichi earthquake). We test the latter set of aftershock parameters separately, since the Miramichi sequence behaved differently from the other three in the region. The Miramichi

aftershock activity was significantly more productive and had longer duration than typical sequences in the St. Lawrence region.
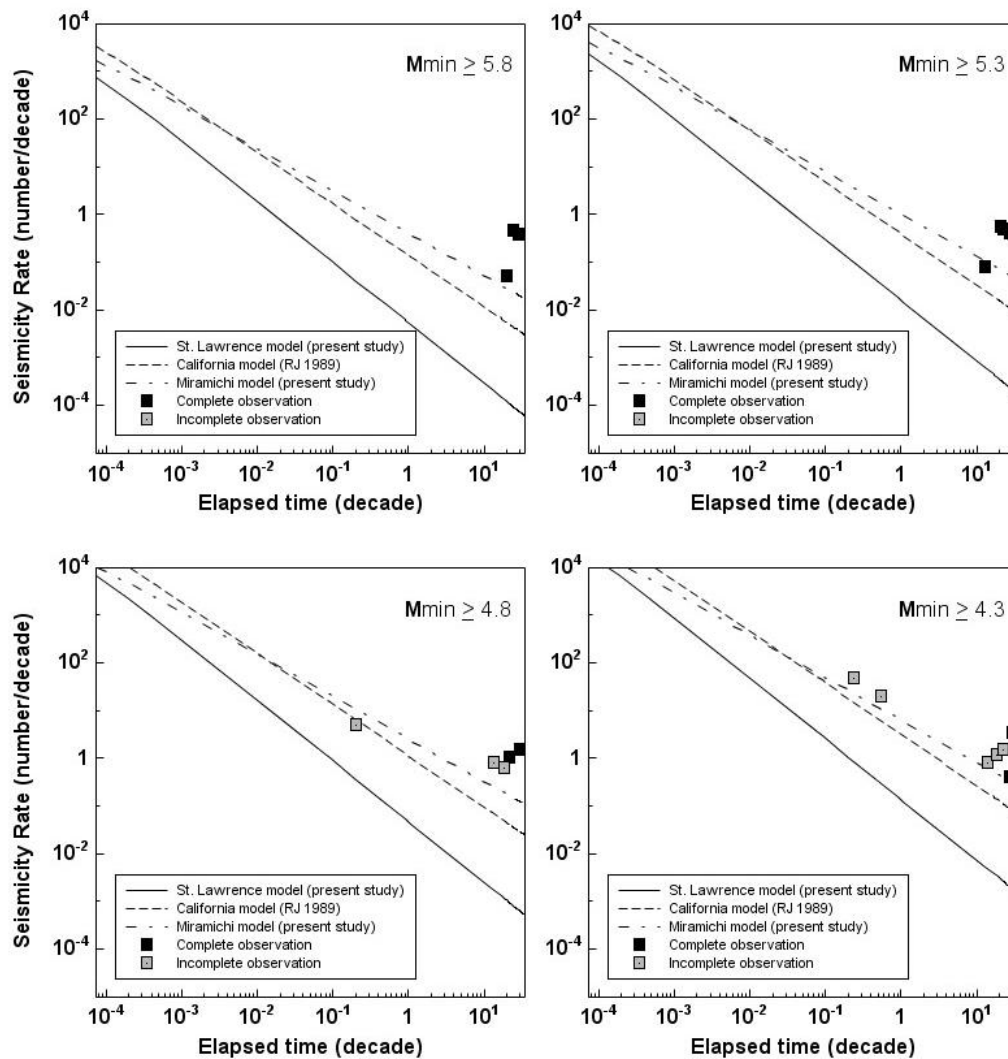
Figure 3-5 Comparison of the predicted and observed event rates for the 1663 M7.0 earthquakes for different magnitude completeness. The complete part of the observation is defined based on the magnitude completeness in Charlevoix reported by GSC (see Figure 3.4). RJ 1989 refers to Reasenberg and Jones 1989.

The comparison between the observed and predicted rates reveals that the present-day seismicity rates are much greater than would be expected from a decaying aftershock sequence from the 1663 **M**7.0 earthquake. This conclusion holds no matter what aftershock parameters are used, and regardless of what choices are made regarding the magnitude of

completeness. Moderate-to-large earthquakes are currently occurring in the Charlevoix seismic zone at a rate that is almost three to five times higher than what we would expect from an aftershock sequence, even if we consider highly-productive sequences such as those in Miramichi and California. To model the contemporary seismicity as aftershock activity from 1663, we would need to postulate that a 1663 earthquake sequence was three to five times more energetic and productive than a typical California sequence. However, if the aftershock activity of the 1663 earthquake was indeed highly productive and long-lasting, then we should have observed numerous major aftershocks in the Charlevoix region following the 1663 earthquake. For such a highly-productive sequence, the Reasenberg and Jones (1989) model would predict the occurrence of more than 20 earthquakes in the magnitude 6 range ($M > 5.5$) within the first 100 years after the mainshock, and ~200 events of $M>4.5$. This differs dramatically from the observed seismicity since 1663 in the Charlevoix area. For example, Ebel (1996) reports the occurrence of just 6 strong events (mN>5, or $M>4.5$) in the focal region of the mainshock in the years following. In our view, it is highly unlikely that tens of earthquakes of $M>5.5$, and hundreds of earthquakes of $M>4.5$, are missing from the historical catalogs, because such events are very widely felt. For example, an earthquake of $M5.5$ in eastern North America would be felt to distances of about 500 km (Atkinson 1993). At the time of the mainshock, the land was populated at several

localities along the St. Lawrence River, and therefore the majority of such events – which

would have been fearful events - should have been reported in the historical accounts (Gouin, 2001). This difference between the predicted aftershock rate and present seismicity, over a wide range of magnitudes, leads us to conclude that current seismicity in the Charlevoix seismic zone is not consistent with a decaying aftershock sequence of the 1663 earthquake. A similar conclusion was reached by Page and Hough (2014) in their consideration of the seismicity of the New Madrid Seismic Zone (central US). Although the contemporary seismicity in Charlevoix does not represent aftershock activity, this does not eliminate the possibility that seismicity in Charlevoix might be still influenced to some extent by the changes in stress imparted by past large earthquakes in the region (Fereidoni and Atkinson, 2013). We examine this hypothesis in the next chapter.

3.6   Aftershock parameters for less productive sequences

One might argue that by considering only those sequences with a sufficient number of events for robust analysis, the regional productivity parameter (*a* value) could be biased towards more productive sequences. This potential bias, however, does not influence our conclusion regarding the long-lived aftershock hypothesis for the 1663 Charlevoix event. The inclusion of less-productive sequences in the calculation of regional properties would lower the mean *a* value obtained for the St. Lawrence region, which would further strengthen the conclusion reached in the previous section.

Nevertheless, to the extent that the results of this study may be used to infer average regional parameters, it is important to investigate what effect the potential bias towards more active sequences might have. In this section, we include the sequences that had lower aftershock productivity (2000 Kipawa **M**4.7, 1997 Cape-Rouge **M**4.5, 1988 Saguenay **M**5.8, and 1979 Charlevoix **M**4.8) in our analysis, in order to provide more insight into the range of aftershock productivity in the region. As these aftershock sequences do not have enough events to reliably calculate the parameters on an event-by-event basis, we stack them together. The stacking technique follows that described by Gross and Kisslinger (1994), Davis and Frohlich (1991), and Nyffenegger and Frohlich (1997), which was developed for the purpose of obtaining meaningful estimates of aftershock parameters for sequences with few aftershocks. The basic idea is that we assign a start time of zero to the mainshocks of each of the sparse sequences, and then combine them together to form a single equivalent large sequence. Based on the magnitudes of the four included mainshocks, we obtain an equivalent mainshock magnitude M_e of 5.29 for the stack, by using the formula of Felzer *et al*. (2003):

$$10^{M_e} = \frac{1}{N}\sum_{i=1}^{N} 10^{M_i} \qquad\qquad (3.4)$$

For the events included in this analysis, the detection threshold is about mN = 1.5 (**M**~0.9) (Du Burger et al, 1991; Bent et al, 2002), due to the presence of local networks. Additionally, the deployment of portable seismic networks during the Kipawa (Bent et al, 2002), Cape-Rouge (Nadeau et al, 1998), and Sagueny (Du Berger et al, 1991) events enhanced the monitoring of aftershock activities during those sequences.

We estimate the Omori parameters for the stacked sequence as follows, considering events of M$\geq$1.0: $K = 1.27, p = 0.97$, and $c = 0.05$(constrained), where the K value has been scaled simply by diving it by the number of mainshocks in the stack (Pollock, 2007). Next, using the GSC's published b-values (Adams and Halchuck, 2003) in the focal region of each sequence, we obtain an average b-value of 0.78, and thereby estimate an a value of -3.24 for the whole stack.

Average aftershock parameters for the region can be estimated by averaging the values obtained for each sequence individually, including the stack of less productive sequences as one event. We obtain the following average regional values for aftershocks in the St. Lawrence region: mean p value = 1.21$\pm$0.26 (median = 1.29), mean b value = 0.91$\pm$0.20 (median = 0.8), mean a value = -2.60$\pm$0.74 (median = -2.59). As expected, the obtained a value is slightly less than indicated previously by considering just the more active sequences.

We acknowledge that the stacking has its own benefits and drawbacks. The stacking of the individual sequences follows the premise of Dietrich (1994) and assumes that aftershock sequences have similar duration. Nyffenegger and Frohlich (1998) clarify the meaning of the p-value calculated from stacked sequences. By the use of simulation, they conclude that in most of the cases where sequences with varying p, N (number of aftershocks), and duration are stacked together, the maximum likelihood estimation of p-value for the stack approximately equals to the weighted mean of the individual sequences p-value. It is not an issue here, as the objective of the paper is to obtain the average of aftershocks parameters in the study region.

3.7 Conclusions

We have studied the temporal behavior of aftershock sequences in the St. Lawrence region by estimating the aftershock parameters in the Reasenberg and Jones (1989) formulation. Our study provides average aftershock statistics in the region by consistent and uniform analysis of recent significant mainshock-aftershock sequences, which can be used in short-term and long-term hazard assessment in the region. The following summarizes the key conclusions of our analysis:

1)   Aftershock sequences in the study region share similar parameter values (see Table 3.2); these may be representative of the seismicity regime in the St. Lawrence region. An apparent exception is the Miramichi sequence, which was more productive and longer than average. This might be attributable to the difference in seismotectonic regime, as the Miramichi sequence occurred in the Appalachians, while the other three events were within the older and deeper Iapetan rift faults of the St. Lawrence and Ottawa valleys.

2)   Even discounting the sequences with especially low activity, the St. Lawrence aftershock sequences are apparently less energetic and productive than average aftershock sequences in California, with the exception of the shallow Miramichi sequence, which had similar productivity to California mainshocks. It is possible that the difference in productivity between St. Lawrence and California aftershock sequences could be related to the difference in the source parameters of the mainshocks and crustal properties. The eastern mainshocks have systematically higher stress drop and the crust is more homogenous in comparison to the west.

3)   Considering the typical behavior of aftershock sequences in the St. Lawrence region and California or Miramichi, the observed seismicity in the Charlevoix Seismic Zone cannot be reconciled with expected rates based on a decaying aftershock sequence from the 1663 earthquake. Since a complete list of aftershocks of the 1663 event is not available, it may not be possible to definitely prove that the observed seismicity in the Charlevoix is not part of a long decaying aftershock sequence. However, we have shown that such an explanation would require a highly-productive sequence (three to five times more productive than California or Miramichi), and would also imply that tens to hundreds of strong and frightening aftershocks went unreported, over a century or more, in an area known for its rich historical records. The more likely explanation is that the 1663 earthquake shares similar aftershock parameters to those observed in other contemporary sequences in the same setting. In this case, it would not be prudent to assume that the current seismicity in the Charlevoix is dying out with time; as such a hypothesis would almost certainly underestimate the contemporary hazard in this region. We conclude that ongoing energetic earthquake activities should be expected to continue in the Charlevoix seismic zone.

3.8 References

Adams, J., & Basham, P. (1989). The seismicity and seismotectonics of Canada: east of The Cordillera. *Geoscience Canada,* **16**(1).

Adams, J., & Halchuk, S. (2003). *Fourth generation seismic hazard maps of Canada: Values for over 650 Canadian localities intended for the 2005 National Building Code of Canada*: Geological Survey of Canada, Open File 4459 , 155 p.

Atkinson, G. M. (1984). Attenuation of strong ground motion in Canada from a random vibrations approach. *Bulletin of the Seismological Society of America,* **74**(6), 2629-2653.

Atkinson, G. M. (1993). Earthquake source spectra in eastern North America. *Bulletin of the Seismological Society of America,* **83**(6), 1778-1798.

Arabasz, W., & Hill, S. (1994). Aftershock temporal behavior and earthquake clustering in the Utah region. *Smith, RB, WJ Arabasz, JC Pechmann, and CM Meertens, Seismicity, ground motion, and crustal deformation—Wasatch Front, Utah, and adjacent Intermountain Seismic Belt, Technical Report,* US Geological Survey Grant(1434-93).

Basham, P., Weichert, D., Anglin, F., & Berry, M. (1982). New Probabilistic Strong Seismic Ground Motion Maps of Canada: A Compilation of Earthquake Source Zones, Methods and Results, *Publications of the Earth Physics Branch*, Energy, Mines, Resources Canada, Open-File 82-33, 202p.

Basham, P. (1989). A Paleozoic-Mesozoic rift framework for seismic hazard assessment in eastern North America. *Current Research*, Geological Survey of Canada, Part F, Paper 89-1F, pp. 45-50, Ottawa.

Basham, P. and J. Adams (1983). *Earthquakes on the continental margin of eastern Canada - Need future large events be confined to the locations of large historical events*, US Geological Survey, Open-File Report 83-843, 456-567.

Bent, A. L., Lamontagne, M., Adams, J., Woodgold, C. R., Halchuk, S., Drysdale, J., Dastous, J. B. (2002). The Kipawa, Quebec "Millennium" earthquake. *Seismological Research Letters,* **73**(2), 285-297.

Boore, D. M., & Atkinson, G. M. (1987). Stochastic prediction of ground motion and

spectral response parameters at hard-rock sites in eastern North America. *Bulletin of the Seismological Society of America,* **77**(2), 440-467.

Burke, K. B., Wetmiller, R. J., Lamontagne, M., Carr, M. J., & Hickey, C. (1989). Microearthquake survey of the Miramichi, New Brunswick, epicentral region, 1985. *Canadian Journal of Earth Sciences,* **26**(12), 2567-2577.

Davis, S. D., & Frohlich, C. (1991). Single-link cluster analysis of earthquake aftershocks: Decay laws and regional variations. *Journal of Geophysical Research: Solid Earth (1978–2012),* **96**(B4), 6335-6350.

Du Berger, R., Roy, D. W., Lamontagne, M., Woussen, G., North, R. G., & Wetmiller, R. J. (1991). The Saguenay (Quebec) earthquake of November 25, 1988: seismologic data and geologic setting. *Tectonophysics*, **186**(1), 59-74.

Ebel, J. E. (1996). The seventeenth century seismicity of northeastern North America. *Seismological Research Letters,* **67**(3), 51-68.

Ebel, J. E., Bonjer, K.-P., & Oncescu, M. C. (2000). Paleoseismicity: Seismicity evidence for past large earthquakes. *Seismological Research Letters,* **71**(2), 283-294.

Ebel, J. E. (2009). Analysis of aftershock and foreshock activity in stable continental regions: implications for aftershock forecasting and the hazard of strong earthquakes. *Seismological Research Letters,* **80**(6), 1062-1068.

Enescu, B., J. Mori, M. Miyazawa, and Y. Kano (2009). Omori-Utsu law c-values associated with recent moderate earthquakes in Japan, *Bulletin of the Seismological Society of America* **99,** 884-891.

Felzer, K. R., Abercrombie, R. E., & Ekström, G. (2003). Secondary aftershocks and their importance for aftershock forecasting. *Bulletin of the Seismological Society of America,* **93**(4), 1433-1448.

Felzer, K. R., Abercrombie, R. E., & Ekström, G. (2004). A common origin for aftershocks, foreshocks, and multiplets. *Bulletin of the Seismological Society of America, **94**(1), 88-98.

Fereidoni, A., Atkinson, G. M., Macias, M., & Goda, K. (2012). CCSC: A composite seismicity catalog for earthquake hazard assessment in major Canadian cities. *Seismological Research Letters,* **83**(1), 179-189.

Fereidoni, A., Atkinson, G. M. (2012), Statistical features of aftershock temporal behavior in

the St. Lawrence Valley, Abstract S54D-08 presented at 2012 Fall Meeting, AGU, San Francisco, Calif., 3-7 Dec.

Fereidoni, A., Atkinson, G. M. (2013), Correlation between static stress changes imparted by the **M**7 1663 earthquake and current seismicity in the Charlevoix seismic zone, presented at the Annual Meeting of the Eastern Section of The Seismological Society of America, ES-SSA, Charlevoix, Canada, 6-8 Oct.

Gouin, P. (2001). Historical earthquakes felt in Quebec (from 1534 to March 1925). *Guérin, Montréal.*

Gross, S. J., & Kisslinger, C. (1994). Tests of models of aftershock rate decay. *Bulletin of the Seismological Society of America,* **84**(5), 1571-1579.

Gutenberg, B., & Richter, C. F. (1954). *Seismicity of the earth and associated phenomena.* Princeton University Press, Princeton, New Jersey, 310 p.

Hasegawa, H. S., & Wetmiller, R. J. (1980). The Charlevoix earthquake of 19 August 1979 and its seismo-tectonic environment. *Seismological Research Letters,* **51**(4), 23-38.

Kagan, Y. Y. (2004). Short-term properties of earthquake catalogs and models of earthquake source, *Bulletin of the Seismological Society of America* **94,** 1207-1228.

Kanamori, H., & Anderson, D. L. (1975). Theoretical basis of some empirical relations in seismology. *Bulletin of the Seismological Society of America,* **65**(5), 1073-1095.

Kisslinger, C. (1996). Aftershocks and fault-zone properties. *Advances in geophysics,* **38**, 1-36.

Lamontagne, M., Bent, A. L., Woodgold, C. R., Ma, S., & Peci, V. (2004). The 16 March 1999 mN 5.1 Côte-Nord earthquake: The largest earthquake ever recorded in the lower St. Lawrence seismic zone, Canada. *Seismological Research Letters,* **75**(2), 299-316.

Lamontagne, M., Hasegawa, H. S., Forsyth, D. A., Buchbinder, G. G., & Cajka, M. (1994). The Mont-Laurier, Québec, earthquake of 19 October 1990 and its seismotectonic environment. *Bulletin of the Seismological Society of America,* **84**(5), 1506-1522.

Ma, S., & Eaton, D. W. (2007). Western Quebec seismic zone (Canada): Clustered, midcrustal seismicity along a Mesozoic hot spot track. *Journal of Geophysical*

Research: Solid Earth (1978–2012), **112**(B6).

Ma, S., & Motazedian, D. (2012). Studies on the June 23, 2010 north Ottawa M W 5.2 earthquake and vicinity seismicity. *Journal of seismology,* **16**(3), 513-534.

McGuire, J. J., Boettcher, M. S., & Jordan, T. H. (2005). Foreshock sequences and short-term earthquake predictability on East Pacific Rise transform faults. *Nature,* **434**(7032), 457-461.

Mikumo, T., & Miyatake, T. (1979). Earthquake sequences on a frictional fault model with non-uniform strengths and relaxation times. *Geophysical Journal of the Royal Astronomical Society,* **59**(3), 497-522.

Nadeau, L., Lamontagne, M., Wetmiller, R., Brouillette, P., Bent, A., & Keating, P. (1998). The November 5, 1998 Cap-Rouge, Quebec Earthquake. *Current Research, part E.* Geological Survey of Canada, P105-115.

Nyffenegger, P., & Frohlich, C. (1998). Recommendations for determining p values for aftershock sequences and catalogs. *Bulletin of the Seismological Society of America,* **88**(5), 1144-1154.

Ogata, Y. (1983). Estimation of the parameters in the modified Omori formula for aftershock frequencies by the maximum likelihood procedure. *Journal of Physics of the Earth,* **31**(2), 115-124.

Ogata, Y. (1999). Seismicity analysis through point-process modeling: A review. *Pure and Applied Geophysics,* **155**(2-4), 471-507.

Page, M. T., & Hough, S. E. (2014). The New Madrid Seismic Zone: Not Dead Yet. *Science* (in print).

Reasenberg, P. A., & Jones, L. M. (1989). Earthquake hazard after a mainshock in California. *Science,* **243**(4895), 1173-1176.

Shcherbakov, R., Goda, K., Ivanian, A., & Atkinson, G. M. (2013). Aftershock Statistics of Major Subduction Earthquakes. *Bulletin of the Seismological Society of America,* **103**(6), 3222-3234. doi: 10.1785/0120120337

Shcherbakov, R., D. L. Turcotte, and J. B. Rundle (2006). Scaling properties of the Parkfield aftershock sequence, *Bulletin of the Seismological Society of America* **96,** S376-S384.

Shcherbakov, R., D. L. Turcotte, and J. B. Rundle (2004). A generalized Omori's law for earthquake aftershock decay, *Geophys.Res.Lett.* **31,** .

Singh, S., & Suárez, G. (1988). Regional variation in the number of aftershocks (mb≧ 5) of large, subduction-zone earthquakes (Mw≧ 7.0). *Bulletin of the Seismological Society of America,* **78**(1), 230-242.

Smith, W. T. (1962). *Earthquakes of eastern Canada and adjacent areas, 1534-1927* (Vol. 26): R. Duhamel, Queen's Printer.

Stein, S., & Liu, M. (2009). Long aftershock sequences within continents and implications for earthquake hazard assessment. *Nature,* **462**(7269), 87-89.

Sturtevant, B., H. Kanamori, and E. E. Brodsky (1996). Seismic triggering by rectified diffusion in geothermal systems, *Journal of Geophysical Research: Solid Earth (1978–2012)* **101,** 25269-25282.

Tuttle, M. P., & Atkinson, G. M. (2010). Localization of large earthquakes in the Charlevoix Seismic Zone, Quebec, Canada, during the past 10,000 years. *Seismological Research Letters*, **81**(1), 140-147.

Utsu, T. (1961). A statistical study on the occurrence of aftershocks. *Geophys. Mag., 30*, 521-605.

Utsu, T., Ogata, Y., & Matsu'ura, R. S. (1995). The centenary of the Omori formula for a decay law of aftershock activity. *Journal of Physics of the Earth*,**43**(1), 1-33.

Utsu, T. (1971). Aftershocks and earthquake statistics (2): further investigation of aftershocks and other earthquake sequences based on a new classification of earthquake sequences. *Journal of the Faculty of Science, Hokkaido University. Series 7, Geophysics,* **3**(4), 197-266.

Wetmiller, R., Adams, J., Anglin, F., Hasegawa, H., & Stevens, A. (1984). Aftershock sequences of the 1982 Miramichi, New Brunswick, earthquakes. *Bulletin of the Seismological Society of America,* **74**(2), 621-653.

Woessner, J., & Wiemer, S. (2005). Assessing the quality of earthquake catalogues: Estimating the magnitude of completeness and its uncertainty. *Bulletin of the Seismological Society of America,* **95**(2), 684-698.

Yamanaka, Y., & Shimazaki, K. (1990). Scaling relationship between the number of aftershocks and the size of the main shock. *Journal of Physics of the Earth,* **38**(4), 305-324.

Chapter 4

4 Correlation between Coulomb stress changes imparted by historic earthquakes and current seismicity in Charlevoix Seismic Zone, eastern Canada[4]

The Charlevoix Seismic Zone (CSZ) is the most seismically active region in eastern Canada and has experienced several large historic events, such as the **M**7 1663 event (where **M** is moment magnitude), as well as ongoing low-level activity. Recent statistical studies (Fereidoni and Atkinson, 2012, 2014) suggest that the contemporary seismicity in Charlevoix cannot be reconciled as part of a long aftershock sequence from the 1663 event. However, this does not eliminate the possibility that current seismicity in Charlevoix might still be influenced by stress changes related to the 1663 event. In this paper we investigate the correlation between the location of contemporary seismicity in the region and the static stress changes imparted by the 1663 earthquake. We model the 1663 earthquake as a primarily thrust event on a SE-dipping fault, which would have produced regions of increased stress that coincide with areas where current microseismicity is concentrated. With our assumed rupture model, we find that ~75-80% of the current seismicity (from 1978 to the present) is located in the area of positive Coulomb stress changes. The relatively good correlation between the models of static stress changes and the seismicity pattern observed in Charelvoix may suggest that the background seismic activity in the region is still influenced by the stress perturbations due to the 1663 shock.

4.1 Introduction

Historically, the Charlevoix Seismic Zone has experienced several damaging earthquakes in the magnitude (M) 6-7 range, with the 1663 M7 earthquake as the largest ever to occur in this region (e.g. Smith 1962). Each year, the CSZ also experiences hundreds of small earthquakes, though most of them are too small to be felt (Adams and Basham, 1989). Based

---

[4] Fereidoni, A., Atkinson, G. M., Correlation between Coulomb stress changes imparted by historic earthquakes and current seismicity in Charlevoix seismic zone, Canada, *Seismological Research Letters*(in print).

on the historical and current rate of activity, the CSZ has highest level of seismic hazard in continental eastern Canada (Figure 4.1). Like other intraplate earthquake zones, such as the New Madrid Seismic Zone (NMSZ) in the central United States (e.g. Frankel et al, 2012), the causes of large earthquakes there are not well understood.

In a broader geologic context, the Charlevoix region lies within a complex geologic setting along the St. Lawrence Valley. As pointed out by Lamontagne (1999), the main geological structures were formed by a series of tectonic events: faulting during the 1100 Ma Grenvillian orogeny; a rifting episode during the 700 Ma Iapetus Ocean opening; the 450 Ma Appalachian orogeny; and a large meteor impact 350 Ma (Rondot, 1979). Consequently, the CSZ is a highly fractured volume, particularly within the impact structure (Lamontagne et al, 2004).

There is uncertainty in the degree of influence that various tectonic events exert on the localization of seismicity in the CSZ, in particular with respect to the control exerted by the Iapetan rift faults. It has been noted that similar rift faults elsewhere along the St. Lawrence River have not been seismically active in historic times (Lamontagne *et al.*, 2004). There is also uncertainty in the temporal distribution of seismicity in the CSZ and how it may be modeled. Tuttle and Atkinson (2010) report paleoseismic evidence for three or more large events (moment magnitude ≥ 6.2) or large-event sequences, in the CSZ over the last 10,000 years. However, the high recurrence rates suggested by historical seismicity – five M= 6-7 events since 1663 and about 10 M=5-6 events since the mid-19th century (Mazzotti et al, 2005) - cannot be easily reconciled with the paleoseismic evidence, as this would require a very high rate of seismic moment release if continuous over a long period of time. Analysis of GPS data in Quebec (Mazzotti et al, 2005) showed that the St. Lawrence Valley is shortening at the average strain rate of $1.7\pm1.0 \times 10^{-9}$ yr^{-1}, with the rate in CSZ being the double the regional average.

In addition, there is a widely-discussed hypothesis that the current seismicity in the CSZ represents a long-lived aftershock sequence of the 1663 **M**~7 earthquake (Basham and Adams, 1983; Basham, 1989; Ebel *et al.*, 2000; Ma and Eaton, 2007; Stein and Liu, 2009), resulting in a concentrated clustering of CSZ seismicity in time. Recent statistical analysis by Fereidoni and Atkinson (2012, 2014) has shown that such a model is not feasible given

the observed seismicity rate and plausible aftershock productivity parameters for the region. Page and Hough (2014) have reached a similar conclusion for the New Madrid Seismic Zone. This however does not eliminate the possibility that the stress perturbations due to the 1663 event might still have some impact on the spatial patterns of seismicity in the region, given the low stressing rate in eastern Canada.
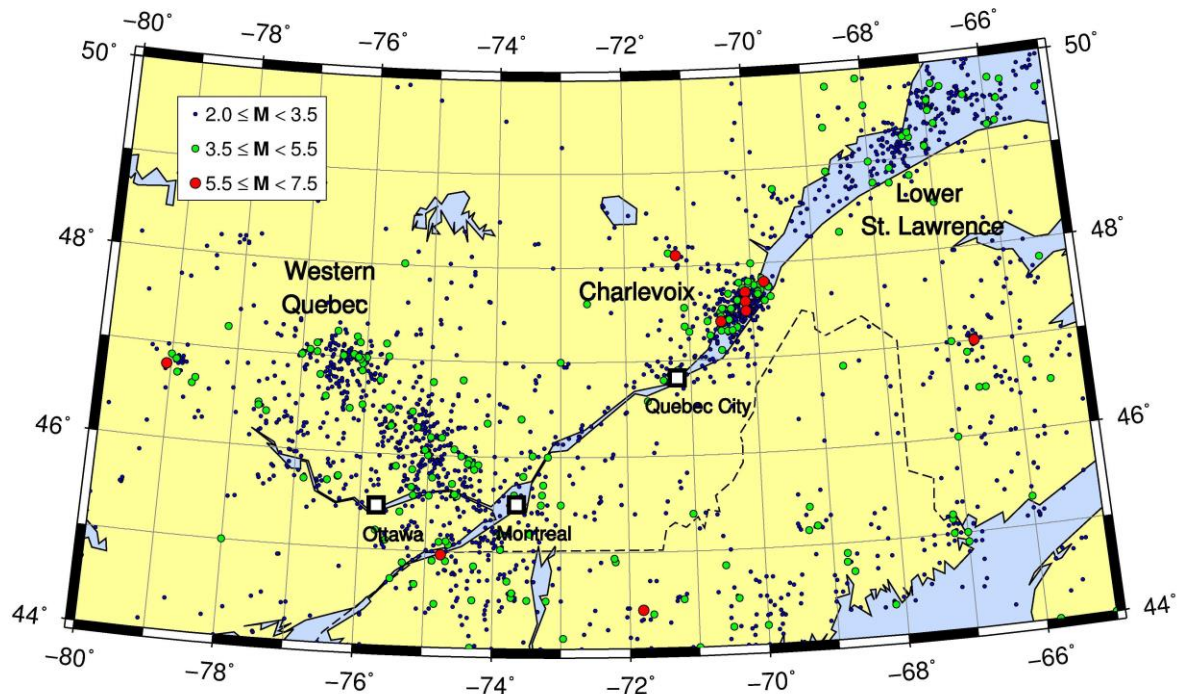
Figure 4-1 Seismicity of the St. Lawrence region, from CCSC catalog.

Many studies aimed at understanding earthquake interactions have focused on the theory of static stress transfer as a possible triggering mechanism (*e.g.* Reasenberg and Simpson, 1992; Lin and Stein, 2004; Ogata and Toda, 2010; Sumy *et al.*, 2014). The majority of such papers have studied the stress changes due to recent well- recorded earthquakes; however some researchers have investigated the stress changes associated with large historical events, despite the inherent limitations imposed by the available information. For example, Nostro *et al.* (1998) explored the static stress interaction between earthquakes and volcanic eruptions in Italy during the past 1000 years. Mueller *et al.* (2004) used the locations of recent recorded seismicity and models of static stress changes to infer the focal region and mechanism of the earthquakes in the 1811-1812 New Madrid sequence. More recently, Ishibe *et al.* (2011)

investigated the correlation between contemporary seismicity and Coulomb stress changes due to large historical strike-slip earthquakes in Japan.

In this paper, we use Coulomb stress theory to investigate whether stress changes caused by the 1663 **M**~7 (where **M** is moment magnitude) earthquake have influence on the location of contemporary seismicity (1978 to the present) in the CSZ. We focus on the stress perturbations caused by the 1663 event, ignoring any stress contributions from the tectonic loading process, consistent with the approach in Toda and Enescu (2011).This is a reasonable approach for the region, given the low strain rate in the St. Lawrence Valley. We compile a suite of plausible rupture scenarios for the 1663 event based on the dominant faulting mechanism in the CSZ. We then present idealized models that illustrate the key features of Coulomb stress changes that are likely to be associated with the event. We show how these models capture much of the observed earthquake distribution, which may explain some puzzling features of seismicity in the CSZ. Finally, we use the general coincidence of background seismicity and the model of Coulomb stress changes to infer a faulting mechanism for the 1663 Charlevoix earthquake and draw conclusions regarding the fault rupture dimensions and event size.

4.2   Seismicity of the Charlevoix Seismic Zone

Since the arrival of European settlers in the 1600s, the CSZ has experienced five damaging earthquakes (Adams and Basham, 1989): in 1663 (**M**7); 1791 (**M**5.5); 1860 (**M**6.1); 1870 (**M**6.6); and 1925 (**M**6.4). The magnitude estimates for these events are drawn from a range of sources as compiled in the Canadian Composite Seismicity Catalogue (CCSC) (Fereidoni *et al.*, 2012). Note that only the last event has an instrumentally-determined moment, and so magnitude estimates of most of the events, including that in 1663, are subject to significant uncertainty. In particular, the magnitude estimate for the 1663 earthquake ranges from m_{bLg} 6.5±0.5 in Gouin (2001) to **M**7.5±0.45 in Ebel (2011). Therefore, the magnitude of the 1663 earthquake still has an uncertainty of at least several tenths of a magnitude unit.

The pattern of contemporary seismicity in the CSZ has been relatively well-defined since the installation of a permanent regional seismic network by the Geological Survey of Canada in 1978. The contemporary earthquakes occur mostly beneath the St. Lawrence River platform as shown in the upper panel of Figure 4.2. The spatial extent of the active zone appears to be

largely controlled by the Iapetan faults and potentially also the meteor impact structure. These Iapetan faults (also called St. Lawrence Paleo-rift faults; Anglin, 1984) were formed in the late Precambrian during opening of the Iapetus Ocean, and were apparently reactivated after the Devonian meteor impact. The hypocenters dip towards the SE and cluster along or between the steeply dipping rift faults (Anglin and Buchbinder, 1981). In addition, the seismicity is not uniformly distributed throughout the CSZ. Most of the low-magnitude ($M <$ 3.5) background activity (about 70%) occurs within the impact structure area, while the larger events ($M \geq 3.5$) appear to occur outside the crater at both ends of the seismic zone. The concentration of the seismicity within the boundaries of the crater is puzzling, as most large impact structures around the world are not seismically active (Solomon and Duxbury, 1987). Lamontagne et al (2004) hypothesized that the larger earthquakes in the CSZ represent reactivation of Iapetan faults in the region, while the smaller events may represent reactivation of smaller fractures within the impact zone, due to local stresses.

When the contemporary seismicity is examined in cross-section through the rift faults (bottom panel of Figure 4.2), the seismicity clusters in two distinct zones separated by an aseismic slab (Anglin and Buchbinder, 1981). This aseismic area coincides with high-velocity bodies (Vlahovic *et al.*, 2003) and the location of major faults beneath the St. Lawrence River. Roughly 80% of earthquakes occur in the depth range of 5-15 km in Grenvillian basement rocks, though some events are as deep as 30 km. Wetmiller and Adams (1990) reported that many of the low-magnitude earthquakes, and probably the nucleation depths of the larger events, are concentrated near a depth of 10 km.

The faulting style that emerges from the CSZ focal mechanisms is mainly thrust to strike-slip faulting. The events occur on fault planes with highly variable orientations, but there are higher numbers of nodal planes in the NE direction (Lamontagne, 1999). It is generally assumed that, on average, most of the larger CSZ earthquakes occur as thrust events on pre-existing SE steeply (~60°) dipping faults (e.g. Baird et al, 2010). This common faulting mechanism is consistent with the focal mechanism obtained for two larger recent events in 1925 and 1979 (Hasegawa and Wetmiller, 1980; Bent, 1992).
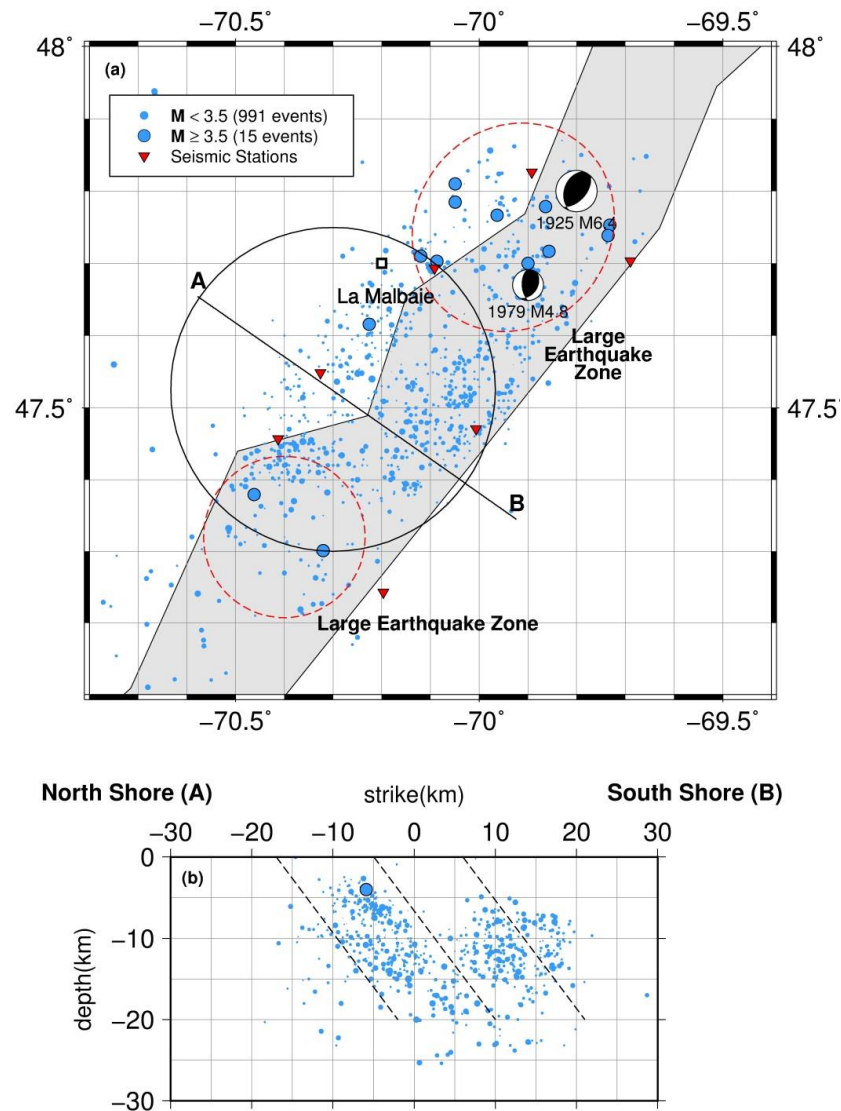
Figure 4-2 Background seismicity in the Charlevoix Seismic Zone (since 1978). Top panel is map view, with focal mechanisms of two of the larger recent earthquakes, 1925 (Bent, 1992) and 1979 (Hasegawa and Wetmiller, 1980), superimposed. Grey shading marks the St. Lawrence River. The two red large circles show where larger earthquakes (M≥3.5, large dots) have occurred, while the black circle roughly marks the outline of the meteor crater where most of the microearthquakes (M<3.5, small dots) occur (Lamontagne and Ranalli, 1997). Bottom panel is a cross-sectional view perpendicular to the trend of the St. Lawrence River. The broken lines represent the interpreted steeply-dipping trends of hypocenters (Anglin, 1984).

4.3   Analysis method

We investigate the static stress interaction between earthquakes here under the standard assumption that increasing the Coulomb stress promotes earthquakes, while decreasing it suppresses failures (e.g. Das and Scholz, 1981; Stein and Lisowski, 1983; Oppenheimer et al, 1988; Harris, 1998). The Coulomb stress change (ΔCFF) is defined in the following equation (King *et al.*, 1994):

$$\Delta CFF = \Delta\tau + \mu'\Delta\sigma \tag{4.1}$$

where $\Delta\tau$ is the shear stress change (positive in the direction of slip), $\Delta\sigma$ is the normal stress change (positive in the direction of fault unclamping), and μ' is the apparent or effective coefficient of friction. To compute the stress perturbation in equation (1), we need to assume a value for the apparent coefficient of friction, which generally ranges from 0.0-0.8. Lin and Stein (2004) suggest that the apparent coefficient of friction appears to be high for thrust faults, perhaps about 0.8. In keeping with this suggestion, we assume $\mu' = 0.8$ for the calculation of ΔCFF. We test the sensitivity of the results to this assumption in later discussions.

 The Coulomb stress change due to an earthquake is resolved on a target fault plane, known as the receiver fault. In general, two types of receiver faults are considered: a specified-fault plane and an optimally-oriented fault plane. The first approach simply assumes that the receiver fault has the same strike, dip, and rake as the mainshock seismic source, considered as the typical faulting mechanism in the region (e.g. Toda et al, 2011; Sumy et al, 2014). In the latter approach, the stress changes are resolved onto a fault plane that maximizes the ΔCFF, and considers both the stress change due to the mainshock and the regional stress field. The latter approach strongly depends on the stress field assumed in the study area, which is unknown in most of the cases. Therefore, in this study we adopt the specified-fault approach, in which we consider the stress changes from large events to be resolved onto planes consistent with the typical faulting mechanism in the CSZ, which indicates thrust faulting on planes that dip steeply to the southeast (*e.g.* Anglin 1984). Table 1 lists the seismic source parameters compiled for the larger earthquakes in the CSZ including the 1663 earthquake and five other earthquakes with **M**≥5.5. We also consider the somewhat-smaller 1979 **M**4.8 earthquake, as this is the largest recent earthquake in the CSZ.

The location and magnitudes of historical earthquakes (in 1663, 1791, 1870, and 1860) are constrained to the best extent possible based on available published information (Smith, 1962; Ebel, 1996; Fereidoni *et al.*, 2012). With regard to the rupture mechanism, we assume these earthquakes as thrust events on a fault plane striking at N035° and steeply dipping southeast, consistent with the orientation of the major rift faults of the CSZ (Lamontagne, 1999). We arbitrarily choose the fault dip as 60° which is a typical dip for thrust faults in the region, and provides a good match to the predominant thrust focal mechanism observed for the larger recent events (Baird *et al.*, 2010). For the events in 1925 (**M**6.4) and 1979 (**M**4.8), for which better information is available from source studies, we adopt the focal mechanism solutions of Bent (1992) and Hasegawa and Wetmiller (1980), respectively.

Our modeling is conducted with the Coulomb 3.3 software (Toda *et al.*, 2011), which calculates the static stress changes resulting from fault rupture in an elastic half space, following the theoretical approach of Okada (1992). Using published empirical relations, we model the size of the seismic sources based on the moment magnitude of the earthquakes. Instead of using the Wells and Coppersmith (1994) relation, which is a commonly-implemented choice in Coulomb 3.3, we use the empirical models in Johnston (1993) for stable continental earthquakes. Since detailed rupture scenarios are not available for the Charlevoix earthquakes, we assume a uniform slip model across the rupture plane (e.g. Johnston, 1993). It is important to note that other empirical relations could be used to derive equally-satisfactory source rupture models, indicating inherent uncertainty in the fault plane parameters. However, the general conclusions drawn in this paper are insensitive to reasonable changes in the fault plane parameters, as the following results and discussions will show.

To compare the calculated ΔCFF with the background seismicity in the CSZ, we use the CCSC as the reference for the background events (Fereidoni *et al.*, 2012), in which all events are catalogued on a homogeneous moment magnitude scale. As the accuracy of the hypocentral locations is important for comparison purposes, we limit our earthquake dataset to shallow earthquakes (depth ≤ 30 km) recorded after 1978 (when relatively dense instrumental coverage began; see Figure 4.2 for station locations). Considering the small extent of our study area and the stable network configuration since 1978, it is reasonable to neglect spatial variability in earthquake detection. We therefore prefer to use all earthquake

locations in the CCSC without setting any specific magnitude threshold. However, we have verified that the result does not change if we impose a set magnitude threshold based on commonly-accepted completeness magnitudes for the region (e.g. Adams and Halchuk, 2003). Therefore this is not an issue of any importance.

Table 4-1 Fault models for CSZ events

Event	Lat.	Long.	M*	L(km)	W(km)	Strike	Dip	Rake	Slip
1663	47.6	70.1	7.0	30	11.0	35	60	90	2.9 m
1791	47.4	70.5	5.5	3.3	3.3	35	60	90	29 cm
1860	47.5	70.1	6.1	8.0	4.1	35	60	90	91 cm
1870	47.4	70.5	6.6	15.0	7.0	35	60	90	1.6 m
1925	47.80	69.80	6.4	15.0	7.0	42	53	105	1.6 m
1979	47.67	69.90	4.8	1.8	1.8	46	76	131	12 cm
* Magnitudes are reported in moment magnitude scale.									

4.4 Coulomb stress changes for the 1663 Charlevoix earthquake

The 1663 **M**~7 Charelvoix earthquake is historically the largest shock in the region, so this event is of particular importance in the interpretation of stress changes in the study area. In this section, we explore the stress interaction between the 1663 earthquake and current background seismicity in the CSZ (1978 to the present) under the hypothesis that small Coulomb stress changes (ΔCFF $\geq$ 0.1 bar, Stein, 1999) can promote events. Based on the assumed threshold of 0.1 bar (Stein, 1991), we examine whether the background activity in the CSZ is promoted in the region of stress increase (ΔCFF $\geq$ 0.1 bar) or inhabited in the region of stress decrease (ΔCFF $\leq$ - 0.1 bar). The Coulomb stress calculation requires defining the slip direction and geometry of the faults that ruptured during the 1663 earthquake. From historical and geological lines of evidence, it is usually concluded that the epicentral area of the 1663 earthquake was in the vicinity of La Malbaie (Figure 4..2), where many profound geological effects were noted (Smith, 1962, Gouin, 2001). In our Coulomb stress modeling, we constrain the location of the centre of the fault center based on the Smith (1962) epicenter at -70.1°W, 47.6°N. We start with the assumption of thrust faulting for the 1663 earthquake on a fault plane (strike: N35°, dip: 60°, rake: 90°) that follows the

orientation of the major rift faults at the CSZ. This assumption is well constrained based on the focal mechanism of the recent largest earthquakes in CSZ that show thrust faulting on north-east south-west striking nodal planes (Bent et al, 2003), with the suggestion being that the 1663 earthquake may have the same focal mechanism (Ebel, 2011). However, we have tested alternative focal mechanisms in a later discussion.

To calculate ΔCFF, we estimate the rupture parameters (slip, rupture dimension) for the 1663 earthquake based on empirical relations that scale the source parameters based on the magnitude of the earthquake (e.g Johnston, 1993; Wells and Coppersmith, 1994). Since the magnitude estimate of the 1663 earthquake is associated with a high level of uncertainty (at least several tenths of a magnitude unit), the rupture parameters are also highly uncertain. We start with an initial model with parameters chosen to be consistent with a **M**7.0 earthquake; we address the issue of the uncertainty in the assumed rupture model in more detail in later discussions. Using the Johnston (1993) scaling relation, it is assumed that the event produced 2.9 m of reverse slip on a 30 km × 11 km rupture plane. It should be noted that the Wells and Coppersmith (1994) relation for thrust events estimate the rupture dimension of 48 km × 22 km for a **M**7.0 earthquake. Since the Johnston (1993) empirical model is developed based on intraplate earthquakes, it is preferred in our study.

Figure 4.3 depicts the resulting pattern of stress changes, along with the locations of recent seismicity (1978 to the present) from the unified CCSC catalog. It can be seen that regions of positive ΔCFF correlate relatively well with the concentration of recent microseismicity in the CSZ. To further test the correlation, we calculate the Coulomb stress change on a 0.005 degree × 0.005 degree horizontal grid. We associate each earthquake in the CCSC catalog to the closest grid node to estimate the Coulomb stress change at the event's hypocentral location. We find that ~80% of earthquakes experience positive Coulomb stress change (ΔCFF ≥ 0.1 bar) that would promote failure and only ~18% of the earthquakes show negative stress change (ΔCFF ≤ - 0.1 bar) that would inhabit failure. Cross sections of the Coulomb stress changes through the center of the fault indicate that lobes of enhanced failure condition (positive ΔCFF) correspond to the distinct zones of activity that are observed in the CSZ. Additionally, the aseismic slab reported in previous studies coincides with the region of reduced Coulomb stress. The general correlation between the stress changes generated by the 1663 event with our assumed rupture parameters and recent microseismicity patterns may

suggest that the 1663 earthquake exerts significant influence over the spatial distribution of contemporary (from 1978 to the present) low-magnitude earthquakes. Indeed, it appears that current seismicity may well be attributable to stress response from the 1663 earthquake.

With our assumed rupture model, the 1663 earthquake exerts only modest stress changes on the areas in which the larger recent events ($\mathbf{M} \geq 3.5$ since 1978) have been located (except for a cluster of seismicity in the northeast).Moreover, with regard to the largest historic earthquakes (also superimposed on Figure 4.3), three out of four events have occurred in regions with minimal stress changes, in the range from -0.17 to 0.17 bar. Considering the large uncertainty (at least tens of kilometers) associated with the location of these historic events, we cannot infer whether or not the stress changes imparted by the 1663 earthquake may have accelerated the occurrence of those events. On the other hand, localization of the recent larger earthquakes outside the region with strong enhanced failure conditions may suggest that the 1663 earthquake does not influence the occurrence of the larger events in the CSZ. This suggestion, however, depends significantly on the geometry of the seismic source assumed. It is likely that all the seismicity in the CSZ, including both microearthquakes and larger events, could be explained by assuming a larger source fault. We return to this point later, in the discussion.
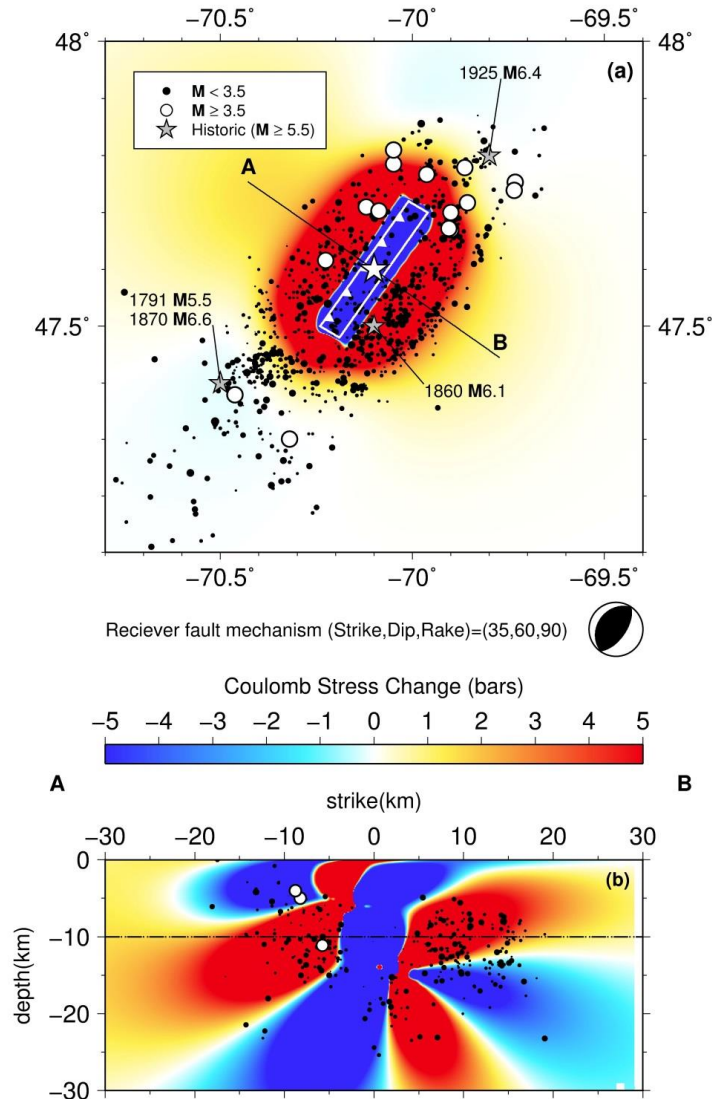
Figure 4-3 Static stress field produced by the 1663 M7.0 event for the focal mechanism shown (strike 35, dip 60, rake 90). Top panel is map view at 10 km depth, in which the fault rupture area is shown as a white large rectangle (hosting 2.9m reverse slip). The white star represents the location of the 1663 earthquake. The green circles indicates the earthquake hypocenters, based on the unified CCSC catalog (since 1978, depth≤30km). The beach ball in the bottom right indicates the fault focal mechanism. The lower panel shows the Coulomb stress changes in a cross-section along the profile A-B, together with earthquake hypocenters within a 20-km-wide band. The dash line indicates the 10 km depth of the map view. Note the general coincidence of microseismicity with lobes of enhanced stress.

4.5 Effects of changing the friction parameter

The Coulomb stress model proposed above has been shown to provide a detectable overall correlation with the observed seismicity pattern in the CSZ, with ~80% of the events occurring within regions exhibiting positive stress changes greater than 0.1 bar. In this section, we examine the effects of changing the apparent coefficient of friction (μ') for the purpose of demonstrating the robustness of the results. We re-calculate the Coulomb stress changes involving the same source parameters as in the above model, but for intermediate (μ'=0.4) and low (μ'=0.2) friction. Low input values for μ' in the Coulomb stress equation have the principal effect of abating the sensitivity to the normal stress changes ($\Delta\sigma$), which perturbs the pattern of stress transfer. Comparison of the results (Figure 4.4) with the previous stress model (Figure 4.3) reveals some noticeable differences. In particular, lowering the apparent friction coefficient strengthens the effect of the shear stress ($\Delta\tau$), which results in broad zones of Coulomb stress decrease perpendicular to the strike of the source fault. Statistical assessment shows that decreasing the value of apparent coefficient of friction reduces the correlation between seismicity and enhanced stress areas. By using μ'=0.4, we find that ~75% of events are occurring in the region of ΔCFF $\geq$ 0.1; this percentage decreases to 66% with the use of μ'=0.2.

In the next step we calculate normal stress changes ($\Delta\sigma$) that involve the same thrust fault model to further investigate the issue. The result given in Figure 4.5 shows the high degree of consistency between the earthquake locations and the calculated unclamping effect, suggesting that the seismicity pattern is sensitive to normal stress changes. We interpret this as evidence that the high value of apparent coefficient of friction appears to be more appropriate for our thrust fault model. The same inference has been made for other thrust faults, as pointed out in Lin and Stein (2004) and references therein. We therefore prefer μ' = 0.8 in the following models, although it should be noted that none of the main conclusions of the paper are significantly affected by changing the apparent coefficient of friction in the Coulomb stress calculation.
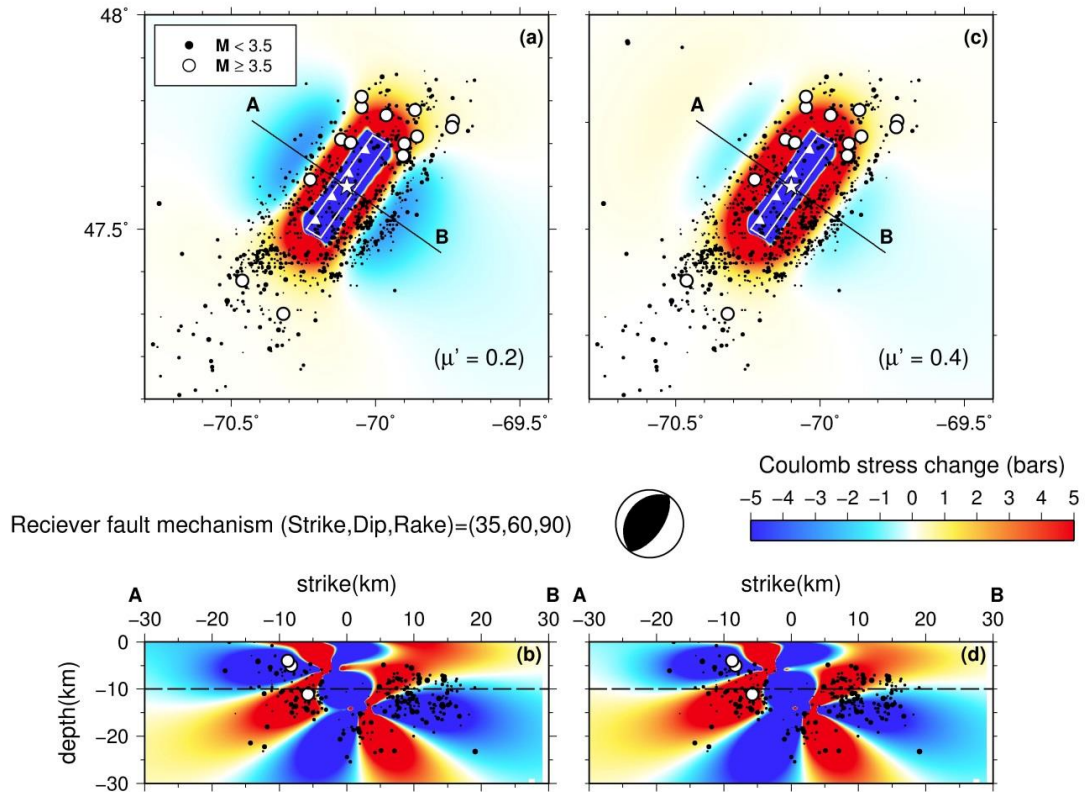
Figure 4-4 Effects of changing the apparent coefficient of friction (µ') on the pattern of the stress transfer. All map views model stress changes at 10 km depth. The source fault model has the same geometry and slip as in the previous figure; the receiver fault is assumed to have the same parameters as the source fault. All cross section view are along the profile A-B, together with earthquake hypocenters along a 20-km-wide band. Calculated stress changes (a)-(b) for low friction (µ'=0.2); (c)-(d) for intermediate friction (µ'=0.4). The symbols are the same as Figure 4.3.
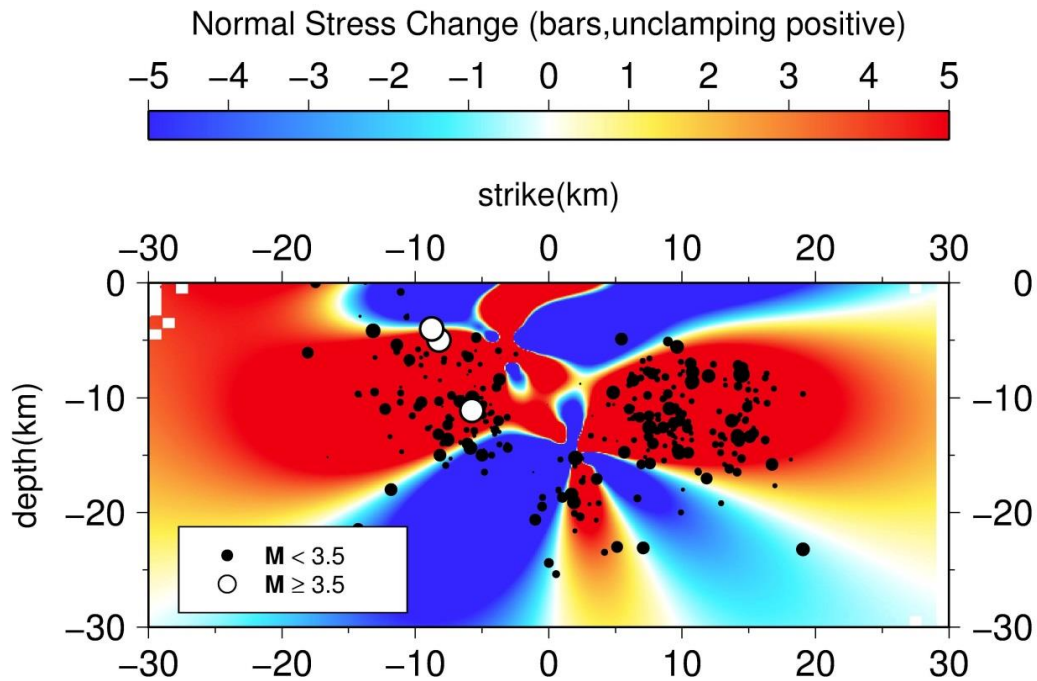
Figure 4-5 A cross section view showing the normal stress changes caused by the source fault model assumed in previous modellings (Figure 4.3 and 4.4). The cross section cuts the center of the source fault along the profile A-B shown in previous figures. The seismicity along a 20-km-wide band is plotted. The symbols are the same as in Figure 4.3.

4.6 Effects of using other source fault models

In this section, we test the sensitivity of our conclusions to the assumed fault source model. In our initial model, we assumed that the fault mechanism was pure thrust. We next test a more realistic model by considering a minor component of strike-slip motion in our faulting mechanism. The new rupture model involves 2.8 m of reverse slip and 0.75 m of strike slip on a fault plane (strike:N42°,dip:53°, rake:105°), that matches the focal mechanism of the1925 Charlevoix earthquake (Bent, 1992), since this focal mechanism also fits very well within the seismotectonic framework of the region. It should be noted that the rupture dimension assumed (30 km × 11 km) is the same as in the previous model. Not surprisingly, the use of the 1925 focal mechanism generates a pattern of ΔCFF which is quite similar to the initial model, with minor differences in detail (i.e. the lobes of slightly reduced stress on either side of the fault plane), as shown in Figure 4.6. The high correlation between

seismicity and enhanced stress areas still remains, with ~75% of the total 1006 events occurring within the regions of positive Coulomb stress increase that are greater or equal to 0.1 bar. Other faulting mechanisms examined (*e.g.* predominantly strike-slip) did not provide a model of stress changes consistent with the observed seismicity.

Another aspect of uncertainty in the assumed rupture scenario for the 1663 earthquake can be explored by calculating the Coulomb stress changes for different rupture dimensions. To do that, we re-calculate ΔCFF as a function of magnitude at 0.25 magnitude unit intervals between **M**6.5 and 8.0, which covers the entire range of magnitude estimates for the 1663 earthquake (Smith, 1962; Ebel, 1996; Gouin, 2001; Ebel, 2011; Locat, 2011). Using the scaling relation of Johnston (1993), the corresponding rupture length varies in a large range from 15 to 150 km (Table 2). In all of the models, we assume the same thrust fault plane as in the initial model (strike: N35°, dip: 60°, rake: 90°). Figure 4.7 and 4.8 show the corresponding stress change patterns; note the geographical coordinate difference from previous figures. In general, we find that 47-75% of the 1062 events locate within the regions of the Coulomb stress increase when the rupture length changes between 15 and 150 km (Table 2). Specifically, the fault areas of 30km×11km and 50km×13km produce a Coulomb stress pattern that has the highest level of correlation with the distribution of the seismicity (~75%); using Johnston (1993), the corresponding magnitude estimates that maximize the correlation are **M**7.0 and **M**7.25, respectively. When the rupture length is smaller (15-22.5 km), the percentage of correlated events reduces to ~61-71%. On the other hand, the use of a longer rupture plane, for example 70km×15km, would produce a larger triggering zone that would cover the entire region of contemporary seismicity (from 1978 to the present), including the moderate-to-large earthquakes at either end of the seismic zone; however, the correlation between earthquakes and the areas of Coulomb stress increase (ΔCFF ≥ 0.1 bar) would decrease to ~70%. If the rupture of the 1663 extended further to the southwest and northeast (for example for the total fault length of 110-150 km), the percentage of correlated events would reduce dramatically, to 47-59%. Therefore, we find that a very long rupture that corresponds to a very high magnitude, in the range of **M**7.75 to **M**8.0, generates stress patterns that considerably diminish the observed correlation with the current seismicity.
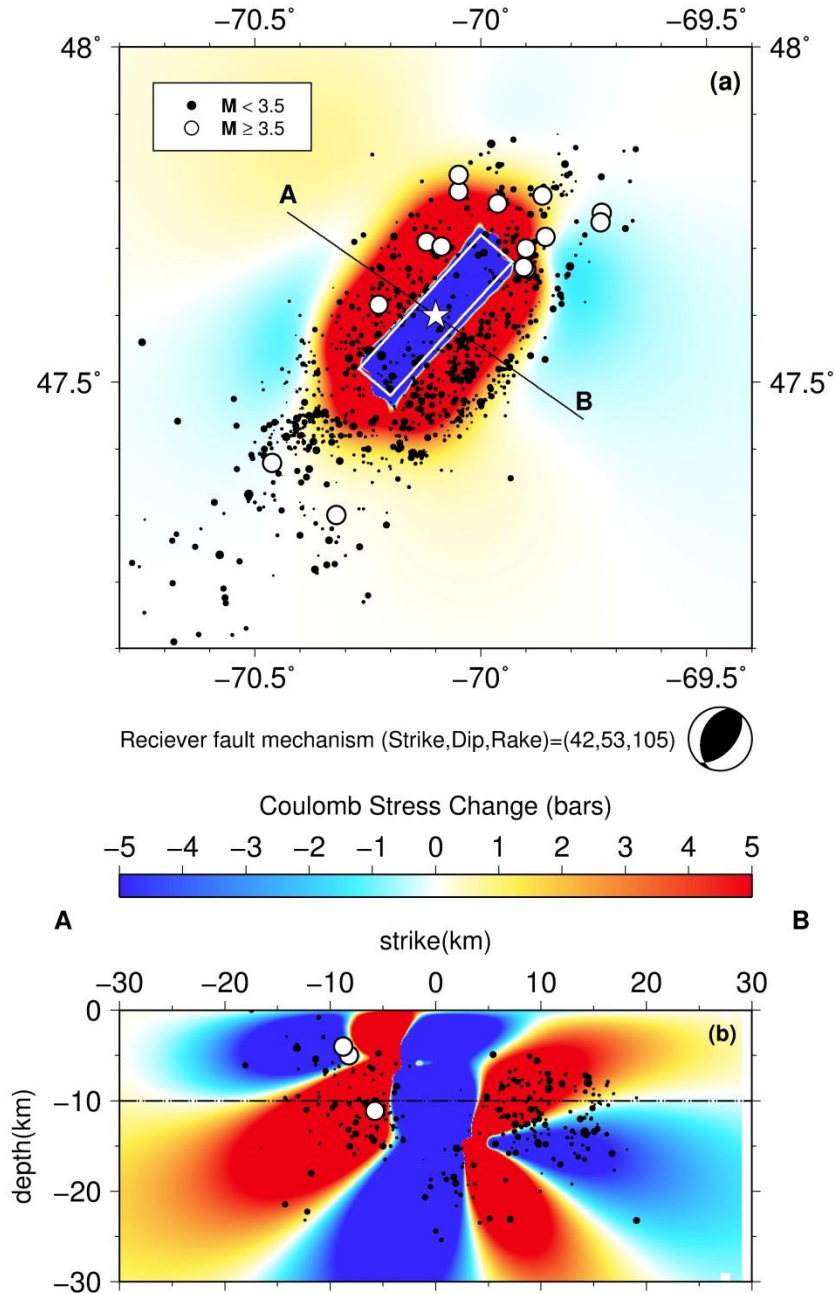
Figure 4-6 Static stress field produced by the 1663 M7.0, assuming that the focal mechanism matches that of the 1925 Charlevoix earthquake (Bent, 1992) with strike 42°, dip 53°, and rake 105°.The source seismic involves precisely the same slip and fault area as adopted in the previous models. The symbols are the same as in Figure 4.3.

Table 4-2 Rupture parameters for various magnitude estimates assumed for the 1663 earthquake and corresponding correlation with the location of the contemporary seismicity

M	L (J93) in km	W (J93) in km	Slip (J93) in m	M* (WC94)	ΔCFF ≥ 0.1 bar	ΔCFF ≤ -0.1 bar
6.5	15	7	1.6	6.15	61%	2%
6.75	22.5	9	2.25	6.41	71%	5%
7	30	11	2.9	6.60	75%	12%
7.25	50	13	4	6.86	75%	19%
7.5	70	15	5.1	7.05	70%	27%
7.75	110	18.5	7.1	7.31	59%	40%
8	150	22	9.1	7.50	47%	51%

Magnitudes are reported in moment magnitude scale.
J93-Johnston (1993)
WC94-Wells and Coppersmith (1994)
* The alternative magnitude estimates are calculated using Wells and Coppersmith (1994) based on the moment magnitude versus fault area relation for thrust events.
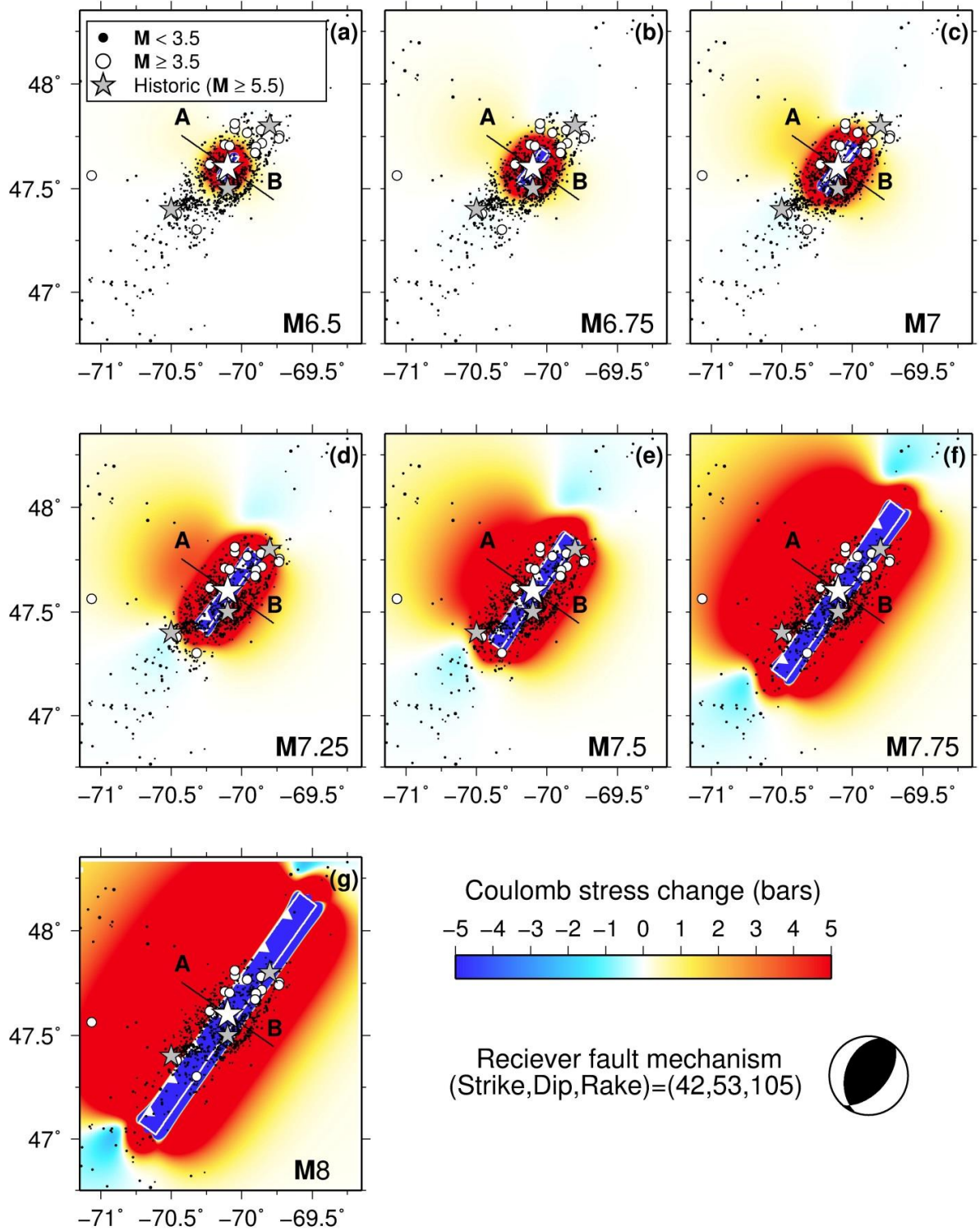
Figure 4-7 Coulomb failure stress resulting from the 1663 earthquake under various hypothesized magnitudes (7.2, 7.5 and 8.0). All map views model corresponding stress changes at 10km depth. Note geographical coordinate difference from Figure (4.3). The

fault areas, shown by white rectangles, has slip on fault planes with strike 42°, dip 53°, and rake 105°, the same as in Figure 4.6. All cross-sectional views are along the profile A-B, and include earthquakes hypocenters within a 20-km-wide band. The symbols are the same as in Figure 4.3.
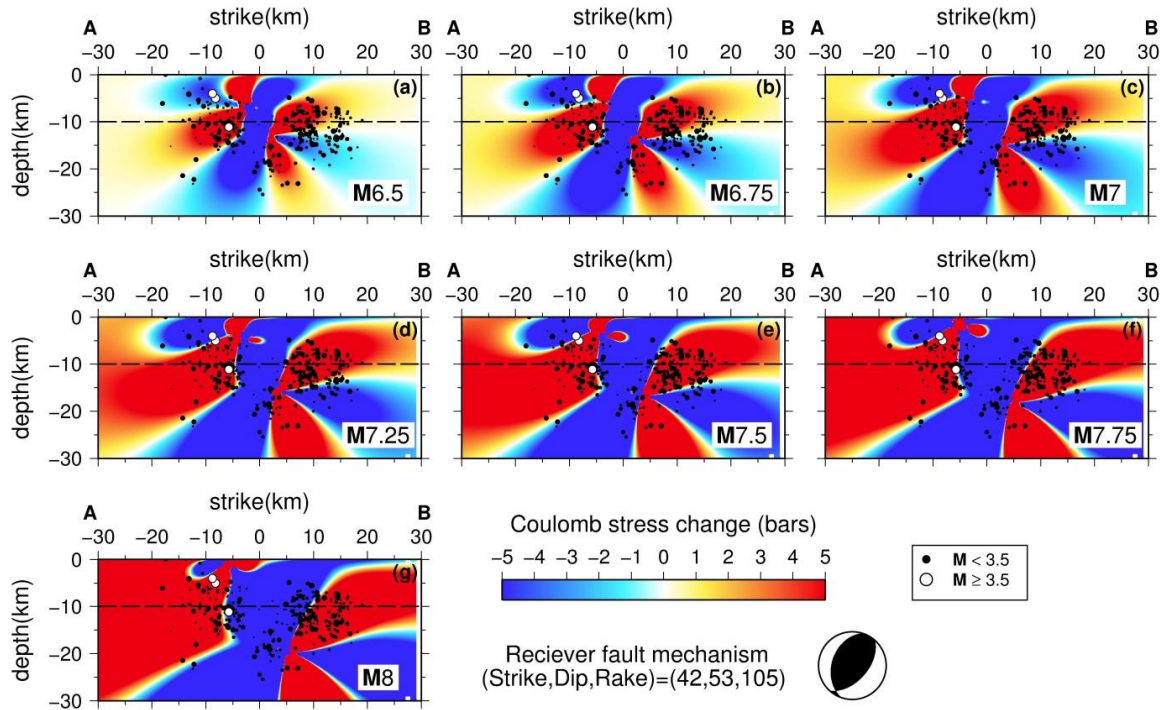
Figure 4-8 Cross-sectional views that correspond to the Coulomb stress maps in Figure 4.7. All cross-sections are along the profile A-B shown in Figure 4.7; supplemented with earthquake hypocentres along a 20-km-wide band. The dash lines indicate the depth of map views in Figure 4.7.

4.7 Coulomb stress changes for other significant CSZ earthquakes

Other stress changes in the CSZ may also affect the spatial distribution of recent seismicity. For example, significant post-1663 earthquakes produce an additional load, on top of the stress changes associated with the 1663 earthquake. Therefore, inclusion of the ΔCFF due to these earthquakes warrants investigation. Here, we include the seismic sources of all earthquakes of **M**$\geq$5.5 that occurred after the 1663 earthquake, as well as the 1979 **M**=4.8 event, because it is the largest recent earthquake in the CSZ. For the 1979 and 1925

earthquakes, we adopt the focal mechanism solutions of Hasegawa and Wetmiller (1980) and Bent (1992), respectively (Table1). For the older events in 1663, 1791, 1860, and 1870, we again consider a predominately thrust event on a fault plane dipping steeply to the southeast (Table 1). Figure 4.9 depicts the combined Coulomb stress effects due to the 1791 **M**5.5, 1860 **M**6.1, 1870 **M**6.6, 1925 **M**6.4, and 1979 **M**4.8 events, added to the stress changes imparted by the 1663 **M**7.0 earthquake. The pattern of the stress changes still generally coincidence with the spatial distribution of the seismicity in the CSZ with ~ 80% of the events locate within the stress triggering zone (ΔCFF $\geq$ 0.1); seismicity clusters at both ends of the zone are located in positive ΔCFF regions.

4.8   Discussion and conclusions

In this study we have explored the influence of the 1663 Charlevoix earthquake on the location of recent seismicity in the region by focusing on the theory of Coulomb stress change. We have used an appropriate rupture geometry and sense of slip, consistent with the thrust faulting mechanisms that are typical in the region, to derive an idealized representation of Coulomb model for the 1663 event. We find that such a model produces a reasonable apparent spatial correlation between the stress changes and the pattern of current seismicity observed in the CSZ, which captures many of the main features of seismicity in the region. The apparent correlation includes the general coincidence of the lobes of enhanced stress with two main clusters of activity observed in previous seismological studies (Anglin and Buchbinder, 1981; Lamontagne and Ranalli, 1997). It is further interesting to note that the aseismic slab that separates these zones correlates well with the region of Coulomb stress decrease, directly adjacent to the hypothesized rupture plane. This is in agreement with Ebel (2011) who notes that the aseismic slab may indicate the fault plane in the 1663 earthquake.

The Coulomb stress modeling provides evidence that the stress changes caused by the 1663 earthquake still exert influence on earthquake occurrence in the Charlevoix region. While the observed correlation with the zone of microseismicity within the Charlevoix impact structure is relatively robust regardless of the rupture model considered, the degree of overlap between the stress-triggering zone and the location of moderate-to-large earthquakes in either end of the zone depends on the hypothesized rupture dimensions. We find the highest correlation (~75-80%) between the location of current seismicity and the regions of stress increase ($\geq$0.1

bar) when the fault rupture for the 1663 earthquake is considered to be between 30 and 50 km in length. These relatively small fault dimensions result in patterns of stress transfer that explain the clusters of low-magnitude earthquakes, but exert a relatively modest influence on the location of larger events. This model is consistent with the hypothesis proposed in Lamontagne *et al.*, 2004. According to Lamontagne et al (2004), the larger earthquakes in the CSZ represent reactivation of Iapetan faults in the region, while the smaller events may represent reactivation of smaller fractures within the impact zone due to local stresses. The local stress distribution due to the occurrence of the 1663 earthquake could have increased the stress and enhanced the failure condition in the weakened zone, leading to a marked increase in the number of small earthquakes within the impact crater. This may explain why the impact structure in the CSZ is seismically active, while similar structures in Canada are aseismic (Adams and Basham, 1989). Alternatively, by assuming a longer rupture plane for the 1663 earthquakes (e.g. 70km $\times$ 15km), all of the seismicity in the CSZ would be roughly located in the areas of increased Coulomb stress. This model which is more consistent with an estimated fault area of 73 km $\times$ 25 km for the 1663 earthquake as inferred by Ebel (2011) provides a credible explanation for localization of both microearthquakes and larger events in the CSZ. However, we find that the correlation between the location of current seismicity and the Coulomb stress change reduces (Table 2) when fault ruptures longer than 50km are considered. This may indicate that the best estimate of the fault rupture for the 1663 earthquake is in the range between 30 and 50 km. Using the Johnston (1993) scaling relation, the corresponding magnitude estimates are **M**7.0 and **M**7.25, respectively. Assuming the same rupture dimensions, one would compute smaller magnitudes, in the range of **M**6.69 to **M**7.02, from the Wells and Coppersmith (1994) magnitude versus fault area relation for thrust events in active tectonic regions. As mentioned earlier, the Johnston (1993) relation is developed based on fault sizes for earthquakes in stable continental regions, which tend to be characterized by higher stress drops, and is therefore preferred in this study.

We acknowledge that our calculations of the Coulomb stress changes depend on the assumed location and geometry of the rupture and the distribution of slip. The conjectural nature of these source parameters generates considerable uncertainty in our model. Therefore, it is possible that the apparent correlation we observed between the model of stress changes and the seismicity pattern is merely fortuitous. However, we have tested the robustness of our

results over a range of plausible rupture and slip geometries, considering uncertainty in both the rupture dimensions and focal mechanisms for the 1663 earthquake. We observe a consistent result, regardless of reasonable changes in the size, orientation and mechanism of faulting, with a large percentage portion of events consistently falling within the regions of positive stress increase above 0.1 bar. The rupture scenarios that best match the seismicity pattern correspond to a thrust event (that may include a minor strike-slip component) due to the reactivation of a SE-dipping fault, with rupture parameters that corresponds to a magnitude in the **M**7.0-7.25 range, based on the Johnston (1993) scaling relationship for fault size. This faulting scenario fits well with our understanding of the seismotectonic framework of the region.

We conclude that the 1663 Charlevoix earthquake widely redistributed the static stress in the surrounding crust, and that this stress change still influences the location of seismicity in the CSZ today. However, we emphasize that this does not mean the current seismicity (from 1978 to the present) represents an aftershock sequence (Fereidoni and Atkinson, 2014). We note that there may be a similar phenomenon observed in the New Madrid Seismic Zone, where the continuing microseismicity is not part of a decaying aftershock sequence (Page and Hough, 2014), but appears to be still influenced by the static stress changes due to large historical earthquakes (Mueller *et al.*, 2004). Page and Hough (2014) proposed one possible explanation that current microseismicity in New Madrid is driven by low-level creep that produces stresses that are roughly consistent with the stress changes caused by the 1811-1812 sequence. In New Madrid, studies have interpreted a barely detectable deformation signal in terms of creep on a down-dip extension of the Reelfoot fault (Frankel et al, 2012). Such a model might potentially be able to reconcile the observations in the Charlevoix Seismic Zone. If the current activity in Charlevoix is the result of ongoing strain accrual, the region will continue to be a source of seismic hazard.
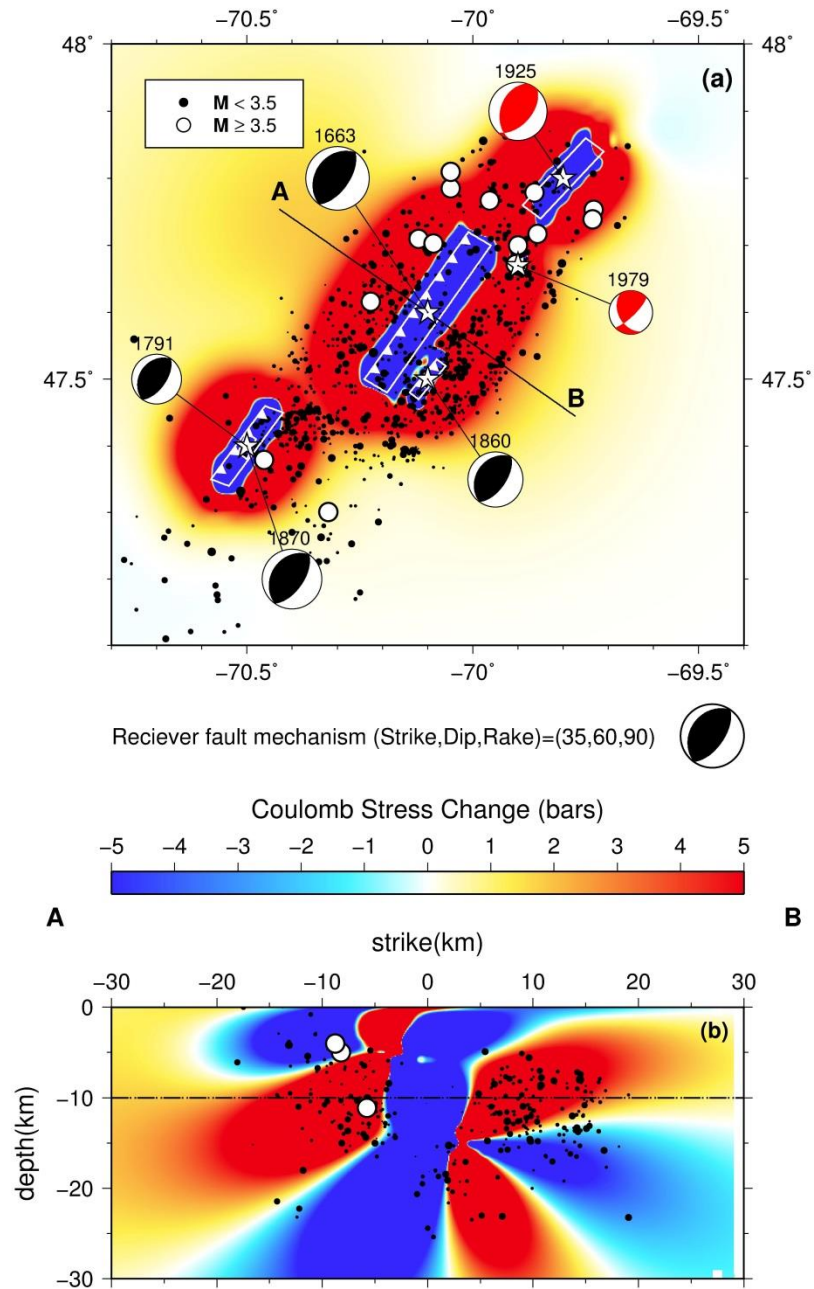
Figure 4-9 The composite Coulomb stress associated with six large earthquakes (the 1663 M7.0, 1791 M5.5, 1860 M6.1, 1870 M6.6, 1925 M6.4, and 1978 M4.8), all at depth 10km. The focal mechanism of the older events (black beach balls) is based on average rift fault geometry while the two recent events (red beach balls) are from Bent (1925) and Hasegawa and Wetmiller (1980), as listed in Table 4-1. Stress changes are resolved on a receiver fault with average rift faults geometry. The symbols are the same as in Figure 4.3.

4.9 References

Adams, J., A. Vonk, D. Pittman, and H. Vatcher (1989). New focal mechanisms for southeastern Canadian earthquakes; Volume II, *Open-File Report - Geological Survey of Canada*.

Adams, J., and P. Basham (1989). The seismicity and seismotectonics of Canada east of the Cordillera, *Geoscience Canada* **16,** 3-16.

Anglin, F., and G. Buchbinder (1981). Microseismicity in the mid-St. Lawrence Valley Charlevoix zone, Quebec, *Bulletin of the Seismological Society of America* **71,** 1553-1560.

Anglin, F. (1984). Seismicity and faulting in the Charlevoix zone of the St. Lawrence Valley, *Bulletin of the Seismological Society of America* **74,** 595-603.

Baird, A. F., S. D. McKinnon, and L. Godin (2010). Relationship between structures, stress and seismicity in the Charlevoix seismic zone revealed by 3-D geomechanical models; implications for the seismotectonics of continental interiors, *Journal of Geophysical Research* **115,** Citation B11402.

Basham, P. W. (1989). Problems with seismic hazard assessment on the eastern Canadian continental margin, *NATO Advanced Study Institutes Series. Series C: Mathematical and Physical Sciences* **266,** 679-686.

Basham, P., and J. Adams (1983). Earthquakes on the continental margin of eastern Canada: Need future large events be confined to the locations of large historical events, *United States Geological Survey Open File Report* **83,** 456-467.

Bent, A. L. (1992). A re-examination of the 1925 Charlevoix, Quebec, earthquake, *Bulletin of the Seismological Society of America* **82,** 2097-2113.

Ebel, J. E. (2011). A new analysis of the magnitude of the February 1663 earthquake at Charlevoix, Quebec, *Bulletin of the Seismological Society of America* **101,** 1024-1038.

Ebel, J. E. (1996). The seventeenth century seismicity of northeastern North America, *Seismological Research Letters* **67,** 51-68.

Ebel, J. E., K. Bonjer, and M. C. Oncescu (2000). Paleoseismicity: Seismicity evidence for past large earthquakes, *Seismological Research Letters* **71,** 283-294.

Fereidoni, A., G. M. Atkinson, M. Macias, and K. Goda (2012). CCSC: A composite seismicity catalog for earthquake hazard assessment in major Canadian cities, *Seismological Research Letters* **83,** 179-189.

Fereidoni, A., G. M. Atkinson (2014). Aftershock Statistics for Earthquakes in the St. Lawrence Valley, *Seismological Research Letters* (in print).

Frankel, A., R. Smalley, and J. Paul (2012). Significant motions between GPS sites in the New Madrid region; implications for seismic hazard, *Bulletin of the Seismological Society of America* **102,** 479-489.

Harris, R. A. (1998). Introduction to special section; stress triggers, stress shadows, and implications for seismic hazard, *Journal of Geophysical Research* **103,** 24-24,358.

Hasegawa, H. S., and R. J. Wetmiller (1980). The Charlevoix earthquake of 19 August 1979 and its seismo-tectonic environment, *Seismological Research Letters* **51,** 23-38.

Ishibe, T., K. Shimazaki, H. Tsuruoka, Y. Yamanaka, and K. Satake (2011). Correlation between Coulomb stress changes imparted by large historical strike-slip earthquakes and current seismicity in Japan, *Earth, planets and space* **63,** 301-314.

Johnston, A. (1993). Average stable continental earthquake source parameters based on constant stress drop scaling, *Seismological Research Letters* **64,** 261.

King, G. C., R. S. Stein, and J. Lin (1994). Static stress changes and the triggering of earthquakes, *Bulletin of the Seismological Society of America* **84,** 935-953.

Lamontagne, M., M. Beauchemin, and T. and Toutin (2004). Earthquakes of the Charlevoix seismic zone, Quebec, *CSEG RECORDS* **October,** 41-44.

Lamontagne, M. (1999). Rheological and geological constraints on the earthquake distribution in the Charlevoix seismic zone, Quebec, Canada, *Open-File Report - Geological Survey of Canada*.

Lamontagne, M., and G. Ranalli (1997). Faults and spatial clustering of earthquakes near La Malbaie, Charlevoix seismic zone, Canada, *Seismological Research Letters* **68,** 337-352.

Lin, J., and R. S. Stein (2004). Stress triggering in thrust and subduction earthquakes and stress interaction between the southern San Andreas and nearby thrust and strike-slip faults, *Journal of Geophysical Research* **109,** B02303.

Locat, J. (2011). La localisation et la magnitude du seisme du 5 fevrier 1663 (Charlevoix) revues a l'aide des mouvements de terrain, *Canadian Geotechnical Journal = Revue Canadienne de Geotechnique* **48,** 1266-1286.

Ma, S., and D. W. Eaton (2007). Western Quebec seismic zone (Canada); clustered midcrustal seismicity along a Mesozoic hot spot track, *Journal of Geophysical Research* **112,** B06305.

Mazzotti, S., & Adams, J. (2005). Rates and uncertainties on seismic moment and deformation in eastern Canada. *Journal of Geophysical Research* **110**.B9.

Mueller, K., S. E. Hough, and R. Bilham (2004). Analysing the 1811–1812 New Madrid earthquakes with recent instrumentally recorded aftershocks, *Nature* **429,** 284-288.

Nostro, C., R. S. Stein, M. Cocco, M. E. Belardinelli, and W. Marzocchi (1998). Two-way coupling between Vesuvius eruptions and southern Apennine earthquakes, Italy, by elastic stress transfer, *Journal of Geophysical Research: Solid Earth (1978–2012)* **103,** 24487-24504.

Ogata, Y., and S. Toda (2010). Bridging great earthquake doublets through silent slip: On-and off-fault aftershocks of the 2006 Kuril Island subduction earthquake toggled by a slow slip on the outer rise normal fault of the 2007 great earthquake, *Journal of Geophysical Research: Solid Earth (1978–2012)* **115,** .

Okada, Y. (1992). Internal deformation due to shear and tensile faults in a half-space, *Bulletin of the Seismological Society of America* **82,** 1018-1040.

Oppenheimer, D. H., P. A. Reasenberg, and R. W. Simpson (1988). Fault plane solutions for the 1984 Morgan Hill, California, earthquake sequence; evidence for the state of stress on the Calaveras Fault, *Journal of Geophysical Research* **93,** 9007-9026.

Page, M. T. and S. E. Hough (2014), The New Madrid Seismic Zone: Not Dead Yet, *Science* **343**, 6172. doi:10.1126/science.1248215.

Reasenberg, P. A., and R. W. Simpson (1992). Response of regional seismicity to the static stress change produced by the Loma Prieta earthquake, *Science* **255,** 1687-1690.

Rondot, J. (1979). Impactite of the charlevoix structure, Quebec, Canada, *Journal of Geophysical Research* **76,** 5414-5423.

Smith, W. E. T. (1962). Earthquakes of eastern Canada and adjacent areas 1534-1927, *Publications of the Dominion Observatory, Ottawa* **26,** 271-301.

Solomon, S. C., and E. D. Duxbury (1987). A test of the longevity of impact-induced faults as preferred sites for later tectonic activity, *Journal of Geophysical Research: Solid Earth (1978–2012)* **92,** E759-E768.

Stein, R. S., and M. Lisowski (1983). The 1979 Homestead Valley earthquake sequence, California; control of aftershocks and postseismic deformation, *Journal of Geophysical Research* **88,** 6477-6490.

Stein, S., and M. Liu (2009). Long aftershock sequences within continents and implications

for earthquake hazard assessment, *Nature* **462,** 87-89.

Sumy, D. F., E. S. Cochran, K. M. Keranen, M. Wei, and G. A. Abers (2014). Observations of static Coulomb stress triggering of the November 2011 M5. 7 Oklahoma earthquake sequence, *Journal of Geophysical Research: Solid Earth* **119,** 1904-1923.

Toda, S., and B. Enescu (2011). Rate/state Coulomb stress transfer model for the CSEP Japan seismicity forecast, *Earth Planets and Space* **63,** 171.

Toda, S., R. S. Stein, V. Sevilgen, and J. Lin (2011), Coulomb 3.3 Graphic-Rich Deformation and Stress-Change Software for Earthquake, Tectonic, and Volcano Research and Teaching – User Guide, *United States Geological Survey Open File Report* 2011-1060, 63 p., available at http://pubs.usgs.gov/of/2011/1060/.

Tuttle, M., and G. Atkinson (2010). Localization of earthquakes in the Charlevoix, Quebec seismic zone in the last 10,000 years. Seism. Res. L., **81**, 140-147.

Vlahovic, G., C. Powell, and M. Lamontagne (2003). A three-dimensional P wave velocity model for the Charlevoix seismic zone, Quebec, Canada, *Journal of Geophysical Research* **108.**

Wells, D. L., and K. J. Coppersmith (1994). New empirical relationships among magnitude, rupture length, rupture width, rupture area, and surface displacement, *Bulletin of the Seismological Society of America* **84,** 974-1002.

Wetmiller, R., and J. Adams (1990). An earthquake doublet in the Charlevoix seismic zone, *Quebec: in Current Research, Part B, Geological Survey of Canada Paper* 105-113.

Chapter 5

5   Conclusions and future works

5.1   Summary

The aim of this thesis was to explore the influence of the 1663 **M**~7 Charlevoix earthquake on the current seismicity in the Charlevoix Seismic Zone. The first part of the thesis focused on developing a suitable baseline of earthquake information. The composite seismicity catalog developed here provides a reliable baseline database for earthquake studies in Canada. The second part of the thesis was devoted to characterization of seismicity in the study region in both time and space, with the goal of developing greater insight into the nature of intraplate seismicity in the Charlevoix region.

In Chapter two, the development of the Canadian Composite Seismicity Catalog (CCSC) was described. For each event in the catalog, all available magnitude types were compiled, and a preferred estimate of moment magnitude was assigned depending on the availability and the quality of data. The CCSC was largely compiled through an automatic procedure, but required manual judgment in selection of the preferred earthquake characterizations. I have applied my best efforts to associate the most complete and reliable information in the composite catalog. However, I acknowledge that the CCSC contains incomplete and uncertain information; this is unavoidable in the creation of a composite catalog.

In Chapter three, the influence of the 1663 earthquake on temporal distribution of seismicity in the Charlevoix Seismic Zone was investigated. For this purpose, the recent significant mainshock-aftershock sequences in the St. Lawrence Valley were analyzed by a consistent and uniform statistical approach with the goal of obtaining the typical behavior of aftershocks. The results provide the plausible range of aftershock parameters in the study region, which can be used in short-term and long-term hazard assessment. The average aftershock statistics obtained in this thesis reveal some key features of the temporal behavior of aftershocks in the study region. Aftershock sequences in the St. Lawrence Valley share similar parameter values, with the exception of the Miramichi sequence for which aftershock activity was more productive and longer than average in the region. Based on the aftershock sequences studied here, the aftershock activity in the St. Lawrence region is apparently less

energetic and productive than average aftershock sequences in California. The difference in productivity between the St. Lawrence and California aftershock sequences could be related to the difference in the source parameters of the mainshocks and crustal properties. The eastern mainshocks have systematically higher stress drop and the crust is more homogenous in comparison to the west. Considering the typical behavior of aftershock sequences in the St. Lawrence region and California or Miramichi, the observed seismicity in the CSZ cannot be reconciled with expected rates based on a decaying aftershock sequence from the 1663 earthquake. An aftershock sequence consistent with the present rate of activity in the CSZ overpredicts the number of moderate-to- large events that were observed in the years following the 1663 mainshock. It is unlikely that tens to hundreds of strong and frightening aftershocks went unreported, over a century or more, in an area known for its rich historical records. The results of this statistical study imply that the current seismicity in Charlevoix is not part of decaying aftershock sequence.

Chapter Four investigates the influence of the 1663 Charlevoix earthquake on the spatial distribution of recent seismicity in the CSZ by focusing on the theory of Coulomb stress changes. With the use of an appropriate rupture geometry and sense of slip, consistent with the typical thrust faulting mechanisms in the region, an idealized representation of Coulomb failure model for the 1663 event is derived. The hypothesized model produces a strong apparent spatial correlation between the stress changes and the pattern of current seismicity observed in the CSZ, which captures many of the main features of seismicity in the region. The stress triggering zone generally corresponds with the regions in which current seismicity clusters. Interestingly, the stress shadow adjacent to the hypothesized rupture plane correlates well with the aseismic slab that separates the clusters of activity. The stress changes associated with the 1663 event include the regions of enhanced failure condition (positive ΔCFF) that correspond to the boundaries of the microearthquake zone within the impact structure in Charlevoix. This may explain the large increase of low-level background seismicity within the crater area. The 1663 event may have enhanced the failure conditions within the region weakened by the impact structure, leading to an increase in local microseismicity. However, the inclusion of moderate to large earthquakes at either end of the seismic zone in the stress-triggering zone depends on the fault size considered. Assuming reasonably large fault planes could provide credible explanation for all of the seismicity in

the Charlevoix region including both microearthquakes and larger events. I acknowledge that the apparent correlation might be merely fortuitous due to the conjectural nature of the source parameters considered in this model. However, the robustness of results over a range of plausible rupture and slip geometries, considering uncertainty in both the magnitude and focal mechanisms for the 1663 earthquake, lend weight to the significance of the correlation. The rupture scenarios that best match the seismicity pattern correspond to a thrust event (that may include a minor strike-slip component) due to the reactivation of a SE-dipping fault, with a magnitude in the **M**7.0-7.5 range. This faulting scenario fits well with the current understanding of the seismotectonic framework of the region, and would explain most of the features of the current observed seismicity.

5.2 Discussion

The evidences from this thesis suggests that the current seismicity in the Charlevoix Seismic Zone is not predominantly composed of the aftershock activity of past large earthquakes; the ongoing seismicity is therefore expected to continue in the region, and the zone should be considered an ongoing source of seismic hazard. However, we emphasize that this does not eliminate the possibility that earthquake activity in Charlevoix is still influenced by the stress changes imparted by the 1663 earthquake in the surrounding crust.

The Coulomb stress analysis used in Chapter 4 shows that the stress triggers and shadow cast by the 1663 earthquake still exert influence on earthquake occurrence in the Charlevoix after centuries. While the degree of overlap between the stress-triggering zone and the location of moderate-to-large earthquakes in either end of the zone depends on the hypothesized rupture dimensions, the observed correlation with the zone of microseismicity within the impact structure is robust regardless of the rupture model considered. It has been proposed in previous studies (Lamontagne et al, 2004) that large earthquakes in the CSZ respond to the reactivation of Iapetan faults in the region; however, for smaller events, smaller fractures within the impact zone might be reactivated by local stresses. The results presented in this thesis provide some support for this hypothesis. The local stress distribution due to the occurrence of the 1663 earthquake could have enhanced the failure condition in the weakened zone, leading to a marked increase in the number of small earthquakes within the impact crater. This may explain why the impact structure in the CSZ is seismically active,

while similar structures in Canada are aseismic (Adams and Basham, 1989).

I acknowledge that the results from Chapter 3 and 4 are in some ways contradictory, as they suggest that the Charlevoix seismicity are not aftershocks, but yet are associated with stress changes caused by the 1663 mainshock. This effectively implies a new class of triggered events that is not consistent with Omori's decay model but still triggered. One may interpret that the "Omori decay" view of triggering is too limited.

There are other examples of such apparent contradictions. Recently, Page and Hough (2014) explored the same contradiction in the New Madrid seismic zone (NMSZ), given the results from the Coulomb stress modeling in an earlier paper by Mueller et al (2004). They proposed one possible explanation for why NMSZ seismicity "looks like aftershocks" when it isn't, namely that present microseismicity is driven by low-level creep that produces stresses that are roughly consistent with the stress changes caused by the 1811-1812 sequence. In New Madrid, studies (e.g. Frankel et al, 2012) have interpreted a barely detectable deformation signal in terms of creep on a down-dip extension of the Reelfoot fault, so this hypothesis has some foundation.

It is interesting to explore whether there is evidence of similar on-going creep in the Charlevoix region. Previous studies of crustal deformation have shown detectable deformation in the Charlevoix Seismic Zone that is higher than the regional average across the St. Lawrence region (Mazzotti and Adams, 2005; Mazzotti et al, 2005). The observed amount of deformation from GPS data could account for very large earthquakes with recurrence period of 400-1300 years. Although Mazzotti et al (2005) showed that the GPS data in the CSZ are compatible with the velocity profile that represents a seismogenic fault above a deep creeping segment, they could not rule out alternative models of crustal deformation (e.g negligible stain rate or weak zone) due to the scatter and uncertainties of the GPS data. Obviously, more precise and denser GPS measurements over the areas with various seismic features in the St. Lawrence Valley could help constrain models for better understating of the seismicity process in this intraplate region and to improve our assessment of seismic hazard.

5.3   Future works

The analysis performed in this thesis provides useful information about the seismicity and hazard in the Charlevoix Seismic Zone. Future works that would further our knowledge of this important intraplate region include the following.

1) The results from this thesis find that the stress trigger and shadow due to the 1663 earthquake may exert an influence on earthquake occurrence that lasts for centuries. An incorporation of viscoelastic effects that modifies the Coulomb stress with time may explain the long-term phenomena observed in the Charlevoix region.

2) Geodetic studies in the CSZ may benefit from the use of a customized deformation model that is appropriate for this intraplate area. Such a model has been implemented by Frankel et al (2012) in the modelling of the GPS measurements in the New Madrid Seismic Zone.

5.4   References

Adams, J., and P. Basham (1989). The seismicity and seismotectonics of Canada east of the Cordillera, *Geosci.Can.* **16,** 3-16.

Frankel, A., R. Smalley, and J. Paul (2012). Significant motions between GPS sites in the New Madrid region; implications for seismic hazard, *Bulletin of the Seismological Society of America* **102,** 479-489.

Page, M. T. and S. E. Hough (2014), The New Madrid Seismic Zone: Not Dead Yet, *Science* **343**, 6172. doi:10.1126/science.1248215.

Mazzotti, S., and J. Adams (2005). Rates and uncertainties on seismic moment and deformation in eastern Canada, *Journal of Geophysical Research: Solid Earth (1978–2012)* **110,** .

Mazzotti, S., T. S. James, J. Henton, and J. Adams (2005). GPS crustal strain, postglacial rebound, and seismic hazard in eastern North America: The Saint Lawrence valley example, *Journal of Geophysical Research: Solid Earth (1978–2012)* **110,** .

Curriculum Vitae

Name: Azadeh Fereidoni

Post-secondary University of Bu-Ali-Sina
Education and Hamedan, Hamedan, Iran
Degrees: 1999-2004 B.Sc.

        University of Tehran
        Tehran, Tehran, Iran
        2004-2007 M.Sc.

        The University of Western Ontario
        London, Ontario, Canada
        2009-2014 Ph.D.

Honours and
Awards: Western Graduate Research Scholarships (WGRS), 2009-2013
        CGU Student Travel Awards, 2011, and 2012
        "Institute for Catastrophic Loss Reduction" Prize, 2012
        AGU Best Student Presentation Award, 2012
        Geophysics Travel Scholarship, 2012
        SSA-ES Best Student Poster Award, 2013

Related Work Teaching Assistant
Experience   The University of Western Ontario
        2009-2013

        Research Assistant
        The University of Western Ontario
        2009-2014